

# Detrital zircon ages and the origins of the Nashoba terrane and Merrimack belt in southeastern New England, USA

J. CHRISTOPHER HEPBURN<sup>1\*</sup>, YVETTE D. KUIPER<sup>2</sup>, KRISTIN J. MCCLARY<sup>1</sup>,  
MARYELLEN L. LOAN<sup>1</sup>, MICHAEL TUBRETT<sup>3</sup>, AND ROBERT BUCHWALDT<sup>4</sup>

1. Department of Earth and Environmental Sciences, Boston College, Chestnut Hill, Massachusetts 02467, USA
2. Department of Geology and Geological Engineering, Colorado School of Mines, Golden, Colorado 80401, USA
3. Department of Earth Sciences, Memorial University of Newfoundland, St. John's, Newfoundland A1B 3X5, Canada
4. Department of Earth and Environment, Boston University, Boston, Massachusetts 02215, USA

\*Corresponding author <john.hepburn@bc.edu>

*Date received: 27 April 2021 | Date accepted: 11 November 2021*

## ABSTRACT

The fault-bounded Nashoba–Putnam terrane, a metamorphosed early Paleozoic, Ganderian arc/back-arc complex in SE New England, lies between rocks of Avalonian affinity to the southeast and middle Paleozoic sedimentary rocks, interpreted as cover on Ganderian basement, in the Merrimack belt to the northwest. U–Pb detrital zircon laser ablation inductively coupled plasma mass spectrometry analysis were conducted on six samples from the Nashoba terrane in Massachusetts and seven samples associated with the Merrimack belt in Massachusetts and SE New Hampshire to investigate their depositional ages and provenance. Samples from the Nashoba terrane yielded major age populations between ~560 and ~540 Ma, consistent with input from local sources formed during the Ediacaran–Cambrian Penobscot orogenic cycle and its basement rocks. Youngest detrital zircons in the terrane, however, are as young as the Early to Middle Ordovician. Six formations from the Merrimack belt were deposited between ~435 and 420 Ma based on youngest zircon age populations and crosscutting plutons, and yielded large ~470–443 Ma age populations. Three of these formations show only Gondwanan provenance. Three others have a mixed Gondwanan-Laurentian signal, which is known to be typical for younger and/or more westerly sedimentary rocks and may indicate that they are the youngest deposits in the Merrimack belt (late Silurian to early Devonian) and/or have been deposited in the equivalent of the more westerly Central Maine basin. Detrital zircon age populations from the Tower Hill Formation, along the faulted contact between the Merrimack belt and Nashoba terrane, are different from either of these tectonic domains and may indicate that the boundary is complex.

---

## RÉSUMÉ

Le terrane limité par des failles de Nashoba-Putnam, un complexe d'arc/arrière-arc métamorphisé gandérien du Paléozoïque précoce dans le sud-est de la Nouvelle-Angleterre, se trouve entre des roches ayant une affinité avalonienne au sud-est et des roches sédimentaires du Paléozoïque moyen, interprétées comme une couverture du socle gandérien, dans la ceinture de Merrimack au nord-ouest. Six échantillons provenant du terrane de Nashoba au Massachusetts et sept échantillons associés à la ceinture de Merrimack au Massachusetts et dans le sud-est du New Hampshire ont fait l'objet d'une analyse par spectrométrie de masse avec plasma à couplage inductif et par ablation par laser de datation U–Pb sur zircon détritique aux fins de l'examen de leurs âges sédimentaires et de leur provenance. Les échantillons provenant du terrane de Nashoba ont révélé des populations principalement âgées entre environ 560 et 540 Ma, ce qui correspond à la contribution des sources locales apparues durant le cycle orogénique édiacarien-cambrien de Penobscot et aux roches de son socle. Les zircons détritiques les plus récents dans le terrane remontent cependant seulement à l'Ordovicien précoce à moyen. Six formations de la ceinture de Merrimack se sont déposées à peu près entre 435 et 420 Ma selon les populations des âges les plus récents sur zircon et les plutons transversaux, et elles ont présenté de vastes populations âgées d'environ 470 à 443 Ma. Trois de ces formations témoignent uniquement d'une provenance gondwanienne. Trois autres évoquent de façon mixte le Gondwanien et le Laurentien, ce qui est reconnu comme un trait typique des roches sédimentaires plus récentes ou plus à l'ouest et qui pourrait révéler qu'il s'agit de dépôts plus récents dans la ceinture de Merrimack (du Silurien tardif au Dévonien précoce) ou qui se seraient mis en place dans l'unité équivalente du bassin plus occidental du centre du Maine. Les populations d'un âge sur zircon détritique de la Formation de Tower Hill le long de la zone de contact faillé entre la ceinture de Merrimack et le terrane de Nashoba diffèrent de l'un et l'autre de ces domaines tectoniques et pourraient indiquer que leur limite est complexe.

[Traduit par la redaction]

## INTRODUCTION

Two Neoproterozoic to early Paleozoic Gondwanan-derived terranes form the eastern portion of southeastern New England: Avalonia to the southeast and the Nashoba-Putnam terrane of Ganderian affinity to its northwest. These are followed westward by a thick succession of Silurian-Devonian cover rocks in the Merrimack belt (Fig. 1). In order to develop a comprehensive overview of the sedimentary and tectonic history of Ganderia in southeastern New England, analyses of detrital zircon from representative metasedimentary rocks in both the Nashoba terrane and Merrimack belt were carried out by U-Pb laser ablation inductively coupled plasma mass spectrometry (LA-ICPMS) to determine their maximum depositional ages, provenance and potential correlations in the northern Appalachians. Six

samples from the Nashoba terrane in Massachusetts and six from the Merrimack belt in Massachusetts and southeastern New Hampshire were analyzed. One additional sample was taken from along the faulted boundary between the Merrimack belt and the Nashoba terrane.

## Geological background

### Nashoba terrane

The Nashoba terrane in eastern Massachusetts (Fig. 1) is an early Paleozoic arc/back-arc complex that, based on Sm/Nd isotope compositions and model ages, developed on an older crustal basement (e.g., Goldsmith 1991a; Hepburn *et al.* 1995; Kay *et al.* 2017; Walsh *et al.* 2021). It has been interpreted as the trailing edge of Ganderia in SE New England

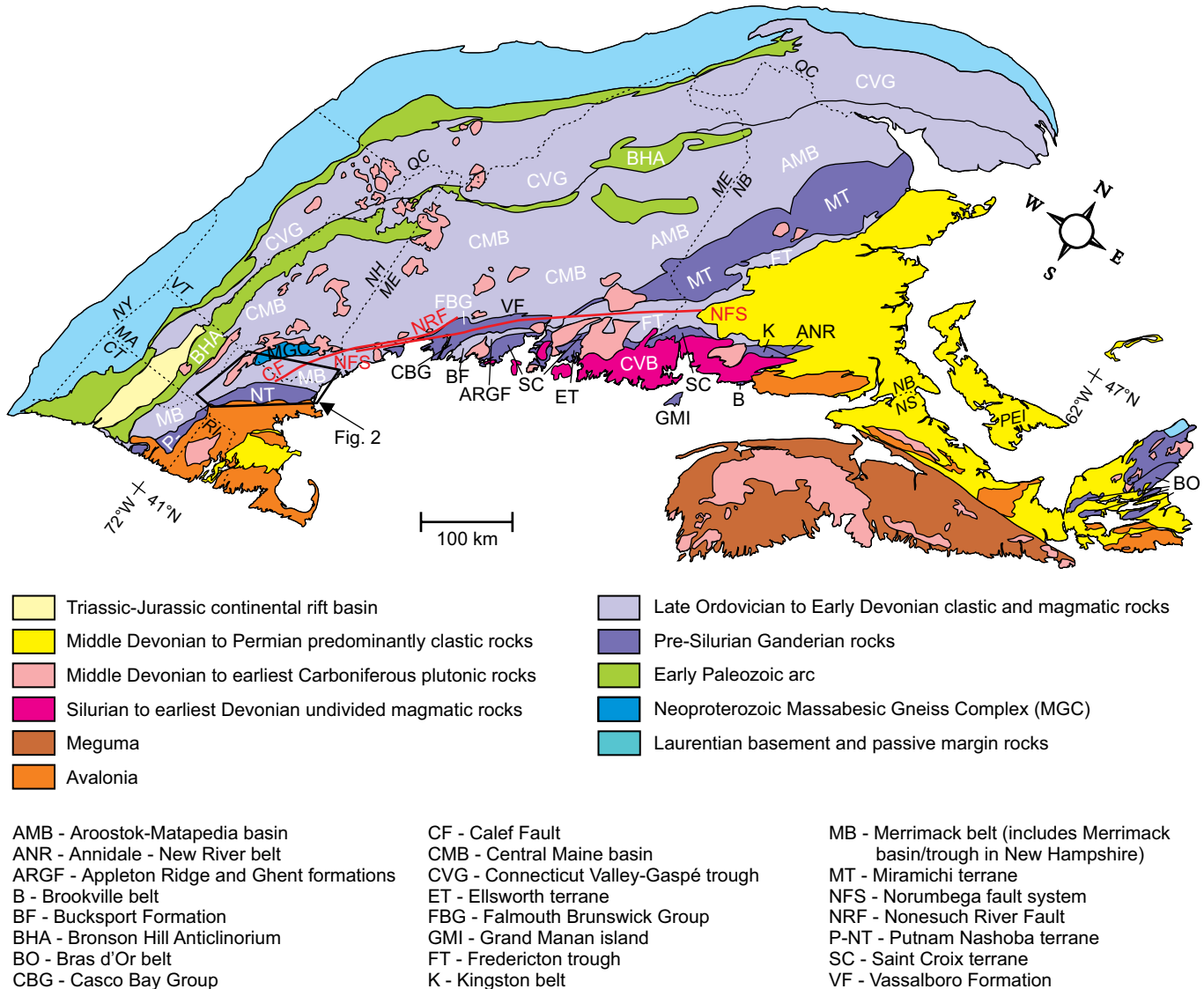


**Figure 1.** Simplified geological map of the northern Appalachians. Modified after Hibbard *et al.* (2006). CT – Connecticut, MA – Massachusetts, ME – Maine, NB – New Brunswick, NH – New Hampshire, NS – Nova Scotia, NY – New York, PEI – Prince Edward Island, RI – Rhode Island, QC – Quebec, VT – Vermont.

(e.g., Hibbard *et al.* 2006; van Staal *et al.* 2009; Walsh *et al.* 2011b, 2015, 2021; Kay *et al.* 2017). The Nashoba terrane consists of highly metamorphosed and multiply deformed early Paleozoic volcanic and volcanogenic sedimentary rocks that are intruded by abundant middle Paleozoic dioritic and granitic plutons (e.g., Wones and Goldsmith 1991; Zartman and Marvin 1991; Hepburn *et al.* 1995). It is separated from the Avalonian rocks to the southeast by the Burlington mylonite zone, which was later overprinted by the more brittle Bloody Bluff fault zone (Castle *et al.* 1976; Zen *et al.* 1983; Skehan *et al.* 1998; Kohut and Hepburn 2004), and from the Merrimack belt to the northwest by the Clinton-Newbury fault zone (Figs. 1, 2; Skehan 1968; Castle *et al.* 1976; Zen *et al.* 1983; Goldsmith 1991b). The stratified units generally dip moderately to steeply northwest (Bell and Alvord 1976; Goldsmith 1991a). In the southeast, the terrane consists largely of mafic metavolcanic and metasedimentary rocks of the Marlboro Formation, while to the northwest predominantly volcanogenic metasedimentary

rocks of the Nashoba Formation dominate (Bell and Alvord 1976; Goldsmith 1991a; Hepburn *et al.* 1995). Other major units include a schistose unit (Tadmuck Brook Schist), an orthogneiss (Fish Brook Gneiss) and a paragneiss (Shawsheen Gneiss) (Fig. 2; Bell and Alvord 1976; Zen *et al.* 1983; Goldsmith 1991a; Hepburn *et al.* 1995). The metavolcanic and metasedimentary units in the southeast are interpreted to have been part of an arc or formed in a near-arc basin, while those in the northwest have been interpreted to represent largely contemporaneous to somewhat younger sedimentary deposits with minor volcanic input in a back-arc basin developed farther from an arc (e.g., Goldsmith 1991a; Hepburn *et al.* 1995; Kay *et al.* 2017).

The terrane is intruded by abundant Silurian to Carboniferous granitic and dioritic plutons. Some of these plutons have been dated using various methods of U-Pb zircon geochronology. These include the  $430 \pm 5$  Ma Sharpner's Pond Diorite (Zartman and Naylor 1984), two phases of the Andover Granite, which are  $419 \pm 0.5$  Ma (Dabrowski

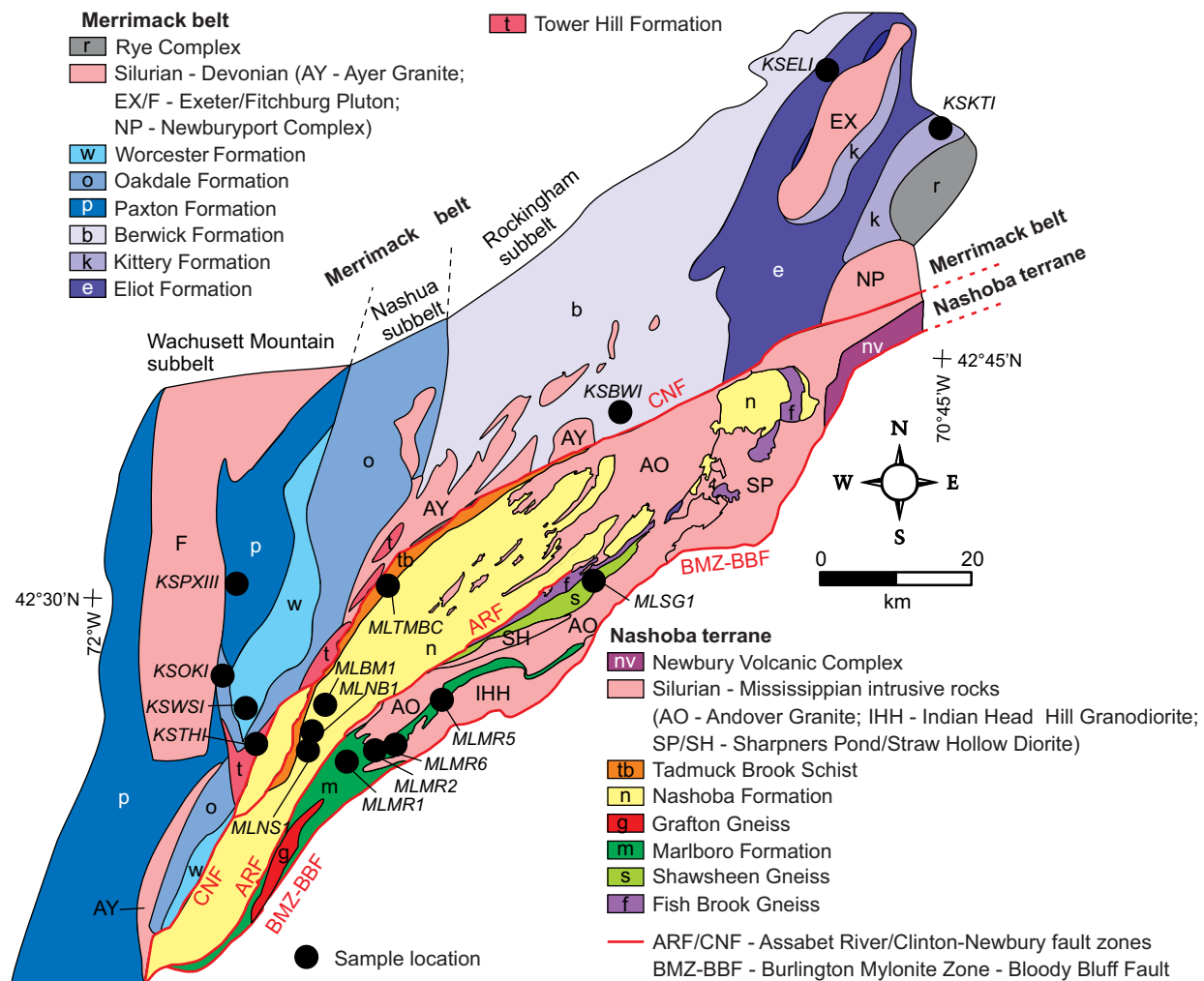


**Figure 2.** Simplified geological map and sample locations (labeled in italic) for the Nashoba terrane and Merrimack belt. Modified after Robinson and Goldsmith (1991), Hepburn *et al.* (1995) and Lyons *et al.* (1997). Subbelts of the Merrimack belt from Robinson and Goldsmith (1991).

2013; Dabrowski *et al.* 2013) and  $412 \pm 2$  Ma (Hepburn *et al.* 1995), the  $420.5 \pm 0.5$  Ma Sudbury granite (Dabrowski 2013; Dabrowski *et al.* 2013), the  $385 \pm 10$  Ma Straw Hollow diorite (Acaster and Bickford 1999) and the  $349 \pm 4$  Ma Indian Head Hill Granite (Hepburn *et al.* 1995).

Previous age determinations on rocks associated with the stratified units in the Nashoba terrane are limited. They include a  $\sim 540$  Ma mafic boudin in the Quinebaug Formation (a unit in the Putnam terrane to the south in Connecticut correlated with the Marlboro Formation), a  $515 \pm 4$  Ma date on the Grafton Gneiss that cross-cuts part of the Marlboro Formation, and a  $500.6 \pm 4.2$  Ma date on a feldspathic granofels in the Marlboro Formation structurally above the Grafton Gneiss (U-Pb zircon SHRIMP, Walsh *et al.* 2009, 2011a, b, 2021). The granofels was derived from a proximal volcanic source and its age is interpreted as the approximate age of deposition (Walsh *et al.* 2021). In addition to the  $\sim 540$ - $500$  Ma volcanic rocks of the Marlboro Formation and the Grafton Gneiss, the Fish Brook orthogneiss (Fig. 2) has also been dated as Cambrian ( $499 +6/-3$  Ma, U-Pb zircon ID-TIMS, Hepburn *et al.* 1995).

Deformation and metamorphism in the Nashoba terrane are primarily a result of the late Silurian–Devonian Acadian orogeny that resulted from accretion of Avalonia and its subsequent westward convergence (e.g., Hepburn *et al.* 1995; van Staal *et al.* 2009, 2020; Kuiper *et al.* 2014; Walsh *et al.* 2015, 2021; Severson 2020). Post-Acadian zircon and monazite in the Nashoba terrane have been interpreted to be a result of the late Devonian Neoacadian and/or Pennsylvanian–Permian Alleghanian orogenic events and/or hydrothermal fluids (Wintsch *et al.* 2007; Stroud *et al.* 2009; Loan 2011; Buchanan *et al.* 2017; Walsh *et al.* 2021).

### *Late Ordovician to Early Devonian cover successions*

Late Ordovician to Early Devonian calcareous and pelitic turbiditic rocks form extensive cover successions on older Ganderian rocks throughout the northern Appalachians from southern New England to Newfoundland (e.g., Williams 1978; Tucker *et al.* 2001; Tremblay and Pinet 2005; Hibbard *et al.* 2006). In New England, these sedimentary rocks show increasing Laurentian affinity to the west where they define the Connecticut Valley-Gaspé trough (Fig. 1; e.g., Hibbard *et al.* 2006; Rankin *et al.* 2007). To the east (Fig. 1), two extensive depocenters of these rocks, the Fredericton trough and Central Maine basin, are defined by their location with respect to inliers of Cambrian–Ordovician basement rocks (e.g., Reusch and van Staal 2012; Ludman *et al.* 2018). However, the terminology that has been applied to these rocks across New England is complex and varied as it includes both structural and sedimentary terms (i.e., belt, synclinorium, basin, trough) as well as various stratigraphic names and correlations. Figure 3 summarizes the principal stratigraphic names by location for the relevant Late Ordovician to Early Devonian cover rocks in eastern and central New England and southern New Brunswick. Below we explain, from north to south, some of the definitions of

basins used by others, and the rationale behind them. We then summarize the definitions used in this contribution, which are largely based on this previous work.

In eastern Maine and New Brunswick, the Fredericton trough lies between the Late Ordovician and older rocks of the St. Croix terrane to the SE and the Miramichi terrane to the NW (Fig. 1; e.g., Reusch and van Staal 2012; Ludman *et al.* 2017, 2018; Dokken *et al.* 2018). The broader Central Maine basin, including the along-strike Aroostock-Matapedia basin to the north, formed between the Miramichi terrane to the SE and older rocks of the Bronson Hill arc and related inliers to the NW (Fig. 1; Osberg *et al.* 1985; Tucker *et al.* 2001; Fyffe *et al.* 2009, 2011; Reusch and van Staal 2012; Bradley and O’Sullivan 2017; Ludman *et al.* 2017, 2018). Both the Fredericton trough and Central Maine basin contain late Ordovician (?) and Silurian sedimentary rocks. Deposition ended in the Fredericton trough by the late Silurian as it was deformed prior to intrusion by the  $421.9 \pm 2.4$  Ma Pocomooshine gabbro-diorite (West *et al.* 1992; Ludman *et al.* 2018), while deposition continued into the Devonian in the Central Maine basin (Osberg 1988; Bradley *et al.* 2000; Tucker *et al.* 2001; Bradley and O’Sullivan 2017; Ludman *et al.* 2018). In south-central Maine and coastal southern Maine the Fredericton trough includes the Late Ordovician (?) and Silurian Ghent, Appleton Ridge and Bucksport formations (Figs. 1, 3; Hussey 1988; Berry and Osberg 1989; Hussey *et al.* 2010; West and Condit 2016; Cartwright *et al.* 2019) that lie southeast of Miramichi terrane-correlative Ordovician and older rocks in the Falmouth-Brunswick Group and Casco Bay Group (West *et al.* 2004, 2006; Hussey *et al.* 2010; Reusch and van Staal 2012; West and Hussey 2016, Hussey and West 2018).

In southwestern Maine and southeastern most New Hampshire, Late Ordovician and Silurian rocks that are approximately along strike, and can be correlated with those of the Fredericton trough and eastern part of the Central Maine basin form the Merrimack basin or Merrimack trough (Lyons *et al.* 1997; Fig. 1) and were originally included in the Merrimack Group (Fig. 3; Eliot, Kittery and Berwick formations; e.g., Hitchcock 1877; Katz 1917; Billings 1956; Lyons *et al.* 1997; Fargo and Bothner 1995; Hussey *et al.* 2010; see Hussey *et al.* 2010 for details). Hussey *et al.* (2010), however, redefined the Merrimack Group in SW Maine and New Hampshire to include only sedimentary rocks interpreted as Late Ordovician–early Silurian (Eliot and Kittery formations) and correlated them with those in the Fredericton trough. They correlated sedimentary rocks interpreted to be late Silurian–Early Devonian (Berwick Formation) with the Central Maine basin. Hussey *et al.* (1999, 2010) suggested that their redefined Late Ordovician–early Silurian Merrimack Group, in addition to the Fredericton trough deposits, including the Bucksport and associated formations of south-central Maine, represent a potentially continuous single basin and named it the Merribuckfred basin (Fig. 3). However, it is now known that the Fredericton trough also includes late Silurian deposits (Dokken *et al.* 2018; Ludman *et al.* 2018). Therefore, the Merribuckfred basin now refers

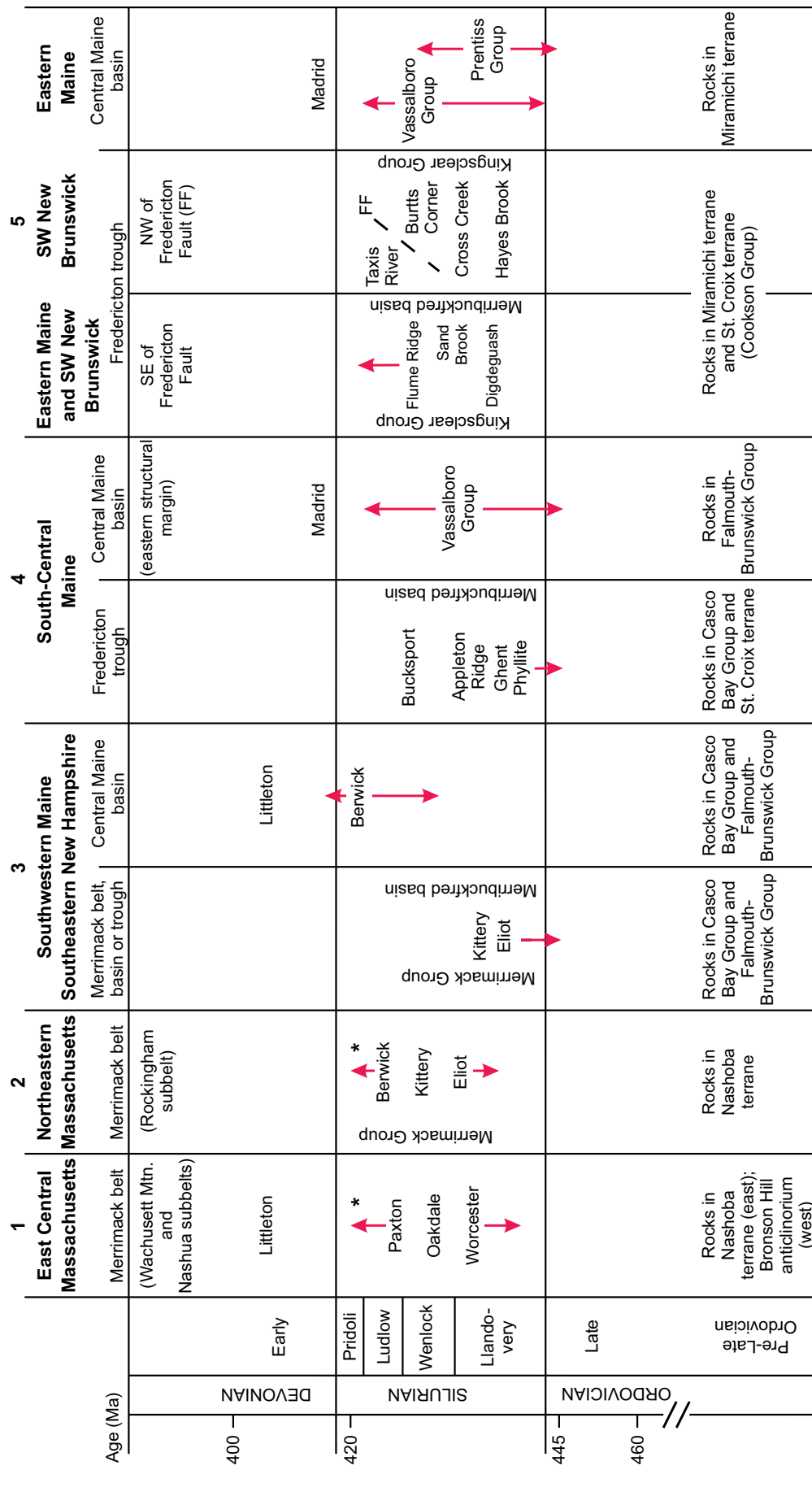


**Figure 3.** Simplified stratigraphy based on previous work for the Late Ordovician, Silurian and Early Devonian cover sequence units referred to in the text for rocks from Massachusetts to SW New Brunswick in the Merrimack belt, Merrimack basin, Fredericton trough and eastern portions of the Central Maine basin (see Figures 1 and 2 for locations). \*Exact ages and stratigraphic order of these units is not well defined in these areas. Merribuckfred basin from Hussey *et al.* (2010). Columns 1 and 2 after Zen *et al.* (1983) and Robinson and Goldsmith (1991). Subbelts after Robinson and Goldsmith (1991), see text and Figure 2. Column 3 after Hussey *et al.* (2010). Column 4 after Cartwright *et al.* (2019). Column 5 after Ludman *et al.* (2017, 2018), Dokken *et al.* (2018) and Cartwright *et al.* (2019).

more to a location than an age range and may include multiple basins deposited through time. We will use Merribuckfred basin as a general term for the Late Ordovician–Silurian basins east of the Miramichi terrane and its equivalents to the south, to differentiate them from the Central Maine basin on the west. We will use Fredericton trough and Merrimack basin when referring to deposits in specific locations (Figs. 1, 3).

The Central Maine basin continues southwest from eastern Maine and New Brunswick into southeastern New Hampshire (Fig. 1; Osberg *et al.* 1985; Zen *et al.* 1983; Lyons *et al.* 1997; Tucker *et al.* 2001; Hibbard *et al.* 2006; Wintsch *et al.* 2007; Hussey *et al.* 2010; Reusch and van Staal 2012). However, Ordovician and older rocks of the Miramichi terrane, Casco Bay Group or Falmouth-Brunswick Group are not present south of southwestern Maine, making the boundary between rocks in the Central Maine and Merribuckfred basins difficult to distinguish. In SE New Hampshire, Dorais *et al.* (2012) and Reusch and van Staal (2012) interpret these basins to be separated by the Ganderian Neoproterozoic Massabesic Gneiss Complex (Fig. 1). However, Hussey *et al.* (2010, 2016) separate these basins east of the Massabesic Gneiss Complex along the Nonesuch River fault in southwestern Maine and its continuation, the Calef fault, in New Hampshire (Fig. 1).

#### **Merrimack belt in Massachusetts and SE New Hampshire**

In Massachusetts, there is no clearly identified boundary between rocks correlative with those in the Merribuckfred or Central Maine basins. Therefore, Zen *et al.* (1983) and Robinson and Goldsmith (1991) included all the late Ordovician (?), Silurian and early Devonian metasedimentary rocks between Ordovician and older rocks in the Nashoba terrane to the east and the Bronson Hill anticlinorium to the west in the Merrimack belt (Figs. 1, 2). However, on some maps, the Central Maine basin continues south into Massachusetts between the Merrimack belt and the Bronson Hill anticlinorium (e.g., Hibbard *et al.* 2006; Rankin *et al.* 2007; Wintsch *et al.* 2007, 2014; Reusch and van Staal 2012; Kopera and Walsh 2014, Walsh *et al.* 2021). Here, we will follow the usage of Zen *et al.* (1983) and Robinson and Goldsmith (1991) and use the inclusive term Merrimack belt to include the Worcester, Oakdale, Paxton, Eliot, Kittery and Berwick formations (Figs. 2, 3) in Massachusetts and SE New Hampshire, but recognize that the Merrimack belt likely includes rocks that can be correlated with those in both the Merribuckfred and Central Maine basins (Tucker *et al.* 2001; Wintsch *et al.* 2007; Hussey *et al.* 2010). The Tower Hill Formation occurs along the Clinton-Newbury fault zone on the east side of the Merrimack belt in east-central Massachusetts (Fig. 2; Zen *et al.* 1983; Robinson and Goldsmith 1991). However, its placement within the Merrimack belt has been debated (see Robinson and Goldsmith 1991) and it will be considered separately below.

The Merrimack belt, excluding the Tower Hill Formation, generally consists of a thick succession of metamorphosed

calcareous and pelitic turbiditic units containing sandstone, siltstone, phyllite and impure quartzite (e.g., Grew 1973; Peck 1976; Robinson 1981; Zen *et al.* 1983; Robinson and Goldsmith 1991; Hussey and Bothner 1993; Lyons *et al.* 1997; Hussey *et al.* 2010). Because of (1) the lack of fossils, (2) the presence of thick successions of similar rock types in various areas, (3) a paucity of clear sedimentary structures to give facing directions, (4) varying degrees of metamorphism across and along strike, and (5) structural complexities due to several generations of folds, the internal stratigraphic order and along-strike correlations of units of the Merrimack belt has long been debated (e.g., Billings 1956, Robinson and Goldsmith 1991, Hussey *et al.* 2010). Robinson and Goldsmith (1991) presented a thorough discussion of the stratigraphic arguments for rocks in the Merrimack belt in central Massachusetts and Hussey *et al.* (2010) for SE New Hampshire. These are not repeated or further discussed here.

The Merrimack belt in Massachusetts is divided into six stratigraphic-tectonic subbelts by Robinson and Goldsmith (1991). Our samples are from the eastern three: the Wachusett Mountain, Nashua and Rockingham subbelts (Fig. 2). The Rockingham subbelt continues into SE New Hampshire and contains the Eliot, Kittery and Berwick formations of the original Merrimack Group (Hitchcock 1877; Katz 1917; Billings 1956; Lyons *et al.* 1997; Fargo and Bothner 1995; Hussey *et al.* 2010). The Tower Hill Formation is within Robinson and Goldsmith's (1991) Nashua subbelt, but occurs along the Clinton-Newbury fault zone adjacent to the contact with the Nashoba terrane and will be discussed separately.

The metamorphic grade of the sedimentary rocks of the Merrimack belt in central Massachusetts varies from lower greenschist facies in the southeast to upper amphibolite facies in the northwest (Thompson and Norton 1968; Zen *et al.* 1983; Goldsmith 1991b; Robinson and Goldsmith 1991; Lyons *et al.* 1997). The Merrimack belt has been intruded by a series of Silurian to Devonian granitic to dioritic plutons (Gore 1976; Zen *et al.* 1983; Zartman and Naylor 1984; Robinson and Goldsmith 1991; Wones and Goldsmith 1991; Zartman and Marvin 1991; Bothner *et al.* 1993, 2009; Fargo and Bothner 1995; Lyons *et al.* 1997; Watts *et al.* 2000; Wintsch *et al.* 2007; Walsh *et al.* 2013a, b, 2015, 2021; Charnock 2015) and is deformed by at least four generations of folds, including large recumbent folds (Peck 1975, 1976; Hepburn 1976; Robinson 1978, 1981; Goldstein 1992, 1994; Goldsmith 1991b; Hussey and Bothner 1993; Kopera and Walsh 2014; Kuiper *et al.* 2014). Deformation and metamorphism in the Merrimack belt resulted from Acadian, Neoacadian and/or Alleghanian events (Zen *et al.* 1983; Goldstein 1994; Attenoukon *et al.* 2006; Attenoukon 2009; Kuiper *et al.* 2014; Kopera and Walsh 2014).

#### **METHODS**

All samples were processed and minerals separated in

the mineral separation laboratory in the Department of Earth and Environmental Sciences at Boston College using standard mineral separation methods. Approximately 150 to 200 zircon grains per sample (if present) were selected by picking all grains from random splits and were then mounted in epoxy. All mounts were then polished with a Struers Labo-Pol 5 in order to expose the inner cores of the zircon grains. Zircon grains were imaged using back-scattered electron (BSE) and cathodoluminescence (CL) image analysis at either the Massachusetts Institute of Technology in Cambridge, Massachusetts, or at the Bruneau Centre for Research and Innovation at Memorial University in St. John's, Newfoundland, Canada. The carbon coating was removed by polishing and the surfaces of the grain mounts were cleaned with dilute nitric acid prior to further analysis.

U–Pb analysis was carried out using laser ablation inductively coupled plasma mass spectrometry (LA-ICPMS) on a Finnigan ELEMENT XR double focusing magnetic-sector field ICPMS connected to a Geolas 193 nm excimer laser at the INCO Innovation Centre at Memorial University in St. John's, Newfoundland (Bennett and Tubrett 2010). Zircon cores and occasionally rims were targeted, based on the CL and BSE images. A 10 µm laser beam was rastered over each selection and sampled a 40×40 µm square spot. For grains less than ~50 µm, or for small zones, the raster was set to 30×30 µm. Laser energy was set at 5 (for Nashoba terrane) or 6 (for Merrimack belt) J/cm<sup>3</sup>, the scan velocity was 10 µm/s, and the laser repetition was set at 8 Hz. Once material was ablated from each grain it was nebulized and introduced into the ELEMENT XR using a mixed Ar-He carrier gas (Bennett and Tubrett 2010). A standard tracer solution was also nebulized with the sample material and included a mixture of natural Tl ( $^{205}\text{Tl}/^{203}\text{Tl} = 2.3871$ ),  $^{209}\text{Bi}$ , and enriched  $^{233}\text{U}$ , and  $^{237}\text{Np}$  (ca. 1 ppb), in a Ar-He carrier gas, this was used to correct for instrumental mass bias (Košler *et al.* 2002).

Standards PL, 91500, and 02123 were used for reference and quality control purposes (Slama *et al.* 2008; Bennett and Tubrett 2010). Each of the three zircon standards were analyzed for every six unknowns. Measurements were taken for each grain using time-resolved data acquisitions that were roughly 120–205 seconds long. Prior to measurements taken of ablated material, data were acquired for the Ar-He gas and tracer solution for approximately 20–30 seconds (Bennett and Tubrett 2010). Elemental masses measured during the time-resolved measurements included: 204(Hg), 203(Tl), 205(Tl), 206(Pb), 207(Pb), 209(Bi), 232(Th), 233(U), 237(Np), 238(U), 249( $^{233}\text{U}$  $^{16}\text{O}$ ), 253( $^{237}\text{Np}$  $^{16}\text{O}$ ) and 254( $^{238}\text{U}$  $^{16}\text{O}$ ) (Bennett and Tubrett 2010). Data correction and reduction was carried out by Mike Tubrett and Wilfredo Diegor at Memorial University of Newfoundland. Raw data were corrected for dead time (20 ns) of the electron multiplier using the Excel spreadsheet-based program LAMdate (Košler *et al.* 2002, 2008). Data reduction included correction for gas blank, laser-induced elemental fractionation (cf. Sylvester and Ghaderi 1997), and instrument mass bias (cf. Horn *et al.* 2000; Košler *et al.* 2002). There was no common Pb correction. Ages of the unknowns were

calculated using LAMdate (Košler *et al.* 2002, 2008) with Isoplot v. 2.06 of Ludwig (1999).

Where possible, approximately 150–200 grains, mostly randomly selected, ensuring representation of various grain sizes and morphologies, were analyzed per sample to provide a strong statistical representation, following Vermeesch's (2004) recommendation that at least 117 grains must be analyzed to be sure that no fraction comprising more than .05 of the population is missed at the 95% confidence level. Concordia diagrams and relative probability plots were made using Isoplot v. 3.7 (Ludwig 2008). Data with a <0.05 probability of concordance, or with a 1σ error for  $^{206}\text{Pb}/^{238}\text{U}$  or  $^{207}\text{Pb}/^{206}\text{Pb}$  ages greater than 10% of the calculated age were excluded from further analysis. Zircon with Th/U ratios <0.1 were considered to have a metamorphic origin (Hoskin and Schaltegger 2003; Rubatto 2017; Yakymchuk *et al.* 2018). If concordant metamorphic grains were present that were older than the youngest igneous-detrital age populations (see below) they were included in the detrital zircon analysis as detrital zircon grains derived from a metamorphic source. The grains younger than the youngest igneous-detrital age populations (Nashoba terrane units only) are plotted and discussed separately. Zircon morphologies were analyzed using transmitted light, BSE and CL images, and compared with age populations. No clear relationships between ages and morphologies emerged. Details can be found in Loan (2011) and Sorota (2013).

Concordia age has recently become the recommended way to report detrital zircon data because it is a mathematical combination of multiple ratios and makes optimal use of all U/Pb and Pb/Pb ratios (Ludwig 1998; Pollock *et al.* 2009). However, we report  $^{206}\text{Pb}/^{238}\text{U}$  ages for zircon <800 Ma and  $^{207}\text{Pb}/^{206}\text{Pb}$  ages for zircon >800 Ma to be consistent with most previous U–Pb detrital zircon studies in the Appalachians. The difference between one method and the other is minimal for data in this study. Uncertainties are reported at the 1σ confidence level. Zircon grains with a probability of concordance less than 0.05, based on 2σ uncertainty, were considered discordant and not used for data interpretation (cf. Košler and Sylvester 2003).

The youngest age population for each sample was determined by taking the weighted average of the  $^{206}\text{Pb}/^{238}\text{U}$  ages for a population of the youngest 3–10 zircon grains with a >0.05 probability of concordance based on 2σ uncertainty. These analyses excluded overgrowths and had Th/U ratios >0.1, and therefore are unlikely to represent metamorphism. Youngest grains were selected to be re-analyzed using CA-TIMS at the Massachusetts Institute of Technology, to improve precision and avoid the effects of Pb-loss (Mattinson 2005; Condon and Bowring 2011). About 3 or 4 grains per sample were selected, but only 13 grains survived sample preparation including chemical annealing. A mixed  $^{205}\text{Pb}$ - $^{233}\text{U}$ - $^{235}\text{U}$  tracer solution (spike) was used. Details of zircon pretreatment, dissolution, and U and Pb chemical extraction procedures are described in Ramezani *et al.* (2007). U and Pb isotopic measurements were performed on a VG Sector-54 multicollector TIMS. Pb and U were loaded together

on a single Re filament in a silica gel–phosphoric acid mixture (Gerstenberger and Haase 1997). Pb isotopes were measured by peak-hopping using a single Daly photomultiplier detector, and U isotopic measurements were made in static mode using multiple Faraday collectors. Details of fractionation and blank corrections are given in Table 1. Data reduction, age calculation, and the generation of concordia plots were carried out using the method of McLean *et al.* (2011), and the statistical reduction and plotting program REDUX (Bowring *et al.* 2011).

## SAMPLE DESCRIPTIONS AND RESULTS

### Nashoba terrane

#### *Sample descriptions and LA-ICPMS detrital zircon results*

Sample locations and LA-ICPMS data are presented in Appendix Tables A1 and A2, respectively. Rock unit and sample descriptions, and data for detrital zircon based on the criteria outlined above are presented in this section (Fig. 4). Data from metamorphic zircon are discussed separately below.

The Marlboro Formation occurs in the southeastern Nashoba terrane (Fig. 2). It is composed largely of hornblende-plagioclase amphibolite, but it also contains felsic granofels, gneiss and metasedimentary rocks that commonly include rusty weathering sillimanite-bearing schist (Bell and Alvord 1976; DiNitto *et al.* 1984; Goldsmith 1991a; Kopera *et al.* 2006). The amphibolites include rocks with basaltic and basaltic-andesite compositions with inferred arc, MORB and alkalic signatures. Whole-rock major and trace-element geochemistry and Sm–Nd isotopes indicate that they formed in a primitive volcanic arc/back-arc setting (DiNitto *et al.* 1984, Goldsmith 1991a, Kay *et al.* 2017) with minimal crustal contamination (Kay *et al.* 2009, 2017; Walsh *et al.* 2015, 2021). This arc has been interpreted to be the source for the majority of the metasedimentary rocks in the Nashoba terrane (Hepburn and Munn 1984, Goldsmith 1991a, Kay *et al.* 2017).

Zircon in metasedimentary rocks of the Marlboro Formation is rare, and commonly metamict. In order to obtain enough grains for a statistical representation, the Marlboro Formation was sampled in four different locations (Fig. 2; Loan 2011). Of the approximately 150 kg of rock processed, a total of only 9 zircon grains yielded concordant data. The data were combined as one sample, MLMRC (Table A2). Sample MLMR1 is from a rusty weathering, black to dark-grey garnet-muscovite-biotite-quartz ( $\pm$  sillimanite) schist interlayered with a biotite-quartz-hornblende-plagioclase amphibolite. Garnet and sillimanite are present in thin layers within the schist and the unit is locally mylonitic. The sample was collected from the pelitic layers only and yielded four concordant analyses. Sample MLMR2 is from a silvery to dark-grey, rusty weathering, fine-grained garnet-biotite-muscovite-quartz schist. It resulted in one concordant anal-

ysis. Sample MLMR5 showed two distinct layers in hand specimen: (1) a muscovite-rich schistose layer and (2) a coarser-grained quartz-rich layer with larger, black, quartz crystals. Black quartz forms due to radiation damage (Klein and Hurlbut 1993). The radiation damage extended to the zircons, resulting in rusty, amorphous, highly metamict grains that gave no concordant data. Sample MLMR6 is from a rusty, heavily weathered garnet-bearing schist that yielded four concordant analyses.

The youngest detrital zircon analysis from the combined Marlboro Formation samples yielded a  $^{206}\text{Pb}/^{238}\text{U}$  age of  $470 \pm 46$  Ma. Sample MLMR6 contained the oldest grain found in the Nashoba terrane with a core of  $\sim 3.36$  Ga and a rim of  $\sim 2.58$  Ga. The relative probability plot of the Marlboro Formation shows a peak in age at  $\sim 532$  Ma and a minor peak at  $\sim 642$  Ma (Fig. 4a).

The Shawsheen Gneiss (Fig. 2) is separated from the Nashoba Formation by the Fish Brook Gneiss and the Assabet River fault zone (Zen *et al.* 1983; Goldsmith 1991a). It is generally quartz-plagioclase-muscovite-biotite schist to paragneiss, which is interpreted to have been derived from the detritus of volcanic rocks of intermediate to mafic composition (Olszewski 1980). Sample MLSG1 is a medium-grained garnet-plagioclase-muscovite-biotite-quartz ( $\pm$  sillimanite) schist to gneiss collected from multiple locations around an industrial park to ensure that a statistical representation of detrital zircon was analyzed.

The Shawsheen Gneiss was previously dated by Olszewski (1980) using U–Pb analyses of zircon on multiple-grain fractions. The resulting discordia chord yielded  $2042 \pm 52$  Ma upper and  $517 \pm 16$  Ma lower intercept ages, but because these are based on only three zircon fractions (Olszewski 1980), the interpretation may not be accurate. Sample MLSG1 yielded 100 concordant detrital zircon analyses. The weighted average  $^{206}\text{Pb}/^{238}\text{U}$  age of the three youngest detrital zircon analyses is  $470 \pm 22$  Ma (MSWD = 0.26). The main age population in the sample is  $\sim 562$  Ma, and a minor population exists at  $\sim 646$  Ma (Fig. 4b). In addition, there are small age clusters at  $\sim 2.1\text{--}2.0$  Ga,  $\sim 1.8\text{--}1.3$  Ga and  $\sim 1.1$  Ga, and a single grain at  $\sim 2.4$  Ga.

The Nashoba Formation occupies about one-third of the Nashoba terrane and is composed largely of biotite-feldspar gneiss and biotite  $\pm$  sillimanite schist with subordinate calc-silicate gneiss, impure feldspathic quartzite and pelitic schist (Bell and Alvord 1976; Zen *et al.* 1983; Hepburn and Munn 1984; Goldsmith 1991a). Hornblende amphibolite dominates the Boxford Member (Bell and Alvord 1976) along the eastern margin of the formation. The Nashoba Formation is metamorphosed in the sillimanite and sillimanite - K-feldspar zones. Samples of the gneiss, schist and calc-silicate gneiss were analyzed.

The Nashoba Formation gneiss (sample MLNB1; Fig. 2) is from a garnet-biotite-muscovite-plagioclase-quartz- ( $\pm$  sillimanite) gneiss. The unit contained interbedded layers of mylonitic gneiss with a few  $\sim 4$  cm thick strongly sheared quartz veins. Areas with large quartz inclusions were not used. The sample yielded 84 concordant detrital zircon analyses.

**Table 1.** CA-TIMS data with LA-ICPMS dates for comparison (see Appendix A2).

Fraction	Composition				Isotopic Ratios				Dates [Ma]				ICP Dates [Ma] $^{206}\text{Pb}/^{238}\text{U}$ [abs.]							
	Th/U	$\text{Pb}^{*}$ (b)	Pb†/	$^{206}\text{Pb}/^{207}\text{Pb}$	$^{206}\text{Pb}/^{235}\text{U}$ (i)	$\pm 2\sigma$	$^{206}\text{Pb}/^{238}\text{U}$ (f,g)	$\pm 2\sigma$	Corr. $^{206}\text{Pb}$ (f,g) coeff.	$^{206}\text{Pb}$ (f,g) [%]	$^{206}\text{Pb}/^{235}\text{U}$ (h) [%]	$\pm 2\sigma$	$^{207}\text{Pb}/^{235}\text{U}$ (h) [abs.]	$^{207}\text{Pb}/^{238}\text{U}$ [abs.]	$\pm 2\sigma$					
	(a) [pg]	Pbc (d)	$^{204}\text{Pb}$ (e)	$^{206}\text{Pb}$ / $^{204}\text{Pb}$ (e)	$^{206}\text{Pb}$ / $^{204}\text{Pb}$ (e)															
<b>Sample MLNB1 - Nashoba Formation Gneiss</b>																				
z002 (mr02a06)	0.34	1.5	196.07	12145.5	0.583	0.21	0.075	0.16	0.82	0.0565	0.12	465.9	0.7	466.5	0.8	469	3	480	13	mr02a06
<b>Sample KSKT1 - Kittry Formation</b>																				
z5 (mr18b11)	0.21	3.1	11	742	0.57	0.98	0.074	0.16	0.55	0.0562	0.9	461.31	0.71	461.1	3.6	460	20	410	10	mr18b11
z21 (mr18b19)	0.71	2.9	6	354	0.60	1.9	0.076	0.25	0.64	0.0568	1.7	473.40	1.10	475	7.1	482	38	417	16	mr18b19
z22 (mr17b32)	1.41	38.3	72	3538	0.53	0.32	0.070	0.11	0.52	0.0557	0.28	434.26	0.46	435	1.1	438.7	6.2	416	11	mr17b32
z50 (mr18a14)	0.85	3.5	8	480	0.53	1.2	0.069	0.16	0.58	0.0556	1.1	432.19	0.68	433	4.2	437	24	409	20	mr18a14
<b>Sample KSBW1 - Berwick Formation</b>																				
BE48 (mr04b29)	0.02	0.3	43.17	2934.1	0.651	0.35	0.078	0.10	0.12	0.0602	0.35	486.35	0.47	508.9	1.4	611	8	414	8	mr04b29
<b>Sample KSOK1 - Oakdale Formation</b>																				
I44 (mr16a24)	0.47	0.4	49.05	2944.1	0.544	0.39	0.070	0.10	0.38	0.0568	0.36	433.70	0.41	441.4	1.4	482	8	436	8	mr16a24
M21 (mr16b23)	0.64	0.5	33.93	1960.1	0.526	0.58	0.068	0.15	0.36	0.0559	0.54	425.53	0.64	429.2	2.0	449	12	409	17	mr16b23
M77 (mr16b112)	0.37	0.8	10.43	657.3	0.612	1.72	0.077	0.17	0.38	0.0576	1.66	478.68	0.78	484.9	6.6	514	36	432	19	mr16b112
<b>Sample KSPXII - Paxton Formation</b>																				
BE23 (se08b31)	1.03	0.4	12.05	645.4	0.552	1.90	0.071	0.37	0.35	0.0565	1.80	441.73	1.60	446.4	6.9	471	40	425	7	se08b31
BE34 (au26a47)	0.45	0.4	21.18	1290.6	0.531	0.88	0.069	0.20	0.13	0.0560	0.88	429.16	0.82	432.6	3.1	451	20	412	18	au26a47
<b>Sample KSWSI - Worcester Formation</b>																				
z23 (mr02a38)	0.32	0.6	46.93	2931.3	0.614	0.46	0.078	0.27	0.62	0.0572	0.36	483.52	1.25	486.1	1.8	498	8	454	9	mr02a38
z83 (mr02a117)	0.37	0.3	6.2	397.7	0.620	2.95	0.078	1.08	0.42	0.0574	2.69	486.29	5.04	490	11.5	507	59	436	17	mr02a117
Blank: $^{206}\text{Pb}/^{204}\text{Pb} = 18.15 \pm 0.48$ ; $^{207}\text{Pb}/^{204}\text{Pb} = 15.306 \pm 0.29$ ; $^{208}\text{Pb}/^{204}\text{Pb} = 37.11 \pm 0.88$ .																				
Mass fractionation correction of 0.25% /amu ± 0.02% /amu (atomic mass unit) was applied to all single collector Daly analyses.																				
(a) Th contents calculated from radiogenic $^{208}\text{Pb}$ and the $^{207}\text{Pb}$ / $^{206}\text{Pb}$ date of the sample, assuming concordance between U-Th and Pb systems.																				
(b) Total mass of radiogenic Pb.																				
(c) Total mass of common Pb.																				
(d) Ratio of radiogenic Pb (including $^{208}\text{Pb}$ ) to common Pb.																				
(e) Measured ratio corrected for fractionation and spike contribution only.																				
(f) Measured ratios corrected for fractionation, tracer, blank, common Pb is lab blank, U blank = 0.1 pg																				
(g) Corrected for Initial Th/U disequilibrium using radiogenic $^{208}\text{Pb}$ and Th/U [magma] = 2.8																				
(h) Isotopic dates calculated using the decay constants $\lambda_{38} = 1.55125\text{E-}10/\text{yr}$ , $\lambda235 = 9.8485\text{E-}10/\text{yr}$ (Jaffey et al. 1971), and for the $^{238}\text{U}/^{235}\text{U} = 137.818 \pm 0.045$ (Hiess et al., 2012)																				

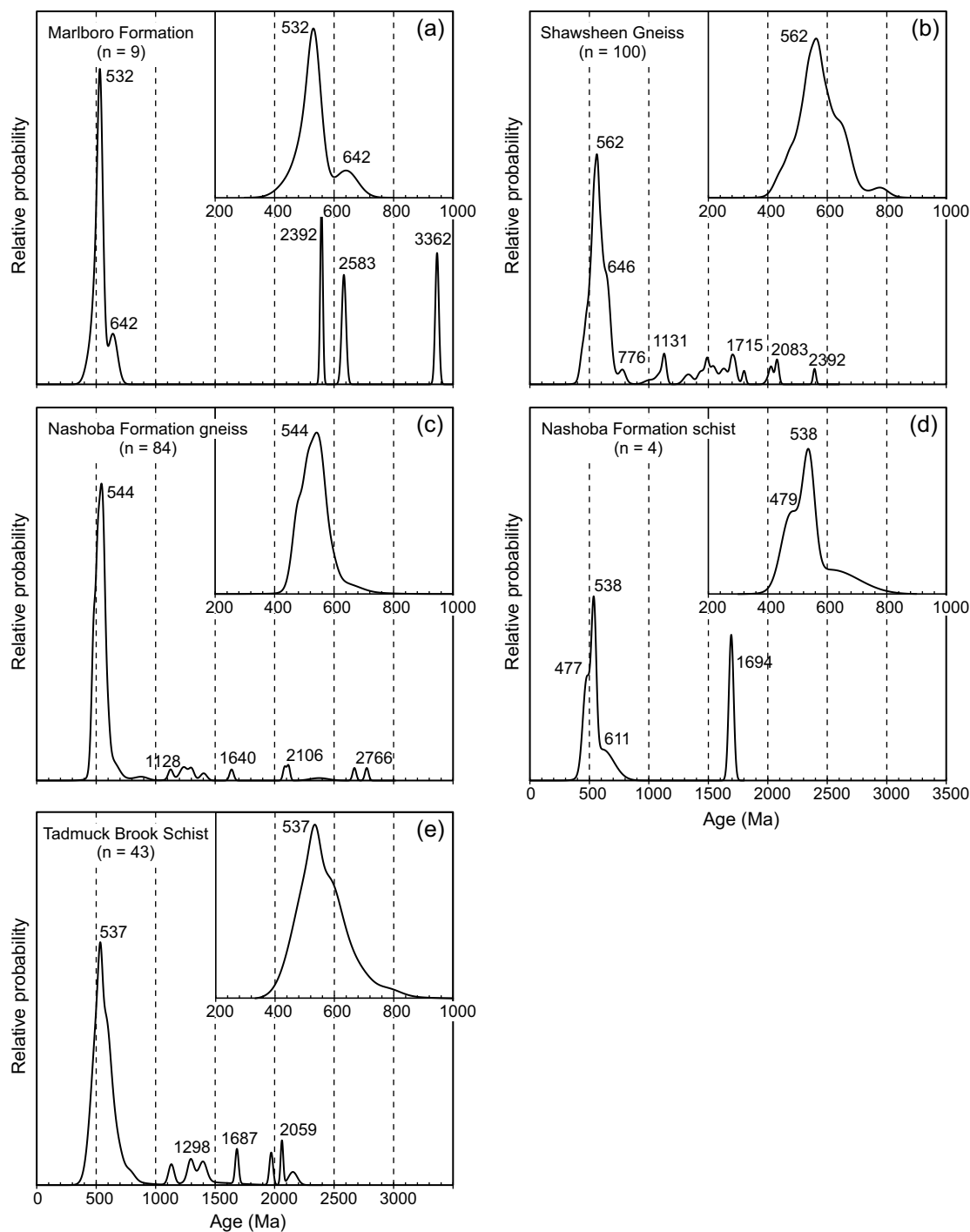


**Figure 4.** Relative probability plots for LA-ICPMS U-Pb detrital zircon data ( $^{206}\text{Pb}/^{238}\text{U}$  ages for zircon  $< 800$  Ma and  $^{207}\text{Pb}/^{206}\text{Pb}$  ages for zircon  $> 800$  Ma) for units of the Nashoba terrane. Inset figures show  $^{206}\text{Pb}/^{238}\text{U}$  ages for zircon  $< 800$  Ma only. Peaks determined using Isoplot. Data are shown in Table A2.

The three youngest grains yielded a weighted average  $^{206}\text{Pb}/^{238}\text{U}$  age of  $462 \pm 20$  Ma (MSWD = 0.061). The major age population is  $\sim 544$  Ma (Fig. 4c). In addition, there are a few  $\sim 2.8\text{--}2.6$  Ga,  $\sim 2.4$  Ga,  $\sim 2.1$  Ga,  $\sim 1.6$  Ga,  $\sim 1.4\text{--}1.1$  Ga zircons.

The Nashoba Formation schist (sample MLNS1; Fig. 2) is a garnet-muscovite-biotite-quartz- ( $\pm$  sillimanite) schist. Of the abundant schistose units in the Nashoba terrane this

sample was selected because of its minimal quartz vein inclusions. However, the sample yielded only 4 concordant detrital zircon analyses, the other 118 concordant analyses being interpreted as metamorphic (Fig. 4d). The youngest detrital zircon in the Nashoba Formation schist yielded a  $^{206}\text{Pb}/^{238}\text{U}$  age of  $477 \pm 32$  Ma. Two remaining detrital grains yielded  $^{206}\text{Pb}/^{238}\text{U}$  ages of  $538 \pm 20$  Ma,  $611 \pm 94$  Ma, and one a  $^{207}\text{Pb}/^{206}\text{Pb}$  age of  $1694 \pm 32$  Ma.

The Nashoba Formation calc-silicate gneiss outcrop (sample MLBM1; Fig. 2) includes rock types ranging from rusty garnet-bearing schist to calc-silicate gneiss and amphibolite. The calc-silicate gneiss sampled contains diopside, actinolite, phlogopitic biotite, and abundant titanite. It likely formed from original more dolomitic layers (Hepburn and Munn 1984). The unit is deformed by a shear zone separating the more calcareous layers of the outcrop from the schistose layers. Samples were taken away from the shear zone and included a mixture of calc-silicate rocks with and without the micaceous lenses. No detrital zircon was found and all zircon analyzed is interpreted to be of metamorphic or carbonate fluid/hydrothermal origin as discussed below.

The Tadmuck Brook Schist is a rusty-weathering micaeuous schist with thin quartzose layers that lies along the northwestern boundary of the Nashoba terrane (Fig. 2) adjacent to the Clinton-Newbury fault zone. The metamorphic grade increases from greenschist facies in the NW to upper amphibolite facies in the SE within the ~1 km thick unit (Jerden and Hepburn 1996; Jerden 1997). It has been uncertain whether the Tadmuck Brook Schist is part of the Nashoba terrane or of the Merrimack belt (Goldsmith 1991a). Sample (MLTMBC; Fig. 2) is from a sillimanite-bearing sulfidic mica schist in the high-grade (southeastern) member and contains thin quartz-rich layers. The Tadmuck Brook Schist has unique mineralogy as it is the only unit that contains scheelite, a fluorescent tungsten-bearing mineral that is commonly associated with high-temperature hydrothermal veins and contact metamorphism in skarns (Klein and Dutrow 2007). The unit also contains abundant titanite. This sample yielded 47 concordant detrital zircon analyses. Due to the small grain size, all the zircons in this sample were ablated using a  $30 \times 30 \mu\text{m}$  square raster, which led to increased uncertainty. The youngest three detrital zircon analyses yielded a weighted average of  $^{206}\text{Pb}/^{238}\text{U}$  ages of  $462 \pm 47 \text{ Ma}$  (MSWD = 0.049). The sample had a major ~537 Ma age peak, and scattered ~2.2–1.9 Ga, ~1.7 Ga and ~1.4–1.1 Ga ages (Fig. 4e).

#### CA-TIMS zircon analysis

Youngest zircon grains of selected samples were re-dated using CA-TIMS methods (Table 1) with the purpose to better constrain the maximum depositional age of the formations. While three or four grains per sample were selected for analysis, not all survived sample preparation and chemical abrasion. Only one grain remained from the Nashoba terrane, sample MLNB1 from the Nashoba Formation gneiss. Its  $^{206}\text{Pb}/^{238}\text{U}$  CA-TIMS age is  $465.9 \pm 0.7 \text{ Ma}$ , which is within error of the weighted average of  $^{206}\text{Pb}/^{238}\text{U}$  LA-ICPMS ages of  $462 \pm 20 \text{ Ma}$  for the three youngest grains from this sample (Table A2; see above).

#### Metamorphic zircon

Nashoba terrane samples from the five formations other than the calc-silicate gneiss contained 159 zircons inter-

preted as metamorphic per the criteria listed above (Fig. 5). They range from ~454 Ma to 324 Ma, with the results for the individual formations as follows: Marlboro Formation, ~443–324 Ma (weighted average of  $^{206}\text{Pb}/^{238}\text{U}$  ages of  $396 \pm 20 \text{ Ma}$ , n = 10, MSWD = 1.6); Shawsheen Gneiss, 422 ± 19 Ma (n = 5, MSWD = 0.27); Nashoba Formation gneiss ~454–353 Ma (or weighted average age of  $408 \pm 13 \text{ Ma}$ , n = 22, MSWD = 5.6); Nashoba Formation schist ~433–327 Ma (or weighted average age of  $377.2 \pm 4.4 \text{ Ma}$ , n = 118, MSWD = 1.9); and Tadmuck Brook Schist  $433 \pm 33 \text{ Ma}$  (n = 4, MSWD = 0.031) (cf. Table A2).

The calc-silicate gneiss (MLMB1) yielded 61  $^{206}\text{Pb}/^{238}\text{U}$  zircon ages of ~434–310 Ma (or weighted average age of  $354.4 \pm 5.9 \text{ Ma}$ , n = 61, MSWD = 2.2; Fig. 5f). Fifty-three of these zircon analyses gave Th/U ratios <0.20, with only one Th/U ratio below 0.10, and 9 analyses gave ratios of 0.20–0.37. These Th/U ratios are higher than the typical <0.1 ratio for metamorphic zircon (Rubatto 2017; Yakymchuk *et al.* 2018). The calc-silicate gneiss is within the stratified succession of the Nashoba terrane, is gradational with the rest of the Nashoba Formation and is similarly metamorphosed under upper amphibolite facies conditions. There is no field evidence to suggest that it is much younger than the other Nashoba terrane rocks. Furthermore, while Th/U ratios >0.1 are not typical for metamorphic zircon, they are not uncommon (Rubatto 2017; Yakymchuk *et al.* 2018). Yakymchuk *et al.* (2018) conclude that “igneous zircon rarely has Th/U < 0.1 and metamorphic zircon can have values ranging from <0.01 to >10.” For these reasons, the ages of zircons in the calc-silicate gneiss are interpreted as metamorphic, likely having formed in the presence of fluids.

Thus, we interpret metamorphic zircon in the Nashoba terrane to have grown between ~433 Ma and ~356 Ma, based on the weighted averages of  $^{206}\text{Pb}/^{238}\text{U}$  ages. The Marlboro Formation, Shawsheen Gneiss, Nashoba Formation Gneiss and Tadmuck Brook Schist generally record older metamorphic zircon ages (weighted average age of  $408.0 \pm 8.8 \text{ Ma}$ , n = 41, MSWD = 3.5) while zircon growth continued until somewhat later in the Nashoba Formation schist and especially the calc-silicate gneiss (weighted combined average age of  $368.4 \pm 4.0 \text{ Ma}$ , n = 180, MSWD = 3.8).

#### Merrimack belt

##### Sample descriptions and LA-ICPMS detrital zircon

The six formations analyzed from the Merrimack belt are presented below in a general NE to SW order (Fig. 2). The Eliot Formation consists of thinly layered grey to green phyllite, calcareous feldspathic metasiltstone and quartzite, quartz-mica schist, and calc-silicate gneiss (Lyons *et al.* 1997; Hussey *et al.* 2010, 2016). It has been interpreted as Silurian–Ordovician based on correlation with parts of the Casco Bay Group in Maine (Hussey *et al.* 2010). Sample KSELI from SE New Hampshire (Fig. 2) consists of generally thin-bedded alternations of tan-grey weathering, turbiditic calcareous quartzite and silvery dark phyllite (Fargo and

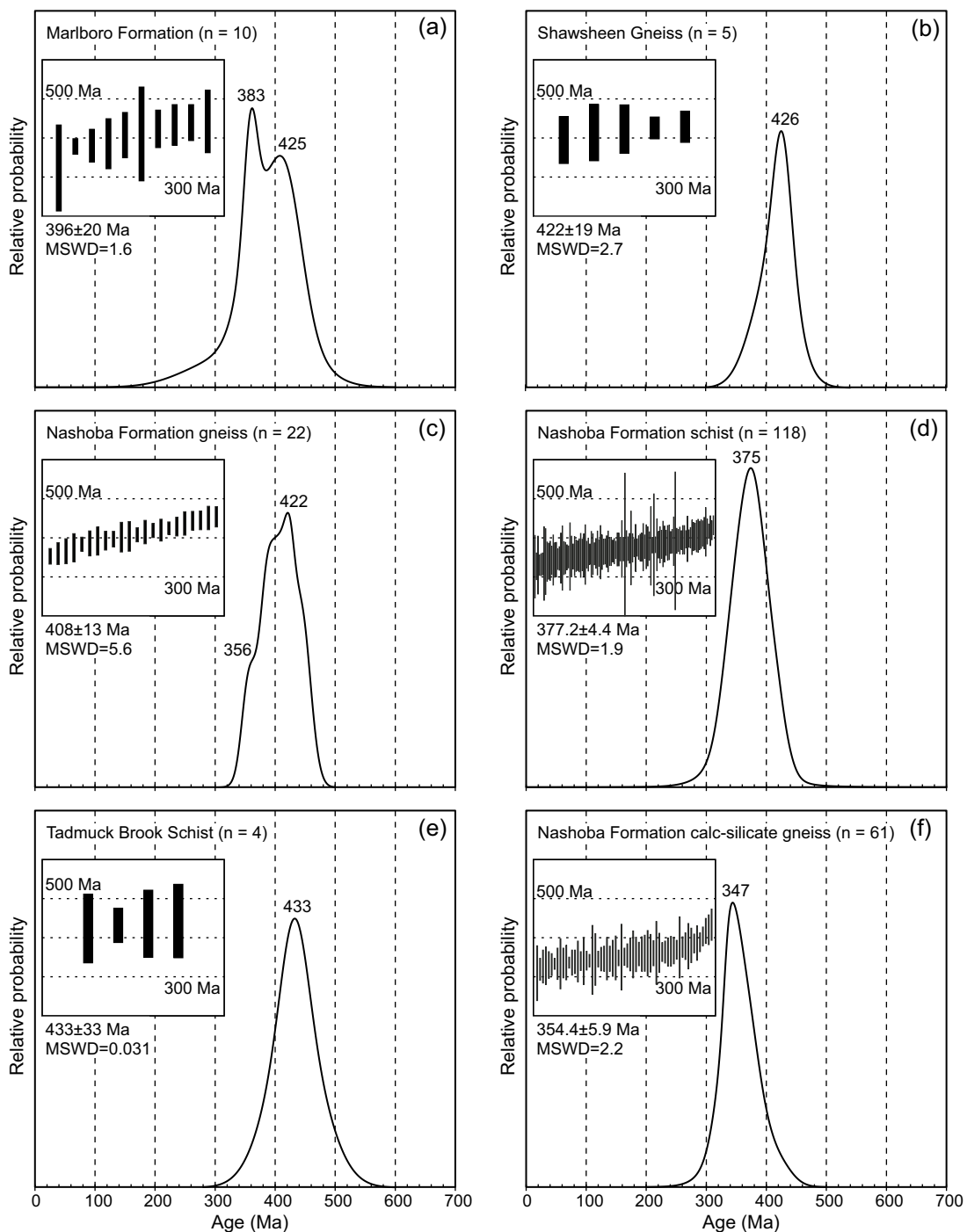


**Figure 5.** Relative probability plots for  $^{206}\text{Pb}/^{238}\text{U}$  ages of metamorphic zircon for units of the Nashoba terrane. Inset figures show float bar charts and weighted averages of  $^{206}\text{Pb}/^{238}\text{U}$  ages with  $2\sigma$  uncertainties. Data are shown in Table A2.

Bothner 1995). Quartz veins were avoided during sample collection and removed prior to crushing. The sample yielded 119 concordant analyses. The weighted average of the  $^{206}\text{Pb}/^{238}\text{U}$  ages of the four youngest detrital zircon grains is  $409 \pm 19$  Ma (MSWD = 0.046). The major population peaks at  $\sim 446$  Ma (Fig. 6a). Two grains are  $\sim 2.9$  Ga and  $\sim 2.7$  Ga and other ages spread between  $\sim 1.9$  Ga and  $\sim 512$  Ma.

The Kittery Formation consists of feldspathic and carbonaceous, ankeritic metaturbidite successions and minor fine-

grained metasiltstone and feldspathic quartzite (Robinson and Goldsmith 1991; Bothner and Hussey 1999; Hussey *et al.* 1984, 2010, 2016). The fine-grained, thinly bedded to laminated rocks and thicker quartzitic beds contain cross lamination and other primary sedimentary structures (Hussey *et al.* 1984, 2010, 2016). Several paleocurrent indicators in the Kittery Formation in New Hampshire suggest a source to the southeast (Rickerich 1983, 1984; Hussey *et al.* 1984). Sample KSKTI (Fig. 2) was taken from an outcrop

in SE New Hampshire, immediately across the Piscataqua River from the type locality in Maine (Katz 1917; Bothner and Hussey 1999) and is a tan weathering, grey to purplish, massive, fine-grained, feldspathic quartzite and quartzitic phyllite. It yielded 101 concordant analyses. The weighted average of  $^{206}\text{Pb}/^{238}\text{U}$  ages of the four youngest detrital zircon grains is  $413 \pm 13$  Ma (MSWD = 0.089). The main age group is  $\sim 461$  Ma, and older populations are  $\sim 2.8$  Ga,  $\sim 1.8\text{--}1.0$  Ga, and  $\sim 769$  and 543 Ma (Fig. 6b).

The Berwick Formation is composed primarily of thin to thick tabular and lenticular beds of calcareous metasiltstone, biotite-rich metasiltstone, purplish biotite-quartz-feldspar granofels, and fine-grained metasandstone (Robinson and Goldsmith 1991; Fargo and Bothner 1995; Hussey *et al.* 2016). Some layers contain actinolite were metamorphosed to the greenschist facies, while at higher metamorphic grade, diopside, hornblende, and plagioclase are common (Robinson and Goldsmith 1991). Most of the Berwick Formation is in the garnet zone, although portions reach the sillimanite zone (Zen *et al.* 1983; Robinson and Goldsmith 1991; Hussey *et al.* 2016). Sample KSBWI, taken from NE Massachusetts (Fig. 2) consists of a fine-grained, light-grey to purplish-grey calcareous metasiltstone with beds a few cm to 1 m thick and interbeds of a dark-grey micaceous phyllite. It yielded 133 concordant analyses. The five youngest zircon grains provided a weighted average of  $^{206}\text{Pb}/^{238}\text{U}$  ages of  $409 \pm 12$  Ma (MSWD = 0.27). Zircon yielded a main age peak at 443 Ma, a few analyses at  $\sim 2.8\text{--}2.7$  Ga and  $\sim 2.3$  Ga and small populations between  $\sim 1.8$  Ga and  $\sim 1.0$  Ga and at  $\sim 634$  Ma (Fig. 6d).

The Oakdale Formation is a thick unit composed of inter-layered brownish-grey to light-grey ankeritic metasiltstone, green-grey to purplish-grey impure quartzite, muscovite schist, and greenish-grey, grey, and dark brown calcareous phyllite (Grew 1973; Hepburn 1976; Peck 1976; Zen *et al.* 1983; Robinson and Goldsmith 1991). Sample KSOKI (Fig. 2) is from the type area in east-central Massachusetts (Emerson 1917; Hepburn 1976; Robinson and Goldsmith 1991) and consists of a grey weathering, light-grey quartz-rich phyllite and micaceous phyllite, interbedded with tan to grey-green weathering beds of metasiltstone and impure quartzite. It yielded 108 concordant zircon analyses. The youngest detrital zircon age population of the four youngest grains is  $431 \pm 12$  Ma (weighted average  $^{206}\text{Pb}/^{238}\text{U}$  age, MSWD = 0.69) and the main age peak is  $\sim 451$  Ma (Fig. 6c). One analysis is  $\sim 2.7$  Ga, and other ages show a continuous spread between  $\sim 2.0$  Ga and the main age population.

The Worcester Formation, also called Worcester Phyllite, is a turbidite succession composed of grey and dark-grey carbonaceous slate, well foliated micaceous phyllite or schist containing andalusite, including chiastolite, interbedded with layers a few centimetres to one metre thick of impure quartzite, calc-silicate or metasiltstone (Grew 1973; Hepburn 1976; Peck 1976; Robinson and Goldsmith 1991). Sample KSWSI (Fig. 2) was taken largely from turbiditic sandy layers in a grey-weathering, light-grey, fine-grained turbidite with fissile phyllite interlayered with metasand-

stone and siltstone layers that range from a few cm to  $\sim 0.5$  m thick. The sample yielded 138 concordant analyses. The weighted average of  $^{206}\text{Pb}/^{238}\text{U}$  ages of the four youngest grains is  $436 \pm 9$  Ma (MSWD = 0.89). The main age group is  $\sim 470$  Ma. One grain is  $\sim 2.2$  Ga, and other populations are between  $\sim 2.0$  Ga and  $\sim 950$  Ma, and  $\sim 800\text{--}470$  Ma (Fig. 6e).

The Paxton Formation contains several sub-lithologies (Robinson and Goldsmith 1991). In the area of our study it is composed predominantly of grey-weathering, slabby, quartz-plagioclase-biotite granofels and well-layered purplish biotite granofels with calcic plagioclase (Robinson *et al.* 1982; Robinson and Goldsmith 1991). Sample KSPXIII from east-central Massachusetts (Fig. 2), is composed of a greenschist grade (garnet zone or lower at the locality sampled) laminated, slabby, quartz-rich, purple-grey granofels to schist. It yielded 113 concordant analyses. The youngest detrital zircon age population for the Paxton Formation is  $426 \pm 6$  Ma (MSWD = 0.56) based on the weighted average of the  $^{206}\text{Pb}/^{238}\text{U}$  ages of the ten youngest grains. The main peak is  $\sim 463$  Ma with a smaller peak at  $\sim 431$  Ma. Two analyses are  $\sim 2.6$  Ga and most other analyses are between  $\sim 1.8\text{--}0.9$  Ga with a few grains between  $\sim 700$  and  $\sim 528$  Ma (Fig. 6f).

### CA-TIMS zircon analyses

Youngest zircon grains of selected samples from the Merrimack belt were re-dated using CA-TIMS methods (Table 1; Fig. 7), but as with the Nashoba terrane samples above, not all survived the processing. All CA-TIMS data for the Merrimack belt were within error of, or older (some much older, see below) than the LA-ICPMS data (Tables 1, A2). The youngest CA-TIMS  $^{206}\text{Pb}/^{238}\text{U}$  ages from five grains from the Kittery, Paxton and Oakdale formations ranged from 434 Ma to 425 Ma.

### Tower Hill Formation

The Tower Hill Formation is a relatively thin unit (up to  $\sim 130$  m thick) along the Clinton-Newbury fault zone (Fig. 2). It is light-grey to buff and consists of massive orthoquartzite beds and subordinate dark-grey phyllite or mica-schist containing biotite, and locally garnet porphyroblasts (Grew 1970, 1973; Peck 1976; Hepburn 1976). However, in places it includes successions of phyllite reaching 65 m in thickness (Robinson and Goldsmith 1991). It is located along the Clinton-Newbury fault and its position in the stratigraphy and potential affinity with the Merrimack belt or Nashoba terrane are unclear (see Robinson and Goldsmith 1991). At the location of sample KSTHI (Fig. 2) in Berlin, Massachusetts it consists of fine-grained, light to dark-grey, massive quartzite. The youngest detrital zircon age population within the 106 concordant analyses is  $513 \pm 15$  Ma (MSWD = 1.01) based on the weighted average of  $^{206}\text{Pb}/^{238}\text{U}$  ages of three grains. One analysis (mr12a30) yielded a  $^{206}\text{Pb}/^{238}\text{U}$  age of  $463 \pm 9$  Ma but is not part of a population. The main population is  $\sim 630$  Ma with a satellite peak at  $\sim 530$  Ma and

a continuum of ages exists from there tapering off to ~1.8 Ga (Fig. 6g). Three grains are ~2.9 Ga and ~2.1 Ga.

## DISCUSSION

### Nashoba terrane

#### *Age of deposition*

Based on the LA-ICPMS results, the youngest detrital zircon population of all samples of the Nashoba terrane combined is  $466 \pm 13$  Ma (MSWD = 0.12, n = 11). Given this, and taking the errors into account, the maximum ages of the Nashoba terrane metasedimentary rocks could range from Early to Late Ordovician. If the higher precision but single CA-TIMS age of  $465.9 \pm 0.7$  Ma (Table 1; Fig. 7) on grain mr02a06 of the Nashoba Formation gneiss (LA-ICPMS age of  $480 \pm 13$  Ma) is representative, portions of the Nashoba Formation could have a maximum depositional age of early Middle Ordovician. Similar results were reported by Walsh *et al.* (2021) for two samples from the Nashoba Formation in southern Massachusetts and its correlative in Connecticut, the Tatnic Hill Formation, where detrital zircons gave an age of deposition between the ~485 Ma age of the youngest detrital zircon, and the ~435 Ma age of metamorphism. Because the 515 Ma granitic Grafton Gneiss cuts some of the mafic metaigneous rocks of the Marlboro Formation, and a ~500 Ma feldspathic granofels structurally overlies these (Walsh *et al.* 2009, 2011a, b, 2021), at least part of the Marlboro Formation is late Cambrian or older. The scarcity of detrital zircon in the metasedimentary rocks of the Marlboro Formation may indicate that they are primarily derived from the local, largely mafic, volcanic rocks of the Marlboro Formation. Thus, at least parts of the Marlboro Formation, and likely portions of the other Nashoba terrane units, are Cambrian, while other units, or parts of them, are Ordovician or younger.

The Assabet River fault zone (Fig. 2) is a major fault zone within the Nashoba terrane, separating the Nashoba Formation and Tadmuck Brook Schist to the northwest from the Shawsheen Gneiss and Marlboro Formation to the southeast (Bell and Alvord 1976; Hepburn and DiNitto 1978; Zen *et al.* 1983; Goldsmith 1991a, b; Kopera *et al.* 2006). To determine the significance of this fault zone, samples from the northwestern and southeastern Nashoba terrane were plotted separately in Figs. 8a and b. Samples from both sides show very similar patterns with a significant ~560–540 Ma detrital zircon age population and minor Mesoproterozoic and Paleoproterozoic populations. Archean grains are rare in both. The similarity of these data indicates that there is no significant difference in detrital age populations across the

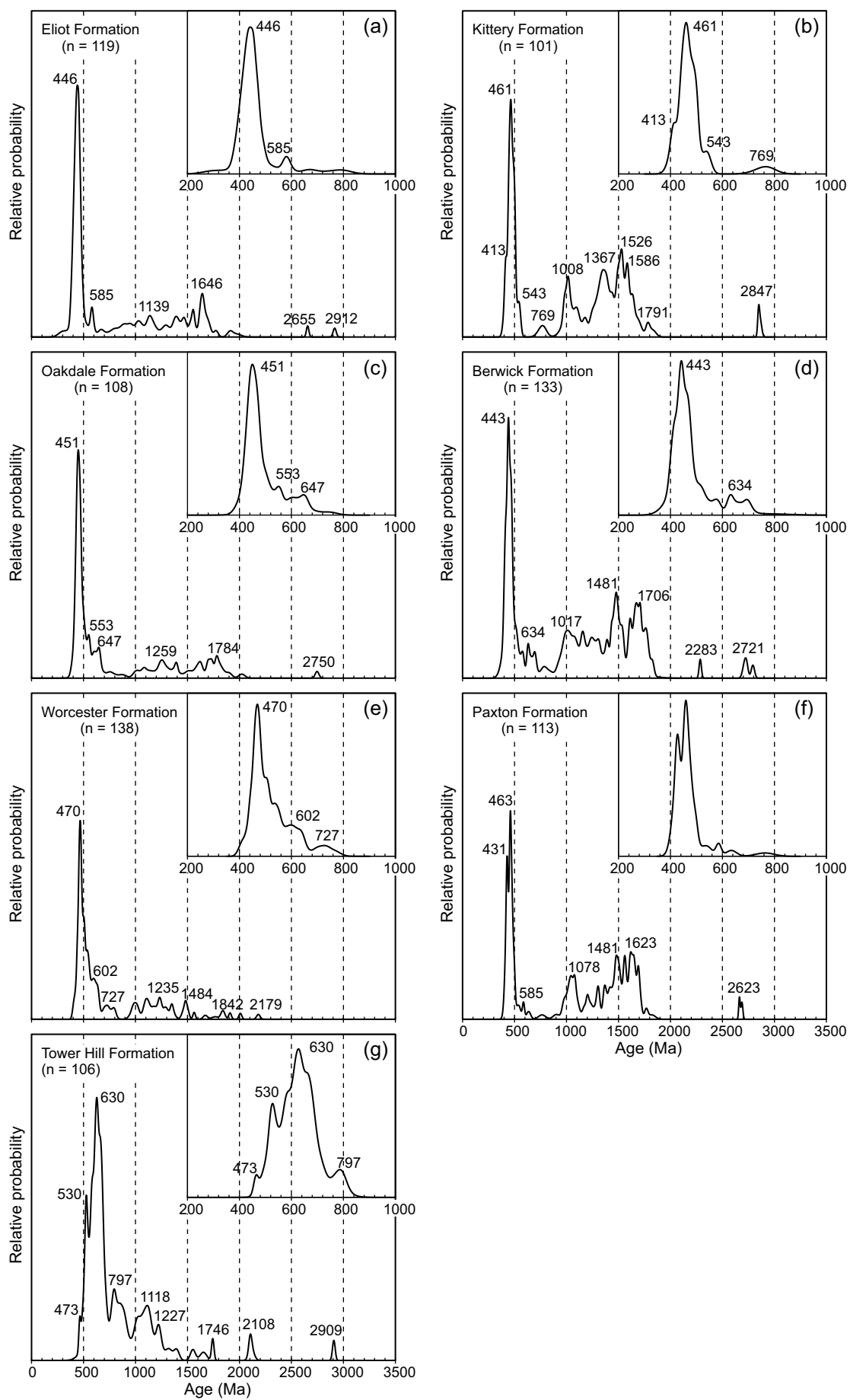
Assabet River fault zone and that it thus does not represent a terrane boundary. The combined Nashoba terrane data are plotted in Fig. 8c. The similarity of the detrital zircon age distribution in the Tadmuck Brook schist (Fig. 4e) to that of the other units of the Nashoba terrane, and its difference from the distributions in the Merrimack belt (Figs. 6, 8f) indicates that it is part of the Nashoba terrane.

#### *Provenance and correlations*

The Nashoba terrane has been interpreted as a primitive arc/back-arc complex (Hepburn *et al.* 1995; Kay *et al.* 2009, 2011, 2017; Walsh *et al.* 2011b, 2015, 2021). Archean and Proterozoic detrital zircon and Mesoproterozoic depleted mantle Sm/Nd model ages (Kay *et al.* 2017) suggest that this complex formed on older crustal material. Paleoproterozoic and Mesoproterozoic detrital zircon in the metasedimentary rock samples support this, and similar youngest zircon age populations and provenance in all four units of the Nashoba terrane indicate that they all formed as part of the same early Paleozoic arc/back-arc complex.

Both Avalonia and at least part of Ganderia experienced active ~650–590 Ma magmatism (e.g., Murphy *et al.* 2004; Fyffe *et al.* 2009; Satkoski *et al.* 2010; Thompson *et al.* 1996, 2007, 2010; Pollock *et al.* 2009; van Staal *et al.* 2009, 2020; Barr *et al.* 2012, 2019). For Ganderia, this abundant arc magmatism continued until the Cambrian, whereas in Avalonia it ceased or greatly decreased by ~565 Ma as Avalonia became a stable platform (Barr *et al.* 2003a; Murphy *et al.* 2004; Samson *et al.* 2005; Rogers *et al.* 2006; Hibbard *et al.* 2007; van Staal *et al.* 2009, 2020; van Staal and Barr 2012). Detrital zircon age populations from the metasedimentary units of the Nashoba terrane are generally consistent with those from the Ediacaran–early Silurian Ganderian rocks from Newfoundland, New Brunswick and east-central Maine (Fig. 9b; e.g., White and Barr 1996; Barr *et al.* 2003b, 2019; Valverde-Vaquero *et al.* 2006b, Pollock *et al.* 2007, 2009; Schulz *et al.* 2008; Fyffe *et al.* 2009; Ludman *et al.* 2018). The large ~540 Ma detrital zircon age population in all units, and the smaller ~640 Ma age population with minor Mesoproterozoic and Paleoproterozoic populations suggest a Ganderian affinity (Barr *et al.* 2014; Rogers *et al.* 2006; Fyffe *et al.* 2009; Pollock *et al.* 2007, 2009). It is less consistent with Avalonia, which is characterized by a large ~640 Ma population and a smaller ~540 Ma population (Fig. 9c; cf. Keppie *et al.* 1998; Thompson and Bowring 2000; Barr *et al.* 2003b, 2012; Murphy *et al.* 2004; Pollock *et al.* 2009; Satkoski *et al.* 2010; Thompson *et al.* 2014). Strongly negative  $\epsilon_{\text{Nd}}(500)$  values and Paleoproterozoic model ages for the metasedimentary rocks in the Nashoba terrane (Kay *et al.* 2017) are also characteristic for Ganderian sedimentary rocks (Samson *et al.* 2000; Schofield and D'Lemos 2000;

**Figure 6. (next page)** Relative probability plots for LA-ICPMS U–Pb detrital zircon data for units of the Merrimack belt and Tower Hill Formation. Main figures show  $^{206}\text{Pb}/^{238}\text{U}$  ages for zircon <800 Ma and  $^{207}\text{Pb}/^{206}\text{Pb}$  ages for zircon >800 Ma, and inset figures show  $^{206}\text{Pb}/^{238}\text{U}$  ages for zircon <800 Ma only. Data are shown in Table A2.



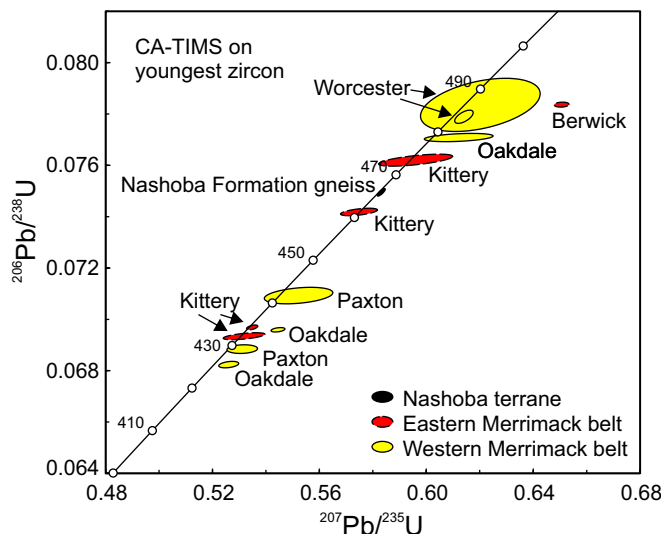


**Figure 7.** U-Pb CA-TIMS data for youngest zircon grains of the Nashoba Formation gneiss of the Nashoba terrane and for various units of the Merrimack belt. Data are shown in Table 1.

Rogers *et al.* 2006; Pollock *et al.* 2012) and not for typical Avalonian crust (Nance and Murphy 1996; Barr *et al.* 1998; Hibbard *et al.* 2007; Thompson *et al.* 2012). We therefore interpret the Nashoba terrane as having Ganderian affinity.

Ganderia is interpreted to have formed along the Iapetus ocean-facing Amazonian margin of Gondwana in the Neo-proterozoic and rifted away in the middle Cambrian, opening the Rheic ocean behind it (Figs. 10a, b) (e.g., van Staal *et al.* 1996, 2009, 2012, 2020; Fyffe *et al.* 2009, 2011; Schulz *et al.* 2008; Pollock *et al.* 2012; Barr *et al.* 2014; van Staal and Barr 2012; Willner *et al.* 2014). Prior to rifting a ~550–528 Ma extensive arc complex developed on the Ganderian margin (Fyffe *et al.* 2011; van Staal and Barr 2012). It formed the basement to the ~515–485 Ma Penobscot arc/back-arc complex that developed on the leading edge of Ganderia as it moved into the Iapetus ocean (Fig. 10b) (Valverde-Vaquero *et al.* 2006a; Rogers *et al.* 2006; Murphy *et al.* 2006; van Staal *et al.* 2009; Fyffe *et al.* 2009, 2011; Zagorevski *et al.* 2007a, b, 2010; van Staal and Barr 2012). At ~486–478 Ma, the Penobscot arc and back-arc fragments consolidated outboard of Laurentia during the Penobscot orogeny (Fig. 10c) (Zagorevski *et al.* 2007b, 2010; van Staal *et al.* 2009; Johnson *et al.* 2009, 2012; van Staal and Barr 2012). Penobscot arc/back-arc rocks are found, south of Newfoundland, in the Brookville, New River and Annidale belts in New Brunswick, the Bras d'Or belt in Cape Breton Island, and the Ellsworth Formation and St. Croix terrane in eastern Maine and share many characteristics with the Nashoba terrane (White *et al.* 1994; Barr *et al.* 1998; Schulz *et al.* 2008; Johnson *et al.* 2009, 2012; Fyffe *et al.* 2011; van Staal and Barr 2012).

Shortly after the Penobscot orogeny, a second expansive arc/back-arc complex (Popelogan-Victoria cycle) formed from ~478–453 Ma on the remnants of the now consolidated Penobscot arc/back-arc deposits (Fig. 10d) (e.g., van

Staal 1994; van Staal *et al.* 1998, 2016; Zagorevski *et al.* 2010; van Staal and Barr 2012; Wilson *et al.* 2017) and opened up the expansive Tetagouche and Exploits back-arc basins in Atlantic Canada – New England and in Newfoundland, respectively. These basins divided the Ganderian terrane into a separate active leading margin and a passive trailing margin (where the Nashoba terrane is located). The leading margin collided with Laurentia at about 455–450 Ma (Taconic phase 3 orogeny of van Staal *et al.* 2009). During the next ~20–25 myr the Tetagouche-Exploits basin gradually closed by west-directed subduction under Laurentia (Salinic orogenic cycle) (Figs. 10e, f) until the trailing margin of Ganderia collided with Laurentia in the terminal 426–420 Ma Salinic orogeny (Fig. 10g) (e.g., van Staal *et al.* 1998, 2003, 2008, 2012, 2016; Valverde-Vaquero *et al.* 2006a; Zagorevski *et al.* 2008; Fyffe *et al.* 2011; Zagorevski and van Staal 2011; van Staal and Barr 2012).

In the Nashoba terrane, igneous rocks of the ~540–500 Ma Marlboro Formation, the 515 Ma Grafton Gneiss and the 499 Ma Fish Brook Gneiss (Hepburn *et al.* 1995; Acaster and Bickford 1999; Walsh *et al.* 2011a, 2015, 2021) originated during the time of formation of the Cambrian Penobscot arc/back-arc complex (Figs. 10a, b) or its Ediacaran–Cambrian basement. An abundance of detrital zircon of that age in metasedimentary units of the Nashoba terrane reflects internal sources within the Penobscot arc/back-arc complex and its basement. Older zircon grains in the Nashoba terrane were eroded into the sedimentary basins from either Gondwanan (Amazonian) sources prior to the Cambrian rifting and drifting of Ganderia, or originated from reworked basement rocks beneath the Nashoba terrane. Such Proterozoic basement is exposed beneath Penobscot-cycle Ganderian rocks in the Brookville and New River terranes and on Grand Manan Island in New Brunswick (Johnson *et al.* 2009, 2012; Fyffe *et al.* 2009, 2011; Pollock *et al.* 2012; van Staal and Barr 2012; Fyffe 2014; Barr *et al.* 2019), the Bras d'Or terrane in Cape Breton Island (Barr *et al.* 1998; van Staal and Barr 2012) and the Islesboro block in coastal Maine (Reusch *et al.* 2018, 2021). The combined LA-ICPMS youngest detrital zircon age population of all samples from the Nashoba terrane ( $466 \pm 13$  Ma) and the single CA-TIMS age ( $465.9 \pm 0.7$  Ma) suggest that Ordovician metasedimentary rocks also exist in the terrane and may have formed during the Popelogan tectonic cycle (Fig. 10d).

### Metamorphic zircon

The Nashoba terrane contains abundant metamorphic zircon grains. These show a significant spread of weighted average ages between ~433 Ma and ~356 Ma (Fig. 5) and primarily indicate zircon growth during the Acadian orogeny. Younger zircon ages, while showing scatter and large uncertainties, likely reflect growth and/or recrystallization that extended into the Neoacadian and Alleghanian orogenies. Metamorphic zircon formed prior to ~425 Ma may have originated during the earlier Salinic orogeny. Our ages are consistent with published ages of metamorphism in the

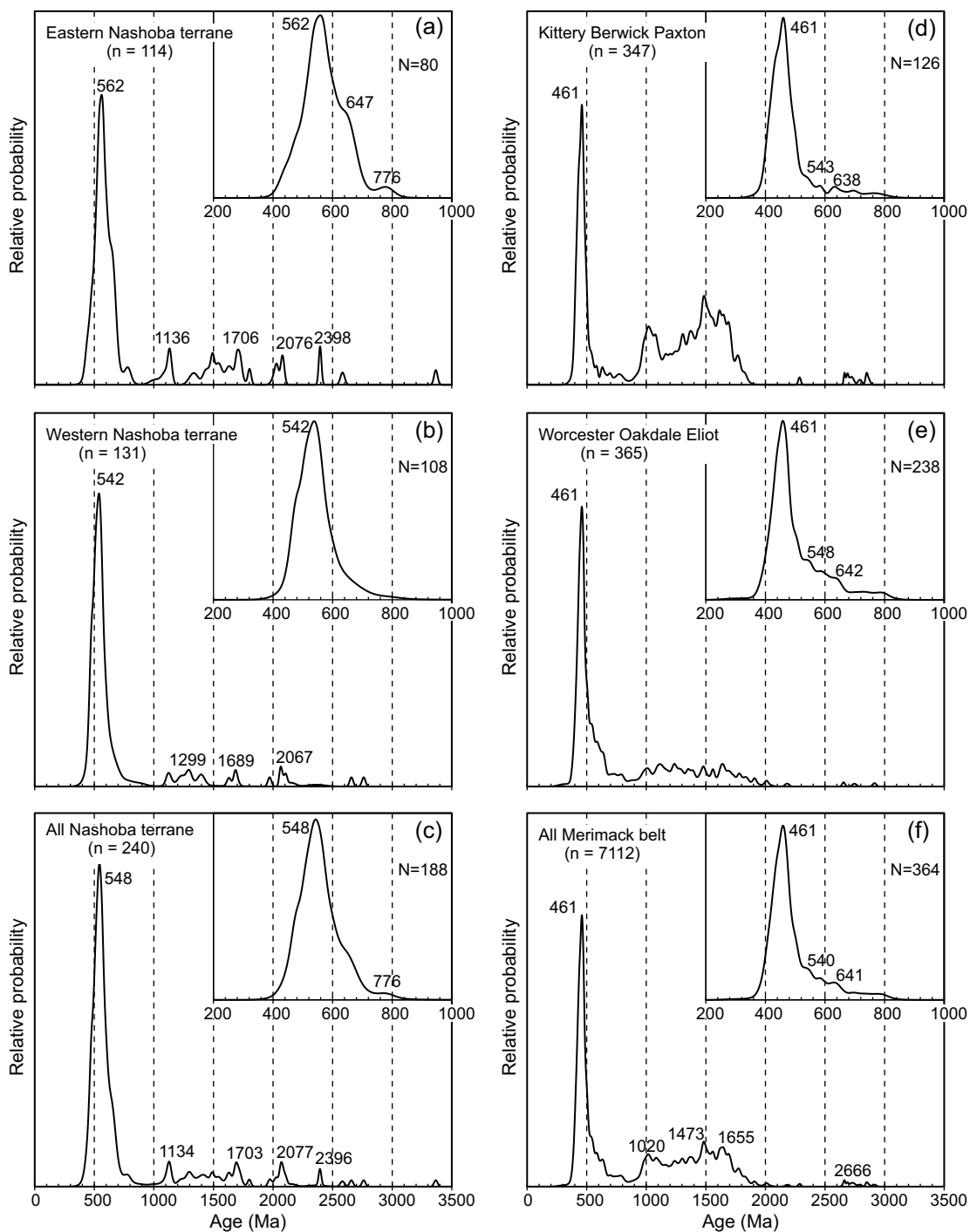


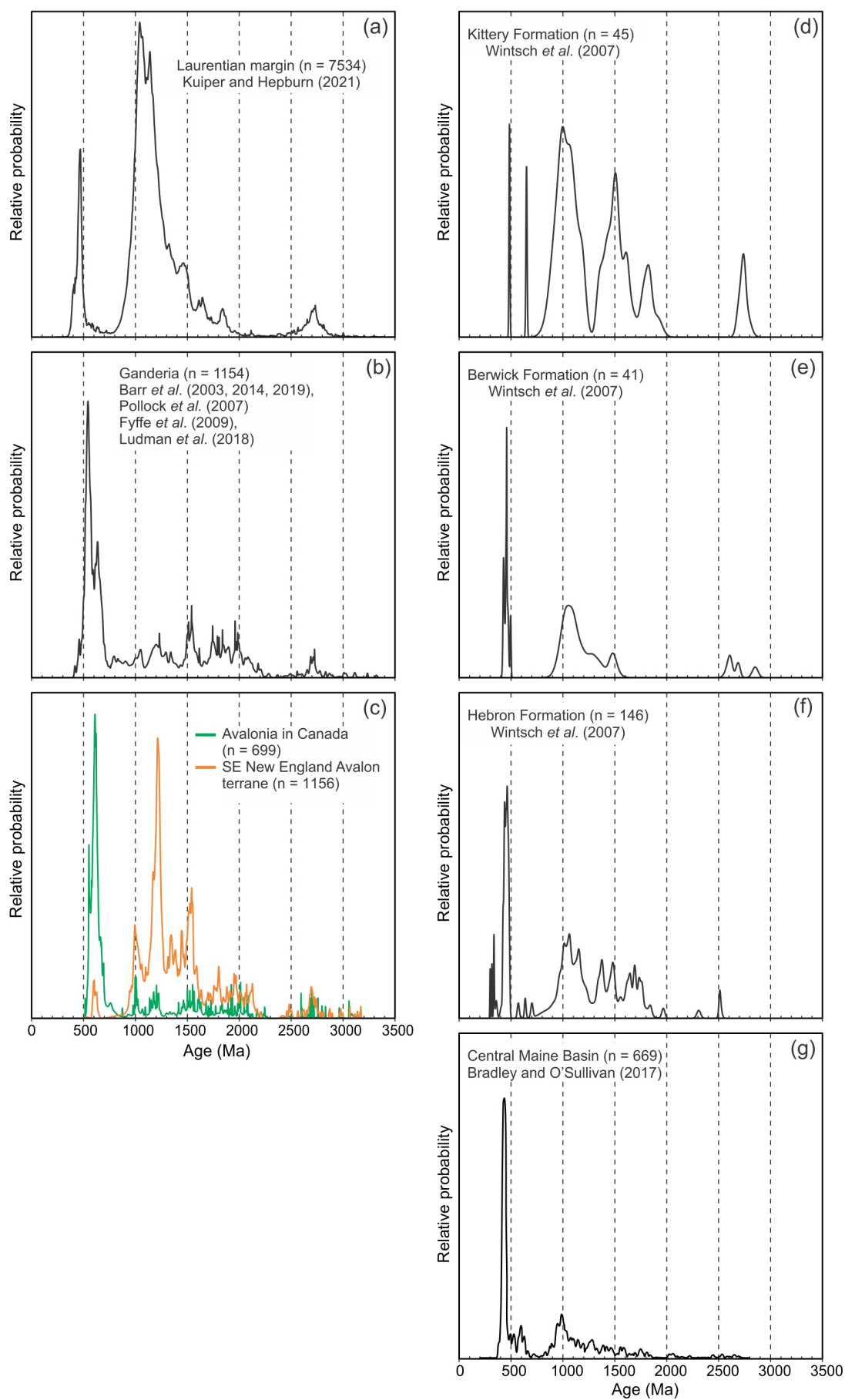
**Figure 8.** Relative probability plots for LA-ICPMS U-Pb detrital zircon data for the eastern, western and all Nashoba terrane (a-c), (d) combined Kittery, Berwick and Paxton formations, (e) combined Worcester, Oakdale and Eliot formations, (f) combined all Merrimack belt. See figures 4 and 6 for data for individual units and further explanation.

Nashoba terrane using various methods (Hepburn *et al.* 1995; Wintsch *et al.* 2007; Stroud *et al.* 2009; Walsh *et al.* 2013a, 2015, 2021; Buchanan *et al.* 2016a, b; Severson 2020). Because the precision of our ages is not higher than those reported previously, and because of consistency between the various data sets, we will not discuss the ages of metamorphism further.

#### Tower Hill Formation

##### Age of deposition and correlations

The youngest LA-ICPMS detrital zircon age population in the Tower Hill Formation is  $513 \pm 15$  Ma (3 grains), considerably older than any of the six formations sampled from the Merrimack belt (Figs. 6, 8f). A single grain from this unit



(not included in the grouping at 513 Ma) has a LA-ICPMS  $^{206}\text{Pb}/^{238}\text{U}$  age of  $463 \pm 9$  Ma, which is within error of the youngest age population of the Nashoba terrane. However, the  $\sim 513$  Ma population is older than any youngest populations in the metasedimentary rocks of the Nashoba terrane and other aspects of the zircon population in the Tower Hill Formation, such as the 630 Ma main age peak, are different from any of the other samples (Figs. 4, 8c). Of particular interest is the  $\sim 950$ – $750$  Ma age population that is not characteristic for known Avalonian or Ganderian rocks.

The  $513 \pm 15$  Ma youngest age population of the Tower Hill Formation is similar to the maximum ages of deposition for Cambrian rocks found in several Ganderian terranes in New England and New Brunswick. These include the Ellsworth Formation of the Ellsworth terrane, the Calais Formation of the St. Croix terrane, and the Baskahegan Lake Formation of the Miramichi terrane (Fyffe *et al.* 2009). However, these formations do not show a large peak at  $\sim 630$  Ma. Basement rocks (Martinon Fm.) below the Ganderian Brookville terrane and on Grand Manan Island in New Brunswick (Flagg Cove and Long Pond Bay Formations, Fyffe *et al.* 2009; Fyffe 2014; Barr *et al.* 2019) do show a Neoproterozoic peak of approximately this age. Rocks with both Cambrian youngest detrital zircon age populations and  $\sim 630$  Ma peaks occur in some samples in the Moretown, Albee and Dead River formations of the Moretown terrane in western Massachusetts, Vermont, New Hampshire and western Maine (Karabinos *et al.* 2017) and the Ganderian Kedears Hill greywacke of North Islesboro, Maine (Reusch *et al.* 2018, 2021). However, because none of their detrital zircon signatures is similar to the Tower Hill formation, no specific correlations can be made. The detrital zircon ages do indicate that the Tower Hill Formation is not a part of the Merrimack belt stratigraphy and that the boundary between the Nashoba terrane and Merrimack belt is complex and likely incorporates exotic fault-bounded slices.

### Merrimack belt

#### *Age of deposition*

The LA-ICPMS youngest detrital zircon populations for individual formations of the Merrimack belt in southeastern New Hampshire and Massachusetts range between  $436 \pm 9$  Ma (Worcester Formation) and  $409 \pm 12$  Ma (Berwick Formation). The CA-TIMS  $^{206}\text{Pb}/^{238}\text{U}$  ages for the five youngest detrital zircon grains from the Merrimack belt samples are between 434 and 425 Ma. Three CA-TIMS ages from the Merrimack belt are within error of LA-ICPMS analyses that were used as part of the youngest populations (Tables 1,

A2). These include two grains from the Oakdale Formation (mr16b23, LA-ICPMS:  $409 \pm 17$  Ma, CA-TIMS:  $425.53 \pm 0.64$  Ma and mr16a24 LA-ICPMS:  $436 \pm 8$  Ma, CA-TIMS:  $433.70 \pm 0.41$  Ma respectively) and grain au26a47 of the Paxton Formation (LA-ICPMS:  $412 \pm 18$  Ma, CA-TIMS:  $429.16 \pm 0.82$  Ma). The remainder of the CA-TIMS ages on grains from the youngest groups of zircons are older than the LA-ICPMS ages, up to  $\sim 30$  myr for a grain from the Worcester Formation with a CA-TIMS age of 486 Ma (Table 1). This may reflect either unaccounted for Pb-loss in the LA-ICPMS analyses or the presence of older cores that survived chemical abrasion better than overgrowths prior to analysis. These older CA-TIMS ages are not interpreted as reflecting the ages of the youngest zircon populations.

The CA-TIMS ages for the three youngest detrital zircons in the Oakdale and Paxton formations (434–426 Ma) are consistent with the  $429 \pm 5$  Ma LA-ICPMS youngest detrital zircon age population ( $\text{MSWD} = 0.82$ ,  $n = 18$ ) for the three formations in the central Massachusetts portion of the belt (Worcester, Oakdale, and Paxton formations). The Worcester Formation is intruded by a  $424 \pm 3$  Ma phase of the Ayer granodiorite at Eddy Pond, near Auburn, Massachusetts (U–Pb secondary ion mass spectrometry (SIMS) zircon data; Walsh *et al.* 2013a; Walsh and Merschat 2015), and the Oakdale Formation is intruded by the  $420.1 \pm 0.1$  Ma Clinton facies of the Ayer granodiorite (U–Pb CA-TIMS zircon data; Charnock 2015). Therefore, the ages of these two formations are constrained between  $\sim 434$  Ma and  $\sim 420$  Ma (late Llandovery to Pridoli).

The combined youngest detrital zircon age population for the Kittery, Eliot and Berwick formations in the northeastern part of the sample area is  $411 \pm 8$  Ma ( $\text{MSWD} = 0.14$ ,  $n = 13$ ). The LA-ICPMS weighted average of  $^{206}\text{Pb}/^{238}\text{U}$  ages of the four youngest detrital zircon grains from the Eliot Formation is  $409 \pm 19$  ( $\text{MSWD} = 0.046$ ), of the four youngest grains from the Kittery Formation is  $413 \pm 13$  Ma ( $\text{MSWD} = 0.089$ ), and of the five youngest detrital zircon grains from the Berwick Formation is  $409 \pm 12$  Ma ( $\text{MSWD} = 0.27$ ). Two grains from the Kittery Formation youngest population yielded CA-TIMS ages of 432 Ma and 434 Ma (Table 1). The previously folded and regionally metamorphosed Kittery and Eliot formations are intruded in SE New Hampshire by the  $418 \pm 1$  Ma Newburyport quartz diorite and the  $407.4 \pm 0.5$  Ma Exeter diorite (U–Pb ID-TIMS and CA-TIMS zircon data; Bothner *et al.* 1993, 2009; Hussey and Bothner 1993; Fargo and Bothner 1995; Wintsch *et al.* 2007). The Berwick Formation was intruded by the  $407 \pm 4$  Ma Devens Long Pond facies of the Aver Granite in Westford, Massachusetts (U–Pb SHRIMP, Walsh *et al.* 2013b, 2021). This indicates that at least the Kittery and Eliot formations must be older

**Figure 9.** (previous page) Relative probability plots for (a) Laurentia, (b) Ganderia, (c) Avalonia, compiled by Severson *et al.* (in press), from Keppie *et al.* (1998); Barr *et al.* (2003b); Murphy *et al.* (2004); Hepburn *et al.* (2008); Pollock *et al.* (2009); Satkoski *et al.* (2010); Thompson *et al.* (2012); Willner *et al.* (2013); Henderson *et al.* (2016); Barr *et al.* (2019); Kuijper *et al.* (in press). (d, e, f) Kittery Berwick and Hebron formations of Wintsch *et al.* (2007), and (g) the Central Maine basin of Bradley and O’Sullivan (2017).

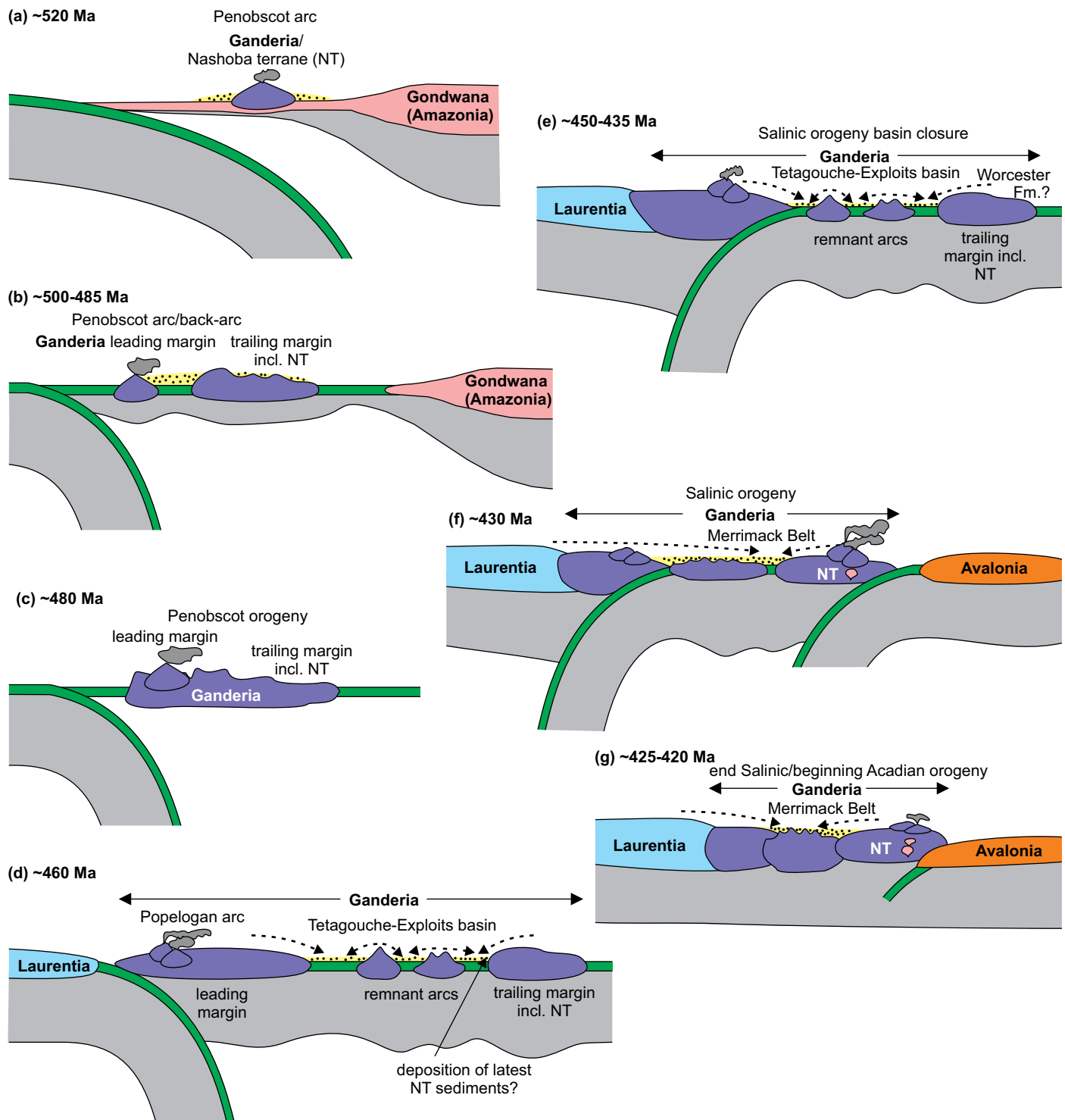


**Figure 10.** Simplified schematic diagrams showing the suggested development of the Nashoba terrane and Merrimack belt through time. Variation and movement of terranes along strike is not represented. Dashed arrows indicate sedimentary source areas.

than 418 Ma and that the LA-ICPMS youngest average detrital zircon age for these formations is inconsistently young.

Based on the LA-ICPMS and CA-TIMS data and the dated intrusive rocks, the Merrimack belt units in Massachusetts and SE NH are interpreted to have been deposited

between ~434 Ma and ~420 Ma. However, since the Berwick and Paxton formations are not intruded by any pre-407 Ma dated igneous rocks in the area their minimum age limit is not well constrained, and they could be somewhat younger.

### *Correlations and changes in provenance through time*

In Massachusetts and SE New Hampshire, the Merrimack belt rocks have ages of deposition between ~434 and ~420 Ma, large Middle to Late Ordovician zircon populations, smaller ~500–800 Ma populations, significant Mesoproterozoic populations, and scattered Archean grains. The Mesoproterozoic populations are much more prominent in the Kittery, Berwick and Paxton formations than in the Eliot, Oakdale, and Worcester formations (Figs. 6, 8d, e). While both Laurentia and Gondwana are potential viable sources for Mesoproterozoic zircon (e.g., Murphy *et al.* 2004; Fyffe *et al.* 2009; Pollock *et al.* 2009; Barr *et al.* 2019; Figs. 9a, b), Laurentia is a better source for ~1.2–1.0 Ga zircon (e.g., Cawood and Nemchin 2001; Hibbard *et al.* 2007; Waldron *et al.* 2014, 2018; Dokken *et al.* 2018; Severson 2020; Kuiper and Hepburn 2021). Furthermore, ~2.2–2.0 Ga zircons are largely absent in Laurentia, while Gondwana provides some zircon of this age, and Neoproterozoic zircon is characteristic for Gondwana, but not for Laurentia (Figs. 9a, b; Pollock *et al.* 2007; Waldron *et al.* 2009, 2014; Severson 2020). In the Merrimack belt samples the detrital zircon signatures of the Kittery, Berwick and Paxton formations show a Mesoproterozoic population, including a prominent 1.2–1.0 Ga population, no ~2.2–2.0 Ga grains and minor Neoproterozoic zircon, indicating evidence of Laurentian input. In contrast, the Eliot, Oakdale, and Worcester formations have a much smaller Mesoproterozoic population, three ~2.2–2.0 Ga grains and abundant Neoproterozoic zircon (Figs. 6, 8d, e), indicating Gondwanan but not Laurentian input.

In south-central Maine, Cartwright *et al.* (2019) concluded that detrital zircon in the older rocks of the Fredericton trough (Llandovery Appleton Ridge Formation and Ghent Phyllite; Figs. 1, 3) have a Gondwanan source and no evidence of Laurentian sediment input, similar to the Llandovery Digdeguash Formation of the Kingsclear Group, southeast of the Fredericton fault (northern extent of the Norumbega fault system; Fig. 1) in southern New Brunswick (Dokken *et al.* 2018). However, the overlying Wenlock–Ludlow Flume Ridge Formation in the eastern Fredericton trough in New Brunswick and the Llandovery Hayes Brook and Wenlock–Ludlow Burts Corner formations northwest of the Fredericton fault contain detrital zircon with Mesoproterozoic Laurentian input (Dokken *et al.* 2018). Likewise, rocks deposited in the Central Maine basin (Vassalboro Group) contain mixed Gondwanan and Laurentian detrital zircon signatures with Mesoproterozoic Laurentian input to its eastern structural margin in central Maine (Cartwright *et al.* 2019). Thus, rocks that contain a Laurentian detrital zircon signature were either deposited in a more westerly location, i.e., in the Central Maine basin or western portion of the Fredericton trough, or else are younger deposits in the eastern Fredericton trough.

In the Merrimack belt in Massachusetts and SE New Hampshire the Worcester, Oakdale and Eliot formations, with minor Laurentian Mesoproterozoic detrital zircon likely correlate with the early Silurian deposits in the Frederic-

ton trough in Maine and New Brunswick. The mixed detrital zircon source of the Kittery Formation with the presence of Laurentian detrital Mesoproterozoic input is consistent with the younger Silurian rocks in the Fredericton trough in New Brunswick (Dokken 2018) and the interpretation of Hussey *et al.* (2010) and Wintsch *et al.* (2007) that it represents the youngest deposit in the Merrimack Group in SE Maine and New Hampshire. The Paxton and Berwick formations (Figs. 6d, f) also have mixed Gondwanan and Laurentian detrital zircon signatures. Hussey *et al.* (2010, 2016; cf. Wintsch *et al.* 2007) place the Berwick Formation stratigraphically above the Kittery and Eliot formations in SE Maine and New Hampshire and interpret it as part of the Central Maine basin. The similar lithologies of the Paxton and Berwick formations, their similar detrital zircon signatures including Laurentian 1.2–1.0 detrital zircons, and the fact that neither is known to be crosscut by late Silurian–Early Devonian plutons support their potential correlation (Robinson and Goldsmith 1991). Thus, the Paxton and Berwick formations are interpreted to be the youngest rocks of those sampled in the Merrimack belt in SE New Hampshire and Massachusetts, consistent with interpretations by Hussey *et al.* (2010, 2016; cf. Wintsch *et al.* 2007) and further suggesting that the Paxton Formation was likely deposited in the Central Maine basin or its equivalent in Massachusetts.

Dokken *et al.* (2018) and Cartwright *et al.* (2019) propose that Laurentian detrital material only reached the eastern Fredericton trough by the middle Silurian and that a barrier existed between Laurentian margin and Gondwanan sources prior to this time (see also Ludman *et al.* 2018). A similar barrier may have existed during the deposition of the Worcester, Oakdale and Eliot formations, which was not present during deposition of the Kittery, Paxton and Berwick formations.

Our detrital zircon age populations for the Kittery and Berwick formations are generally similar to those based on the SHRIMP U–Pb analysis of Wintsch *et al.* (2007; Figs. 9d, e). Although minor differences exist in the sizes of the populations, these may be a result of differences in the number of analyses. Wintsch *et al.* (2007) correlated the Berwick Formation in Maine with the Hebron Formation in Connecticut. The Hebron Formation has a zircon age distribution (Fig. 9f) similar to the Berwick Formation, although the Hebron Formation contains a relatively larger ~1.2–1.0 Ga Laurentian population. This may be a result of local provenance differences, e.g., a higher local input from a Grenville source. Alternatively, it may indicate that the Hebron Formation, where sampled, is somewhat younger than the Berwick Formation, resulting in an increased Laurentian signal. The similarity of the detrital zircon distributions in the Berwick, Paxton and Hebron formations to those of samples from the Central Maine basin (Fig. 9g; Bradley and O’Sullivan 2017) indicate that they all were likely deposited in the Central Maine basin or its equivalent in Massachusetts and Connecticut.

### Potential source areas and tectonic synthesis

The Merrimack belt in Massachusetts and SE New Hampshire, the Merribuckfred basin and eastern portion of the Central Maine basin in Maine and New Brunswick all show a mix of Gondwanan and Laurentian sources. Here we briefly summarize the spatial and temporal differences in sources for the Merribuckfred and Central Maine basins, from north to south, so as to better identify the sources for Merrimack belt. Ludman *et al.* (2018, 2019) interpret the rocks in the Fredericton trough in eastern Maine to have originated largely from Gondwanan sources, either from emergent basement highlands underlain by Ganderian rocks such as in the Miramichi terrane, or by Wenlock–Ludlow time, from arc sources to the east as Avalonia approached and docked with the trailing edge of Ganderia. Such arc sources are present in the Coastal Volcanic belt in eastern Maine and the Kingston belt in New Brunswick (Fig. 1; Gates and Moench 1981; Seaman *et al.* 1999, 2019; Barr *et al.* 2002; Van Wagoner *et al.* 2002; Piñán-Llamas and Hepburn 2013; Ludman *et al.* 2017, 2018). In southern coastal Maine, Hussey *et al.* (2010) interpreted the Llandovery Bucksport and Appleton Ridge formations in the Fredericton trough to have Gondwanan sources and to have been deposited between a western Ganderian Ordovician arc (present in the Casco Bay and Falmouth-Brunswick Groups; Fig. 1) and the eastern trailing margin of Ganderia. Similarly, late Ordovician (?) to early Silurian deposits in the eastern Fredericton trough in New Brunswick (Dokken *et al.* 2018) and in south-central Maine (Cartwright *et al.* 2019) show only Gondwanan sources. However, younger deposits in the Kingsclear Group in the eastern Fredericton trough in southern New Brunswick and those in the western Fredericton trough (Fig. 3) include Laurentian detrital zircon material (Dokken *et al.* 2018).

The majority of the zircon in the Merrimack belt in Massachusetts and SE New Hampshire (Figs. 6, 8f) has Gondwanan affinity and most formed during the ~478–453 Ma Popelogan-Victoria volcanic arc/back-arc cycle that included the opening of the broad Tetagouche-Exploits back-arc basin (Fig. 10d; e.g., Valverde-Vaquero *et al.* 2006a; Fyffe *et al.* 2009; Johnson *et al.* 2009; Zagorevski *et al.* 2007a, 2010; van Staal and Barr 2012; Wilson *et al.* 2015; van Staal *et al.* 2016). Input of zircons into the Merrimack belt during the existence of the Tetagouche-Exploits back-arc basin likely came from erosion of emergent local highlands underlain by Ganderian Ordovician rocks, such as in the Miramichi and St. Croix terranes in eastern Maine and New Brunswick (Fig. 10e; Fyffe 1995; Fyffe *et al.* 2009, 2011; Ludman *et al.* 2017, 2018) and in the Casco Bay and Falmouth-Brunswick Groups in south-central and coastal southern Maine (West *et al.* 2003, 2004, 2008; Gerbi and West 2007; Hussey 2010, West and Hussey 2016, Hussey and West 2018). Input of Laurentian-derived zircons to the eastern portions of the trailing margin of Ganderia during this time was probably minor as the Tetagouche-Exploits basin and perhaps these highlands formed a barrier to Laurentian zircon transport

(Fig. 10e), but was more prominent to the west in the Central Maine basin (Bradley and O’Sullivan 2017; Cartwright *et al.* 2019).

The boundary between the Merribuckfred and Central Maine basins in New England has been interpreted as the line of closure of the Tetagouche-Exploits basin (the Dog Bay line in Newfoundland) during the Salinic orogeny (Reusch and van Staal 2012). During the closure of this basin, it is likely that the younger Silurian deposits in the Merrimack belt (Kittery, Berwick and Paxton formations) received increasing amounts of Laurentian detritus (Fig. 10f). By the middle Silurian, when the Tetagouche-Exploits basin was closing, the oceanic crust between the approaching Avalonia and Ganderia was subducting below the trailing margin of Ganderia (Fig. 10f). The Silurian volcanic arc formed at this time is represented in Massachusetts by the Newbury Volcanic Complex (Shride 1976a, b; Zen *et al.* 1983) along the northeastern boundary of the Nashoba terrane (Fig. 2). Avalonia collided by ~425 Ma (Fig. 10g; e.g., Fyffe *et al.* 1999; Bradley *et al.* 2000; van Staal *et al.* 2009; van Staal and Barr 2012; Piñán-Llamas and Hepburn 2013; Wilson *et al.* 2017). Paleocurrent directions in the Kittery Formation in the Merrimack belt suggest that some of the youngest detritus was sourced east of the belt (Rickerich 1983, 1984; Hussey *et al.* 1984). Thus, middle to late Silurian detrital zircon in the Merrimack belt could have been derived from the Salinic orogen and Laurentian margin to the west and/or from arc volcanism and orogenesis related to the approach and collision of Avalonia to the east (Figs. 10f, g). As the Acadian orogenic front advanced westward, earlier deposits to the east were uplifted and likely provided reworked detritus for younger, more westerly, deposits in the Central Maine basin (Bradley *et al.* 2000; Hussey *et al.* 2010; Bradley and O’Sullivan 2017; Ludman *et al.* 2018).

## SUMMARY

### Nashoba terrane

Detrital zircon from five units in the Nashoba terrane in eastern Massachusetts have similar U–Pb LA-ICPMS age patterns with main age peaks between ~560 and ~540 Ma and an average peak for all Nashoba terrane samples at 548 Ma. The Shawsheen Gneiss and Marlboro Formation have small peaks at ~640 Ma and all samples have input between ~1.1 and 1.7 Ga, scattered grains between ~2.0 and 2.1 Ga and a few grains at ~2.4 Ga. One sample from the Marlboro Formation has a detrital core with an Archean age of 3.36 Ga. Populations of youngest detrital zircons ranged from  $470 \pm 22$  Ma to  $462 \pm 20$  Ma with an average of  $466 \pm 13$  Ma. CA-TIMS analysis of one grain from the youngest population of the Nashoba Formation gneiss gave a  $^{206}\text{Pb}/^{238}\text{U}$  age of  $465.9 \pm 0.7$  Ma. The similarity of the zircon detrital pattern of the Tadmuck Brook schist to that of the other units indicates that it is part of the Nashoba terrane.

The strong ~540 Ma peak in the detrital zircon abun-

dance with a much smaller ~640 Ma peak indicates that the Nashoba terrane is a part of Ganderia, a conclusion that is consistent with earlier work (e.g., Hepburn 2004; Walsh *et al.* 2011b, 2013a, 2021; Kay *et al.* 2017). The large input of ~540 Ma zircons indicates that most of the detrital input was from local sources formed during the Cambrian Penobscot orogenic cycle and its Ediacaran basement.

Metamorphic zircon is common in the Nashoba terrane and yielded an approximately continuous spectrum of ages from ~440 Ma to ~335 Ma, consistent with previous studies.

### Tower Hill Formation

The Tower Hill Formation lies along the terrane bounding Clinton-Newbury fault zone and has significantly different detrital zircon abundances than either the Nashoba terrane or Merrimack belt metasedimentary rocks. The main population is ~630 Ma, with a continuum of ages from that age to ~1.8 Ga and three grains at ~2.9 Ga and ~2.1 Ga. The youngest detrital zircon population is  $513 \pm 15$  Ma based on the weighted average of three grains. Zircon data from the Tower Hill Formation indicates that it is different from the rocks of the Merrimack belt and Nashoba terrane, suggesting that the boundary between the Nashoba terrane and Merrimack basin is complex.

### Merrimack belt

Metasedimentary rocks of the Merrimack belt in Massachusetts and SE New Hampshire yielded large Ordovician zircon populations (average peaks at 443–460 Ma), smaller 500–800 Ma populations and scattered Archean grains. Some units (Worcester, Oakdale and Eliot formations) show only Gondwanan provenance, while three units (Kittery, Paxton and Berwick formations) include a minor, but significant Mesoproterozoic Laurentian provenance input. This may indicate that these formations are younger than the others and/or were deposited in a more westerly position in the equivalent of the Central Maine basin. All units were deposited between ~435 and ~420 Ma based on youngest LA-ICPMS and CA-TIMS zircon populations and the ages of crosscutting plutons. The majority of the sedimentary material was derived from Ordovician Ganderian arcs and basement, or reworked arc material, due to the expansion and contraction of the Tetagouche-Exploits basin during the Popelogan/Victoria arc/back-arc cycle and Salinic orogeny. Late Silurian deposits in the Merrimack basin originated from input of both Laurentian material from the west and arc and orogenic sources to the east as the seaway between Ganderia and Avalonia closed by subduction under the trailing edge of Ganderia and the beginning of Acadian orogenesis.

### ACKNOWLEDGEMENTS

We would like to thank Wally Bothner for many helpful

discussions and field trips to the Merrimack belt in New Hampshire. Wilfredo Diegor is thanked for help with some of the LA-ICPMS analysis, data correction and reduction at the Memorial University of Newfoundland. We thank journal reviewers Douglas Reusch and John Waldron for their careful reviews and helpful suggestions that led to improvements in the clarity and presentation of the manuscript. David West is thanked for his helpful editorial handling of the manuscript.

Research was funded by Geological Society of America Graduate Student Research Grants to MLL and KJM, an ExxonMobil Geoscience Grant to KJM, and a Boston College Research Incentive Grant to YDK.

### REFERENCES

- Acaster, M. and Bickford, M.E. 1999. Geochronology and geochemistry of Putnam-Nashoba terrane metavolcanic and plutonic rocks, eastern Massachusetts: Constraints on the early Paleozoic evolution of eastern North America. Geological Society of America, Bulletin, 111, pp. 240–253. [https://doi.org/10.1130/0016-7606\(1999\)111<0240:-GAGOPN>2.3.CO;2](https://doi.org/10.1130/0016-7606(1999)111<0240:-GAGOPN>2.3.CO;2)
- Attenoukon, M.B. 2009. Thermochronological and petrographic constraints on the timing of terrane assembly in eastern New England. Unpublished Ph.D. thesis, Indiana University, Bloomington, Indiana, 300 p.
- Attenoukon, M.B., Kunk, M.J., and Wintsch, R.P. 2006. Constraining the absolute age of multiple fabric-forming events in polymetamorphic argillites, Merrimack Terrane, Massachusetts. Geological Society of America, Northeastern Section, 41st Annual Meeting Abstracts with Programs, 38, no. 2, p. 86. <https://gsa.confex.com/gsa/2006NE/webprogram/Paper100887.html>
- Barr, S.M., Raeside, R.P., and White, C.E. 1998. Geological correlations between Cape Breton Island and Newfoundland, Northern Appalachian orogen. Canadian Journal of Earth Sciences, 35, p.1252–1270. <https://doi.org/10.1139/e98-016>
- Barr, S.M., White, C.E., and Miller, B.V. 2002. The Kingston terrane, southern New Brunswick, Canada: Evidence for an Early Silurian volcanic arc. Geological Society of America, Bulletin, 114, pp. 964–982. [https://doi.org/10.1130/0016-7606\(2002\)114<0964:TKTSNB>2.0.CO;2](https://doi.org/10.1130/0016-7606(2002)114<0964:TKTSNB>2.0.CO;2)
- Barr, S.M., White, C.E., and Miller, B.V. 2003a. Age and geochemistry of Late Neoproterozoic and early Cambrian igneous rocks in southern New Brunswick: similarities and contrasts. Atlantic Geology, 39, pp. 55–73. <https://doi.org/10.4138/1050>
- Barr, S.M., Davis, D.W., Kamo, S., and White, C.E. 2003b. Significance of U–Pb detrital zircon ages in quartzite from peri-Gondwanan terranes, New Brunswick and Nova Scotia, Canada. Precambrian Research, 126, pp. 123–145. [https://doi.org/10.1016/S0301-9268\(03\)00192-X](https://doi.org/10.1016/S0301-9268(03)00192-X)
- Barr, S.M., Hamilton, M.A., Samson, S.D., Satkoski, A.M.,

- and White, C.E. 2012. Provenance variations in northern Appalachian Avalonia based on detrital zircon age patterns in Ediacaran and Cambrian sedimentary rocks, New Brunswick and Nova Scotia, Canada. *Canadian Journal of Earth Sciences*, 49, pp. 533–546. <https://doi.org/10.1139/e11-070>
- Barr, S.M., White, C.E., Davis, D.W., McClelland, W.C., and van Staal, C.R. 2014. Infrastructure and provenance of Ganderia: evidence from detrital zircon ages in the Brookville terrane, southern New Brunswick, Canada. *Precambrian Research*, 246, pp. 358–370. <https://doi.org/10.1016/j.precamres.2014.03.022>
- Barr, S.M., van Rooyen, D., Miller, B.V., White, C.E., and Johnson, S.C. 2019. Detrital zircon signatures in Precambrian and Paleozoic sedimentary units in Ganderia and Avalonia of southern New Brunswick, Canada - more pieces of the puzzle. *Atlantic Geology*, 55, pp. 275–322. <https://doi.org/10.4138/atgeol.2019.010>
- Bell, K.G. and Alvord, D.C. 1976. Pre-Silurian stratigraphy of Northeastern Massachusetts. In *Contributions to the stratigraphy of New England*. Edited by L.R. Page. Geological Society of America, Memoir, 148, pp. 179–216. <https://doi.org/10.1130/MEM148-p179>
- Bennett, V. and Tubrett, M. 2010. U–Pb isotopic age dating by LAM ICP-MS, INCO Innovation Centre, Memorial University: sample preparation methodology and analytical techniques. In *Yukon Exploration and Geology 2009*. Edited by K.E. MacFarlane, L.H Weston, and L.R. Blackburn. Yukon Geological Survey, pp. 47–55.
- Berry, H.N., IV and Osberg, P.H. 1989. A stratigraphic synthesis of eastern Maine and western New Brunswick. In *Studies in Maine Geology, Volume 2*. Edited by R.D. Tucker and R.G. Marvinney. Maine Geological Survey, Augusta, Maine, pp. 1–32.
- Billings, M.P. 1956. The Geology of New Hampshire: Part 2. Bedrock Geology. New Hampshire State Planning and Development Commission, Concord, 203 p.
- Bothner, W.A. and Hussey, A.M., II 1999. Norumbega connections: Casco Bay, Maine, to Massachusetts? In *Norumbega Fault System of the Northern Appalachians*. Edited by A. Ludman and D.P. West, Jr. Geological Society of America, Special Paper, 331, pp. 59–72. <https://doi.org/10.1130/0-8137-2331-0.59>
- Bothner, W.A., Gaudette, H.E., Fargo, T.G., Bowring, S.A., and Isachsen, C.E. 1993. Zircon and sphene U/Pb ages of the Exeter pluton: Constraints on the Merrimack Group and part of the Avalon composite terrane. Geological Society of America, Abstracts with Programs, 25, no. 6, p. 485.
- Bothner, W.A., Blackburn, T., Bowring, S., Buchwaldt, R., and Hussey, A.M., II 2009. Temporal constraints on Paleozoic plutonism in southwestern Maine and southeastern New Hampshire: Revisions and implications. Geological Society of America, Northeastern Section, 44th Annual Meeting, Abstracts with Programs, 41, no. 3, p. 32. <https://gsa.confex.com/gsa/2009NE/webprogram/Paper155255.html>
- Bowring, J.F., McLean, N.M., and Bowring, S.A. 2011. Engineering cyber infrastructure for U–Pb geochronology: Tripoli and U–Pb\_Redux. *Geochemistry, Geophysics, Geosystems*, 12, Q0AA19. <https://doi.org/10.1029/2010GC003479>
- Bradley, D.C. and O’Sullivan, P. 2017. Detrital zircon geochronology of pre-and syncollisional strata, Acadian orogen, Maine Appalachians. *Basin Research*, 29, pp. 571–590. <https://doi.org/10.1111/bre.12188>
- Bradley, D.C., Tucker, R.D., Lux, D., Harris, A.G., and McGregor, D.C. 2000. Migration of the Appalachian Orogen and foreland basin across the Northern Appalachians of Maine and adjacent Areas. U.S. Geological Survey, Professional Paper, 1624, 49 p. <https://doi.org/10.3133/pp1624>
- Buchanan II, J.W., Kuiper, Y.D., Hepburn, J.C., and Kelly, N.M. 2016a. Linking partial melting in the Nashoba Formation to the Andover Granite, Eastern Massachusetts. Geological Society of America, Northeastern Section, 51st Annual Meeting, Abstracts with Program, 48. <https://gsa.confex.com/gsa/2016NE/webprogram/Paper271913.html>
- Buchanan II, J.W., Kuiper, Y.D., Williams, M.L., and Hepburn, J.C. 2016b. Ductile extrusion of the Nashoba Formation during convergence of the Avalon terrane with the composite Laurentian margin, Eastern Massachusetts. Geological Society of America Annual General Meeting, Abstracts with Programs, 48. <https://gsa.confex.com/gsa/2016AM/webprogram/Paper284455.html>
- Buchanan II, J.W., Kuiper, Y.D., Hepburn, J.C., Williams, M.L. 2017. Constraints on Devonian-Carboniferous deformation in the Nashoba terrane, Eastern Massachusetts. Geological Society of America, Joint 52nd Northeastern and 51st North-Central Annual Section Meeting, Abstracts with Programs, 49, no. 2. <https://gsa.confex.com/gsa/2017NE/meetingapp.cgi/Paper/290834>
- Cartwright, S.F.A., West, Jr., D.P. and Amidon, W.H. 2019. Depositional constraints from detrital zircon geochronology of strata from multiple lithotectonic belts in south-central Maine, USA. *Atlantic Geology*, 55, pp. 93–136. <https://doi.org/10.4138/atgeol.2019.003>
- Castle, R.O., Dixon, H.R., Grew, E.S., Griscom, A., and Zietz, I. 1976. Structural dislocations in eastern Massachusetts. U.S. Geological Survey, Bulletin, 1410, 39 p.
- Cawood, P.A. and Nemchin, A.A. 2001. Paleogeographic development of the East Laurentian margin: Constraints from U–Pb dating of detrital zircons in the Newfoundland Appalachians. *Geological Society of America, Bulletin*, 113, pp. 1234–1246. [https://doi.org/10.1130/0016-7606\(2001\)113<1234:PDOTEL>2.0.CO;2](https://doi.org/10.1130/0016-7606(2001)113<1234:PDOTEL>2.0.CO;2)
- Charnock, R.D. 2015. Origin and evolution of the southeastern Merrimack belt, Massachusetts. Unpublished M.S. thesis, Colorado School of Mines, Boulder, Colorado, 107 p.
- Condon, D.J. and Bowring, S.A. 2011. A user’s guide to Neoproterozoic geochronology. In *The Geological record of Neoproterozoic glaciations*. Edited by E. Arnaud, G.

- P. Halverson, and G. Shields-Zhou. Geological Society, London, Memoirs, 36, Chapter 9, pp. 135–149. <https://doi.org/10.1144/M36.9>
- Dabrowski, D. 2013. Implications of Silurian granite genesis to the tectonic history of the Nashoba terrane, Eastern Massachusetts. Unpublished M.S. thesis, Boston College, Chestnut Hill, Massachusetts, 118 p.
- Dabrowski, D., Hepburn, J. C., and Kuiper, Y. 2013. Geochronological constraints on the origin of the Andover granite and its relationship to the tectonic history of the Nashoba terrane, eastern Massachusetts. Geological Society of America, Northeastern Section, 48th Annual Meeting, Abstracts with Programs, 45, no. 1, p. 91. <https://gsa.confex.com/gsa/2013NE/webprogram/Paper215158.html>
- DiNitto, R.G., Hepburn, J.C., Durfee Cardoza, K., and Hill, M. 1984. The Marlboro Formation in its type area and associated rocks just west of the Bloody Bluff fault zone, Marlborough area, Massachusetts. In *Geology of the coastal lowlands, Boston, Massachusetts to Kennebunk, Maine*. Edited by L. Hanson. New England Intercollegiate Geological Conference, 76th Annual Meeting, Salem, Massachusetts, pp. 271–291.
- Dokken, R.J., Waldron, J.W.F., and Dufrane, S.W. 2018. Detrital zircon geochronology of the Fredericton trough, New Brunswick Canada: constraints on the Silurian closure of remnant Iapetus ocean. *American Journal of Science*, 318, pp. 684–725. <https://doi.org/10.2475/06.2018.03>
- Dorais, M.J., Wintsch, R.P., Kunk, M.J., Aleinikoff, J., Burton, W., Underdown, C., and Kerwin, C.M. 2012. P-T-t conditions, Nd and Pb isotopic compositions and detrital zircon geochronology of the Massabesic Gneiss Complex, New Hampshire: Isotopic and metamorphic evidence for the identification of Gander basement, Central New England. *American Journal of Science*, 312, pp. 1049–1097. <https://doi.org/10.2475/10.2012.01>
- Emerson, B.K. 1917. Geology of Massachusetts and Rhode Island. U.S. Geological Survey, Bulletin, 597, 289 p.
- Fargo, T. and Bothner, W.A. 1995. Polydeformation in the Merrimack Group, southeastern New Hampshire and southwestern Maine. In *Guidebook to fieldtrips in southern Maine and adjacent New Hampshire*. Edited by A.M. Hussey, II and R.A. Johnson. New England Intercollegiate Geological Conference, 87, pp. 15–28.
- Fyffe, L.R. 1995. Fredericton belt. In *Geology of the Appalachian-Caledonian Orogen in Canada and Greenland*. Edited by H. Williams. Geological Survey of Canada, *Geology of Canada*, 6, pp. 351–354.
- Fyffe, L.R. 2014. The Grand Manan terrane of New Brunswick: Tectonostratigraphy and relationship to the Gondwanan margin of the Iapetus Ocean. *Geoscience Canada*, 41, pp. 483–502. <https://doi.org/10.12789/geo-can.2014.41.051>
- Fyffe, L.R., Pickerill, R.K., and Stringer, P. 1999. Stratigraphy, sedimentology and structure of the Oak Bay and Waweig formations, Mascarene basin: implications for the paleotectonic evolution of southwestern New Brunswick. *Atlantic Geology*, 35, pp. 59–84. <https://doi.org/10.4138/2024>
- Fyffe, L.R., Barr, S.M., Johnson, S.C., McLeod, M.J., McNicoll, V.J., Valverde-Vaquero, P., van Staal, C.R., and White, C.E. 2009. Detrital zircon ages from Neoproterozoic and Early Paleozoic conglomerate and sandstone units of New Brunswick and coastal Maine: implications for the tectonic evolution of Ganderia. *Atlantic Geology*, 45, pp. 110–144. <https://doi.org/10.4138/atgeol.2009.006>
- Fyffe, L.R., Johnson, S.C., and van Staal, C.R. 2011. A review of Proterozoic to Early Paleozoic lithotectonic terranes in the northeastern Appalachian orogen of New Brunswick, Canada, and their tectonic evolution during Penobscot, Taconic, Salinic, and Acadian orogenesis. *Atlantic Geology*, 47, pp. 211–248. <https://doi.org/10.4138/atgeol.2011.010>
- Gates, O. and Moench, R. 1981. Bimodal Silurian and Lower Devonian volcanic rock assemblages in the Machias-Eastport area, Maine. U.S. Geological Survey, Professional Paper, 1184, 32 p. <https://doi.org/10.3133/pp1184>
- Gerbi, C.C. and West, D.P., Jr. 2007. Use of U-Pb geochronology to identify successive spatially overlapping tectonic episodes during Silurian-Devonian orogenesis in south-central Maine, USA. *Geological Society of America, Bulletin*, 119, pp. 1218–1231. <https://doi.org/10.1130/B26162.1>
- Gerstenberger, H. and Haase, G. 1997. A highly effective emitter substance for mass spectrometric Pb isotope ratio determinations. *Chemical Geology*, 136, pp. 309–312. [https://doi.org/10.1016/S0009-2541\(96\)00033-2](https://doi.org/10.1016/S0009-2541(96)00033-2)
- Goldsmith, R. 1991a. Stratigraphy of the Nashoba Zone, eastern Massachusetts: An enigmatic terrane. In *The bedrock geology of Massachusetts*. Edited by N. L. Hatch, Jr. United States Geological Survey, Professional Paper, 1366 E-J, pp. F1–F22.
- Goldsmith, R. 1991b. Structural and metamorphic history of eastern Massachusetts. In *The bedrock geology of Massachusetts*. Edited by N. L. Hatch, Jr. United States Geological Survey, Professional Paper, 1366 E-J, pp. H1–H63.
- Goldstein, A.G. 1992. Motion of the Clinton-Newbury and related faults and multiple deformation of the Merrimack Group in eastern Massachusetts: Aspects of the Alleghanian orogeny in southeastern New England. In *Guidebook for field trips in the Connecticut Valley region of Massachusetts and adjacent states*. Edited by P. Robinson and J.B. Brady. New England Intercollegiate Geological Conference, 84th Annual Meeting, Amherst, Massachusetts. University of Massachusetts, Amherst, Massachusetts, *Geoscience Contribution Series* 66-1, pp. 120–131.
- Goldstein, A.G. 1994. A shear zone origin for Alleghanian (Permian) multiple deformation in eastern Massachusetts. *Tectonics*, 13, pp. 62–77. <https://doi.org/10.1029/93TC02522>
- Gore, R.Z. 1976. Ayer crystalline complex of Ayer, Harvard, and Clinton, Massachusetts. In *Studies in New England geology*. Edited by P.C. Lyons and A.H. Brownlow. Geological Society of America, Memoir, 146, pp. 103–124.

- <https://doi.org/10.1130/ME146-p103>
- Grew, E.S. 1970. Geology of the Pennsylvanian and pre-Pennsylvanian rocks of the Worcester area, Massachusetts. Unpublished Ph.D. thesis, Harvard University, Cambridge, Massachusetts, 263 p.
- Grew, E.S. 1973. Stratigraphy of the Pennsylvanian and pre-Pennsylvanian rocks of the Worcester area, Massachusetts. *American Journal of Science*, 273, pp. 113–129. <https://doi.org/10.2475/ajs.273.2.113>
- Henderson, B.J., Collins, W.J., Murphy, J.B., Gutierrez-Alonso, G., and Hand, M. 2016. Gondwanan basement terranes of the Variscan-Appalachian orogen: Baltican, Saharan, and West African isotopic fingerprints in Avalonia, Iberia, and the Armorican terranes. *Tectonophysics*, 681, pp. 279–304. <https://doi.org/10.1016/j.tecto.2015.11.020>
- Hepburn, J.C. 1976. Lower Paleozoic rocks west of the Clinton-Newbury fault zone, Worcester area, Massachusetts. In *Geology of Southeastern New England*. Edited by B. Cameron. New England Intercollegiate Geological Conference, 68th Annual meeting, Boston, Massachusetts, Princeton, New Jersey, Science Press, pp. 366–382.
- Hepburn, J.C. 2004. The peri-Gondwanan Nashoba terrane of Eastern Massachusetts: An Early Paleozoic arc-related complex and its accretionary history. In *Guidebook to field trips from Boston, MA to Saco Bay, ME*. Edited by L. Hanson. New England Intercollegiate Geological Conference, 96th Annual Meeting, Salem, Massachusetts, pp. 17–38.
- Hepburn, J.C. and DiNitto, R.G. 1978. Preliminary bedrock geologic map of the Marlborough quadrangle, Middlesex and Worcester counties, Massachusetts. United States Geological Survey, Open-File Report 78-222, 29 p., scale 1:24 000. <https://doi.org/10.3133/ofr78222>
- Hepburn, J.C. and Munn, B. 1984. A geologic traverse across the Nashoba block, eastern Massachusetts. In *Geology of the Coastal Lowlands Boston, Massachusetts to Kennebunk, Maine*. Edited by L. Hanson. New England Intercollegiate Geological Conf., 76th Annual Meeting, Salem, Massachusetts, pp. 103–123.
- Hepburn, J.C., Dunning, G.R., and Hon, R. 1995. Geochronology and regional tectonic implications of Silurian deformation in the Nashoba Terrane, Southeastern New England, U.S.A. In *Current perspectives in the Appalachian-Caledonian orogen*. Edited by J.P. Hibbard, C.R. van Staal, and P.A. Cawood. Geological Association of Canada, Special Paper, 41, pp. 349–366.
- Hepburn, J.C., Fernández-Suárez, J., Jenner, G.A., and Belousova, E.A. 2008. Significance of detrital zircon ages from the Westboro quartzite, Avalon terrane, eastern Massachusetts. Geological Society of America, Northeastern Section, 43rd Annual Meeting, Abstracts with Programs, v. 40, no. 2, p. 14. <https://gsa.confex.com/gsa/2008NE/webprogram/Paper134762.html>
- Hiess, J., Condon, D.J., McLean, N., and Noble, S.R. 2012.  $^{238}\text{U}/^{235}\text{U}$  systematics in terrestrial uranium-bearing minerals. *Science*, 335, pp. 1610–1614. <https://doi.org/10.1126/science.1215507>
- Hibbard, J.P., van Staal, C.R., Rankin, D.W., and Williams, H. 2006. Lithotectonic map of the Appalachian orogen, Canada–United States of America. Geological Survey of Canada, map 2096A, scale 1:1 500 000. <https://doi.org/10.4095/221912>
- Hibbard, J.P., van Staal, C.R., and Rankin, D.W. 2007. A comparative analysis of pre-Silurian crustal building blocks of the Northern and Southern Appalachian orogen. *American Journal of Science*, 307, pp. 23–45. <https://doi.org/10.2475/01.2007.02>
- Hitchcock, C.H. 1877. The Geology of New Hampshire: Part II Stratigraphic Geology. Edward A. Jenks, State Printer, Concord, New Hampshire, 684 p.
- Horn, I., Rudnick R.L., and McDonough, W.F. 2000. Precise elemental and isotope ratio determination by simultaneous solution nebulization and laser ablation-ICP-MS: application to U-Pb geochronology. *Chemical Geology*, 167, pp. 403–423. [https://doi.org/10.1016/S0009-2541\(99\)00168-0](https://doi.org/10.1016/S0009-2541(99)00168-0)
- Hoskin, P.W.O. and Schaltegger, U. 2003. The composition of zircon and igneous and metamorphic petrogenesis. In *Reviews in mineralogy and geochemistry*. Edited by J.M. Hanchar and P.W.O. Hoskin. Mineralogical Society of America, Washington, D.C., 53, pp. 27–62. <https://doi.org/10.2113/0530027>
- Hussey, A.M., II 1988. Lithotectonic stratigraphy, deformation, plutonism, and metamorphism, greater Casco Bay region, southwestern Maine. In *Studies in Maine Geology: Volume 1. Structure and Stratigraphy*. Edited by R.D. Tucker and R.G. Marvinney. Maine Geological Survey, Augusta, Maine, pp. 17–34.
- Hussey, A.M., II and Bothner, W.A. 1993. Geology of the coastal lithotectonic belt, SW Maine and SE New Hampshire. In *Fieldtrip guidebook for the Northeastern United States*, Boston GSA. Edited by J. T. Cheney and J.C. Hepburn. Geological Society of America Annual Meeting, Boston, Massachusetts, 1, Contribution #67, Department of Geology and Geography, University of Massachusetts, Amherst, Massachusetts, pp. K1–K19.
- Hussey, A.M., II and West, D.P., Jr. 2018. Bedrock geology of the Brunswick quadrangle Maine. Maine Geological Survey, Map 18-04, scale 1:24 000.
- Hussey, A.M., II, Rickerich, S.F., and Bothner, W.A. 1984. Sedimentology and multiple deformation of the Kittery Formation, southwestern Maine and southeastern New Hampshire. In *Geology of the Coastal Lowlands; Boston, MA to Kennebunk, Maine*. Edited by L.S. Hanson. New England Intercollegiate Geological Conference Guidebook, Department of Geological Sciences, Salem State College, Salem, Massachusetts, pp. 47–53.
- Hussey, A.M., II, Ludman, A., Bothner, W.A., and West, D.P. 1999. Fredericton and Merrimack troughs: Once one or always two?. Geological Society of America, Abstracts

- with Programs, 31, no. 1, p. A-25.
- Hussey, A.M., II, Bothner, W.A., and Aleinikoff, J. 2010. The tectono-stratigraphic framework and evolution of southwestern Maine and southeastern New Hampshire. In *From Rodinia to Pangea: The Lithotectonic record of the Appalachian region*. Edited by R.P. Tollo, M.J. Bartholomew, J.P. Hibbard, and P.M. Karabinos. Geological Society of America, Memoir 206, pp. 205–230. [https://doi.org/10.1130/2010.1206\(10\)](https://doi.org/10.1130/2010.1206(10))
- Hussey, A.M., II, Bothner, W.A., and Thompson, P.J. 2016. Bedrock geology of the Kittery 1:100 000 quadrangle, Southwestern Maine and Southeastern New Hampshire. Maine Geological Survey, Bulletin, 45, 99 p.
- Jaffey, A.H., Flynn, K.E., Glendenin, L.E., Bentley, W.C., and Essling, A.M. 1971. Precision measurement of half-lives and specific activities of  $^{235}\text{U}$  and  $^{238}\text{U}$ . Physical Review C: Nuclear Physics, 4, pp. 1889–1906. <https://doi.org/10.1103/PhysRevC.4.1889>
- Jerden, J.L. Jr. 1997. Polyphase metamorphism and structure of the Tadmuck Brook Schist, eastern Massachusetts. Unpublished M.S. thesis, Boston College, Chestnut Hill, Massachusetts, 250 p.
- Jerden, J. L., Jr. and Hepburn, J. C. 1996. The Tadmuck Brook Schist, a phyllonite (?) between the Nashoba terrane and the Merrimack trough, eastern Massachusetts. Geological Society of America, Abstracts with Programs, 28, no. 3, p.68.
- Johnson, S.C., McLeod, M.J., Fyffe, L.R., and Dunning, G.R. 2009. Stratigraphy, geochemistry, and geochronology of the Annidale and New River belts, and the development of the Penobscot arc in southern New Brunswick. In *Mineral Resource Report 2009-2*. Edited by G.L. Martin. New Brunswick Division of Natural Resources; Minerals, Policy, and Planning Division, pp. 141–218.
- Johnson, S.C., Fyffe, L.R., McLeod, M.J., and Dunning, G.R. 2012. U-Pb ages, geochemistry, and tectonomagmatic history of the Cambro-Ordovician Annidale Group: A remnant of the Penobscot arc system in southern New Brunswick? Canadian Journal of Earth Sciences, 49, pp. 166–188. <https://doi.org/10.1139/e11-031>
- Karabinos, P., Macdonald, F.A., and Crowley, J.L. 2017. Bridging the gap between the foreland and hinterland I: geochronology and plate tectonic geometry of Ordovician magmatism and terrane accretion of the Laurentian margin of New England. American Journal of Science, 317, pp. 515–554. <https://doi.org/10.2475/05.2017.01>
- Katz, F.J. 1917. Stratigraphy in southwestern Maine and southeastern New Hampshire. U.S. Geological Survey, Professional Paper, 108, pp. 165–177. <https://doi.org/10.3133/pp108I>
- Kay, A., Hepburn, J.C., Kuiper, Y.D. and Inglis, J. 2009. Nd isotopic constraints on the origin of the Nashoba terrane, Eastern Massachusetts. Geological Society of America, Northeastern Section, 44th Annual Meeting, Abstracts with Programs, 41, no. 1, p. 98. <https://gsa.confex.com/gsa/2009NE/webprogram/Paper15584.html>
- Kay, A., Hepburn, J.C., and Kuiper, Y.D. 2011. Trace ele-  
ment and Sm–Nd isotopic geochemical characteristics of the Nashoba terrane, Eastern Massachusetts. Geological Society of America, Northeastern (46th Annual) and North-Central (45th Annual) Joint Meeting, Abstracts with Programs, 43, no. 1, p.150. <https://gsa.confex.com/gsa/2011NE/webprogram/Paper185370.html>
- Kay, A., Hepburn, J.C., Kuiper, Y.D., and Baxter, E.F. 2017. Geological evidence for a Ganderian arc/back-arc remnant in the Nashoba terrane, SE New England, USA. American Journal of Science, 317, pp. 413–448. <https://doi.org/10.2475/04.2017.01>
- Keppie, J. D., Davic, D.W., and Krough, T.E. 1998. U–Pb geochronological constraints on Precambrian stratified units in the Avalon composite terrane of Nova Scotia, Canada: tectonic implications. Canadian Journal of Earth Sciences, 35, pp. 222–236. <https://doi.org/10.1139/e97-109>
- Klein, C. and Dutrow, B., 2007. Manual of Mineral Science, 23rd edition, John Wiley and Sons, Hoboken, New Jersey, 716 p.
- Klein, C. and Hurlbut, C., Jr. 1993. Manual of Mineralogy, 21st edition, John Wiley and Sons, New York, 681 p.
- Kohut, E.J. and Hepburn, J.C. 2004. Mylonites and brittle shear zones along the western edge of the Avalon terrane west of Boston. In *Guidebook to field trips from Boston, MA to Saco Bay, ME*. Edited by L.S. Hanson. New England Intercollegiate Geological Conference, 96th Ann. Mtg., Salem, Massachusetts, pp. 89–110.
- Kopera, J.P. and Walsh, G.J. 2014. The eastern Merrimack terrane in Massachusetts: Revisiting metamorphism, deformation and plutonism. In *Guidebook to field trips in southeastern New England (MA-NH-RI)*. Edited by M. D. Thompson. New England Intercollegiate Geological Conference, 106th Annual Meeting, Wellesley, Massachusetts, pp. A3–1–20.
- Kopera J., Hepburn J.C., and DiNitto R. 2006. Bedrock geologic map of the Marlborough quadrangle, Massachusetts. Office of the Massachusetts State Geologist, Geologic Map 06-01, scale 1:24 000.
- Košler, J. and Sylvester, P.J. 2003. Present trends and the future of zircon in geochronology; laser ablation ICPMS. Reviews in Mineralogy and Geochemistry, 53, pp. 243–275. <https://doi.org/10.2113/0530243>
- Košler, J., Fonneland, H., Sylvester, P., Tubrett, M., and Pedersen, R. 2002. U–Pb dating of detrital zircons for sediment provenance studies—a comparison of laser ablation ICPMS and SIMS techniques. Chemical Geology, 182, pp. 605–618. [https://doi.org/10.1016/S0009-2541\(01\)00341-2](https://doi.org/10.1016/S0009-2541(01)00341-2)
- Košler, J., Forst, L., and Sláma, J. 2008. LamDate and Lam-Tool: spreadsheet-based data reduction for laser ablation ICP-MS. Laser Ablation-ICP-MS in the Earth Sciences: Current Practices and Outstanding Issues. Mineralogical Association of Canada, Short Course Series, 40, pp. 315–317.
- Kuiper, Y.D. and Hepburn, J.C. 2021. Detrital zircon populations of the eastern Laurentian margin in the Appalachians. Geology, 49, pp. 233–237. <https://doi.org/10.1130/>

G48012.1

- Kuiper, Y.D., Buchanan, J.W., Charnock, R., Hepburn, J.C., and Kopera, J.P. 2014. Structural history of the Nashoba terrane-Merrimack terrane boundary zone, eastern Massachusetts. In *Guidebook to field trips in Southeastern New England (MA-NH-RI)*. Edited by M.D. Thompson. New England Intercollegiate Geological Conference, 106th Annual Meeting, Wellesley, Massachusetts, pp. C4-1–C4-12.
- Kuiper, Y.D., Murray, D.P., Ellison, S., and Crowley, J.L. in press. U-Pb detrital zircon analysis of sedimentary rocks of the southeastern New England Avalon terrane in the US Appalachians: Evidence for a separate crustal block. In *New developments in the Appalachian-Caledonian-Variscan orogen*. Edited by Y.D. Kuiper, J.B. Murphy, R.D. Nance, R.A. Strachan, and M.D. Thompson. Geological Society of America, Special Paper 544. [https://doi.org/10.1130/2021.2554\(05\)](https://doi.org/10.1130/2021.2554(05))
- Loan, M.L. 2011. New constraints on the age and deposition of the metasedimentary rocks in the Nashoba terrane, SE New England. Unpublished M.S. thesis, Boston College, Chestnut Hill, Massachusetts, 125 p.
- Ludman, A., Hopeck, J., and Berry, H.N. IV 2017. Provenance and paleogeography of post-Middle Ordovician, pre-Devonian sedimentary basins on the Gander composite terrane, eastern and east-central Maine; implications for Silurian tectonics in the northern Appalachians. *Atlantic Geology*, 53, pp. 63–85. <https://doi.org/10.4138/atgeol.2017.003>
- Ludman, A., Aleinikoff, J., Berry, H.N., IV, and Hopeck, J.T. 2018. SHRIMP U-Pb zircon evidence for age, provenance, and tectonic history of early Paleozoic Ganderian rocks, east-central Maine, USA. *Atlantic Geology*, 54, pp. 335–387. <https://doi.org/10.4138/atgeol.2018.012>
- Ludman, A., Aleinikoff, J. N., and Devlin, B. 2019. Interpreting detrital zircon provenance in the context of regional stratigraphic and tectonic models: an example from Late Ordovician - Early Devonian cover rocks on Ganderia, eastern Maine. Geological Society of America, Northeastern Section, 54th Annual Meeting, Abstracts with Programs, 51, no. 1. <https://gsa.confex.com/gsa/2019NE/meetingapp.cgi/Paper/325696>
- Ludwig, K. L. 1998. On the treatment of concordant uranium-lead ages. *Geochimica et Cosmochimica Acta*, 62, pp. 665–676. [https://doi.org/10.1016/S0016-7037\(98\)00059-3](https://doi.org/10.1016/S0016-7037(98)00059-3)
- Ludwig K.L. 1999. User's manual for Isoplot/EX, version 2.06: a geochronological toolkit for Microsoft Excel. Berkeley Geochronology Center, Special Publication, 1a, 49 p.
- Ludwig K.L. 2008. Isoplot 3.7. A geochronological toolkit for Microsoft Excel. Berkeley Geochronology Center, Special Publication, 4, rev., 77 p.
- Lyons, J. B., Bothner, W. A., Moench, R. H., and Thompson, J. B. 1997. Bedrock geologic map of New Hampshire. U.S. Geological Survey, scale 1:250 000.
- Mattinson, J.M. 2005. Zircon U-Pb chemical abrasion ("CA-TIMS") method: Combined annealing and multi-step partial dissolution analysis for improved precision and accuracy of zircon ages. *Chemical Geology*, 220, pp. 47–66. <https://doi.org/10.1016/j.chemgeo.2005.03.011>
- McLean, N.M., Bowring, J.F., and Bowring, S.A. 2011. An algorithm for U-Pb isotope dilution data reduction and uncertainty propagation: *Geochemistry, Geophysics, Geosystems*, 12, Q0AA18. <https://doi.org/10.1029/2010GC003478>
- Murphy, J.B., Pisarevsky, S.A., Nance, R.D., and Keppie, J.D. 2004. Neoproterozoic - Early Paleozoic evolution of peri-Gondwanan terranes: implications for Laurentia-Gondwana connections. *International Journal of Earth Science (Geologische Rundschau)*, 93, pp. 659–682. <https://doi.org/10.1007/s00531-004-0412-9>
- Murphy, J.B., Gutierrez-Alonso, G., Nance, R.D., Fernandez-Suarez, J., Keppie, J.D., Quesada, C., Strachan, R.A., and Dostal, J. 2006. Origin of the Rheic Ocean: Rifting along a Neoproterozoic suture? *Geology*, 34, pp. 325–328. <https://doi.org/10.1130/G22068.1>
- Nance, R.D. and Murphy, J.B. 1996. Basement isotopic signatures and Neoproterozoic paleogeography of Avalonian-Cadomian and related terranes in the circum-North Atlantic. In *Avalonian and related peri-Gondwanan terranes of the circum-North Atlantic*. Edited by N.D. Nance and M.D. Thompson. Geological Society of America, Special Paper, 304, pp. 333–346. <https://doi.org/10.1130/0-8137-2304-3.333>
- Olszewski, W.J., Jr. 1980. The geochronology of some stratified metamorphic rocks in northeastern Massachusetts. *Canadian Journal of Earth Sciences*, 17, pp. 1407–1416. <https://doi.org/10.1139/e80-148>
- Osberg, P.H. 1988. Geologic relations within the shale-wacke sequence in south-central Maine. In *Studies in Maine Geology: Volume 1. Structure and Stratigraphy*. Edited by R.D. Tucker and R.G. Marvinney. Maine Geological Survey, Augusta, Maine, pp. 51–73.
- Osberg, P.H., Hussey, A.M., II, and Boone, G.M. 1985. Bedrock geologic map of Maine. Maine Geological Survey, scale 1:500 000.
- Peck, J.H. 1975. Preliminary bedrock geologic map of the Clinton quadrangle, Worcester County, Mass. U.S. Geological Survey, Open File Report, 75-658, 30 p., scale 1:24 000. <https://doi.org/10.3133/ofr75658>
- Peck, J.H. 1976. Silurian and Devonian stratigraphy in the Clinton quadrangle, central Massachusetts. In *Contributions to the stratigraphy of New England*. Edited by L.R. Page. Geological Society of America, Memoir, 148, pp. 241–252. <https://doi.org/10.1130/MEM148-p241>
- Piñán-Llamas, A. and Hepburn, J.C. 2013. Geochemistry of the Silurian-Devonian volcanic rocks in the Coastal Volcanic Belt, Machias-Eastport area, Maine: Evidence for a pre-Acadian arc. *Geological Society of America, Bulletin*, 125, pp. 1930–1942. <https://doi.org/10.1130/B30776.1>
- Pollock, J.C., Wilton, D.H.C., van Staal, C.R., and Morrissey, K.D. 2007. U-Pb zircon geochronological constraints on the Late Ordovician-Early Silurian collision of Ganderia and Laurentia along the Dog Bay Line: The terminal Iapetan suture in the Newfoundland Appalachians. Amer-

- ican Journal of Science, 307, pp. 399–433. <https://doi.org/10.2475/02.2007.04>
- Pollock, J.C., Hibbard, J.P., and Sylvester, P.J. 2009. Early Ordovician rifting of Avalonia and birth of the Rheic Ocean: U-Pb detrital zircon constraints from Newfoundland. Geological Society, London, Journal, 166, pp. 501–515. <https://doi.org/10.1144/0016-76492008-088>
- Pollock, J.C., Hibbard, J.P., and van Staal, C.R. 2012. A paleogeographical review of the peri-Gondwanan realm of the Appalachian orogen. Canadian Journal of Earth Sciences, 49, pp. 259–288. <https://doi.org/10.1139/e11-049>
- Ramezani, J., Schmitz, M., Davydov, V., Bowring, S., Snyder, W., and Northrup, C. 2007. High-precision U-Pb zircon age constraints on the Carboniferous-Permian boundary in the southern Urals stratotype. Earth and Planetary Science Letters, 256, pp. 244–257. <https://doi.org/10.1016/j.epsl.2007.01.032>
- Rankin, D.W., Coish, R.A., Tucker, R.D., Peng, Z.X., Wilson, S.A., and Rouff, A.A. 2007. Silurian extension in the upper Connecticut Valley, United States and the origin of Middle Paleozoic basins in the Québec embayment. American Journal of Science, 307, pp. 216–264. <https://doi.org/10.2475/01.2007.07>
- Reusch, D.N. and van Staal, C.R. 2012. The Dog Bay - Liberty Line and its significance for Silurian tectonics of the northern Appalachian orogen. Canadian Journal of Earth Science, 49, pp. 239–258. <https://doi.org/10.1139/e11-024>
- Reusch, D.N., Holm-Denoma, C.S. and Slack, J.F. 2018. U-Pb zircon geochronology of Proterozoic and Paleozoic rocks, North Islesboro, coastal Maine (USA): links to West Africa and Penobscottian orogenesis in southeastern Ganderia? Atlantic Geology, 54, pp. 189–211. <https://doi.org/10.4138/atgeol.2018.007>
- Reusch, D.N., Strauss, J. and Smith, L. 2021. Update on detrital zircon U/Pb geochronology from Proterozoic and early Paleozoic rocks of the Penobscot Inlier, Maine. Geological Society of America, Abstracts with Programs, 53, no. 1. <https://doi.org/10.1130/abs/2021NE-361615>
- Rickerich, S.F. 1983. Sedimentology, stratigraphy and structure of the Kittery Formation in the Portsmouth, New Hampshire, Area. Unpublished M.S. thesis, University of New Hampshire, Durham, New Hampshire, 115 p.
- Rickerich, S.F. 1984. Sedimentology and stratigraphy of the Kittery Formation near Portsmouth, New Hampshire. Geological Society of America, Abstracts with Programs, 16, p. 59.
- Robinson, G.R. Jr. 1978. Bedrock geologic map of the Pepperell, Shirley, Townsend quadrangles, and part of the Ayer Quadrangle, Massachusetts and New Hampshire. US Geological Survey, Miscellaneous Field Studies, Map 957, scale 1:24 000.
- Robinson, G.R. Jr. 1981. Bedrock geology of the Nashua River area, Massachusetts-New Hampshire; supplement to USGS Miscellaneous Field Studies Map MF-957 (Bedrock geologic map of the Pepperell, Shirley, Townsend quadrangles, and part of the Ayer Quadrangle, Massachusetts and New Hampshire). U.S. Geological Survey, Open File Report, 81-593, 187 p. <https://doi.org/10.3133/ofr81593>
- Robinson, P. and Goldsmith, R. 1991. Stratigraphy of the Merrimack Belt, Central Massachusetts. In The bedrock geology of Massachusetts. Edited by N.L. Hatch, Jr. United States Geological Survey, Professional Paper, 1366 E-J, pp. G1–G37.
- Robinson, P., Tracy, R.J., Hollocher, K.T. and Dietsch, C.W. 1982. Stratigraphy and structure of the Ware-Barre area, central Massachusetts. In Guidebook for field trips in Connecticut and south-central Massachusetts. New England Intercollegiate Geological Conference, 74th annual meeting. Connecticut Geological and Natural History Survey, Guidebook, 5, pp. 341–373.
- Rogers, N., van Staal, C.R., McNicoll, V., Pollock, J., Zagorevski, A., and Whalen, J. 2006. Neoproterozoic and Cambrian arc magmatism of the Victoria Lake Supergroup: A remnant of Ganderian basement in central Newfoundland? Precambrian Research, 147, pp. 320–341. <https://doi.org/10.1016/j.precamres.2006.01.025>
- Rubatto, D. 2017. Zircon: The metamorphic mineral. Reviews in Mineralogy and Geochemistry, 83, 261–295. <https://doi.org/10.2138/rmg.2017.83.9>
- Samson, S.D., Barr, S.M., and White, C.E. 2000. Nd isotopic characteristics of terranes within the Avalon Zone, southern New Brunswick. Canadian Journal of Earth Sciences, 37, pp. 1039–1052. <https://doi.org/10.1139/e00-015>
- Samson, S.D., D'Lemos, R.S., Miller, B.V., and Hamilton, M.A. 2005. Neoproterozoic palaeogeography of the Cadomia and Avalon terranes: constraints from detrital zircon U-Pb ages. Geological Society, London, Journal, 162, pp. 65–71. <https://doi.org/10.1144/0016-764904-003>
- Satkoski, A.M., Barr, S.M., and Samson, S.D. 2010. Provenance of Late Neoproterozoic and Cambrian sediments in Avalonia: Constraints from detrital zircon ages and Sm-Nd isotopic compositions in southern New Brunswick, Canada. Journal of Geology, 118, pp. 187–200. <https://doi.org/10.1086/649818>
- Schofield, D.I. and D'Lemos, R.S. 2000. Granite petrogenesis in the Gander Zone, NE Newfoundland: Mixing of melts from multiple sources and the role of lithospheric delamination. Canadian Journal of Earth Sciences, 37, pp. 535–547. <https://doi.org/10.1139/e99-116>
- Schulz, K.J., Stewart, D.B., Tucker, R.D., Pollock, J.C., and Ayuso, R.A. 2008. The Ellsworth terrane, coastal Maine: Geochronology, geochemistry, and Nd-Pb isotopic composition - implications for the rifting of Ganderia. Geological Society of America, Bulletin, 120, pp. 1134–1158. <https://doi.org/10.1130/B26336.1>
- Seaman, S.J., Scherer, E.E., Wobus, R.A., Zimmer, J.H., and Sales, J.G. 1999. Late Silurian volcanism in coastal Maine: The Cranberry Island series. Geological Society of America, Bulletin, 111, pp. 686–708. [https://doi.org/10.1130/0016-7606\(1999\)111<0686:LSVICM>2.3.CO;2](https://doi.org/10.1130/0016-7606(1999)111<0686:LSVICM>2.3.CO;2)
- Seaman, S.J., Hon, R., Whitman, M., Wobus, R.A., Hogan, J.P., Chapman, M., Koteas, G.C., Rankin, D., Piñán-Llamas, A., and Hepburn, J.C. 2019. Late Paleozoic super-

- volcano-scale eruptions in Maine, USA. Geological Society of America, Bulletin, 131, pp. 1995–2010. <https://doi.org/10.1130/B32058.1>
- Severson, A.R. 2020. Across- and along-strike structural and geochronological variations of the Nashoba-Putnam and Avalon terranes, eastern Massachusetts, Connecticut, and Rhode Island, southeastern New England Appalachians. Unpublished Ph.D. thesis, Colorado School of Mines, Golden, Colorado, 131 p.
- Severson, A.R., Kuiper, Y.D., Eby, G.N., Lee, H.Y., Hepburn, J.C. in press. New detrital zircon U-Pb ages and Lu-Hf isotopic data from metasedimentary rocks along the western boundary of the composite Avalon terrane in the southeastern New England Appalachians. In *New developments in the Appalachian-Caledonian-Variscan orogen*. Edited by Y.D. Kuiper, J.B. Murphy, R.D. Nance, R.A. Strachan, and M.D. Thompson. Geological Society of America, Special Paper 544. [https://doi.org/10.1130/2021.2554\(04\)](https://doi.org/10.1130/2021.2554(04))
- Shride, A.F. 1976a. Stratigraphy and correlation of the Newbury volcanic complex, northeastern Massachusetts. In *Contributions to the stratigraphy of New England*. Edited by L.R. Page. Geological Society of America, Memoir, 148, pp. 147–177. <https://doi.org/10.1130/MEM148-p147>
- Shride, A.F. 1976b. Stratigraphy and structural setting of the Newbury Volcanic Complex, northeastern Massachusetts. In *Geology of Southeastern New England*. Edited by B. Cameron. New England Intercollegiate Geological Conference, 68th Annual Meeting, Science Press, Princeton, New Jersey, pp. 291–300. [https://scholars.unh.edu/neigc\\_trips/254/](https://scholars.unh.edu/neigc_trips/254/)
- Skehan, J.W. 1968. Fracture tectonics of southeastern New England as illustrated by the Wachusett-Marlborough tunnel, east-central Massachusetts. In *Studies of Appalachian geology-Northern and Maritime*. Edited by E-an Zen, W.S. White, J.B. Hadley, and J.B. Thompson, Jr. Interscience Publishers, New York, pp. 281–290.
- Skehan, J.W., Rast, N., Kohut, E., Hepburn, J.C., and Grimes, S. 1998. Precambrian and Paleozoic mylonites of the Boston Avalon. In *Guidebook to field trips in Rhode Island and adjacent regions of Connecticut and Massachusetts*. Edited by D.P. Murray. New England Intercollegiate Geological Conference, 90th Annual Meeting, University of Rhode Island, Kingston, RI, pp. A3-1–A3-24.
- Sláma, J., Košler, J., Condon, D.J., et al. 2008. Plešovice zircon - A new natural reference material for U-Pb and Hf isotopic microanalysis. *Chemical Geology*, 249, pp. 1–35. <https://doi.org/10.1016/j.chemgeo.2007.11.005>
- Sorota, K.J. 2013. Age and origin of the Merrimack terrane, southeastern New England: A detrital zircon U-Pb geochronology study. Unpublished M.S. thesis, Boston College, Chestnut Hill, Massachusetts, 217 p.
- Stroud, M.M., Markwort, R.J., and Hepburn, J.C. 2009. Refining temporal constraints on metamorphism in the Nashoba terrane, southeastern New England, through monazite dating. *Lithosphere*, 1, pp. 337–342. <https://doi.org/10.1130/L50.1>
- monazite dating. *Lithosphere*, 1, pp. 337–342. <https://doi.org/10.1130/L50.1>
- Sylvester, P.J. and Ghaderi, M. 1997. Trace element analysis of scheelite by excimer laser ablation-inductively coupled plasma-mass spectrometry (ELA-ICP-MS) using a synthetic silicate glass standard. *Chemical Geology*, 141, pp. 49–65. [https://doi.org/10.1016/S0009-2541\(97\)00057-0](https://doi.org/10.1016/S0009-2541(97)00057-0)
- Thompson, J.B., Jr. and Norton, S.A. 1968. Paleozoic regional metamorphism in New England and adjacent areas. In *Studies of Appalachian geology-Northern and Maritime*. Edited by E-an Zen, W.S. White, J.B. Hadley, and J.B. Thompson, Jr. Interscience Publishers, New York, pp. 319–328.
- Thompson, M.D. and Bowring, S.A. 2000. Age of the Squantum “Tillite,” Boston Basin, Massachusetts, U-Pb zircon constraints on terminal Neoproterozoic glaciation. *American Journal of Science*, 300, pp. 630–655. <https://doi.org/10.2475/ajs.300.8.630>
- Thompson, M.D., Hermes, O.D., Bowring, S.A., Isachsen, C.E., Besancon, J.R., and Kelly, K.L. 1996. Tectonostratigraphic implications of Late Proterozoic U-Pb zircon ages in the Avalon Zone of southeastern New England. In *Avalonian and related peri-Gondwanan terranes of the circum-North Atlantic*. Edited by R.D. Nance and M.D. Thompson. Geological Society of America, Special Paper, 304, pp. 179–191. <https://doi.org/10.1130/0-8137-2304-3.179>
- Thompson, M.D., Grunow, A.M., and Ramezani, J. 2007. Late Neoproterozoic paleogeography of the southeastern New England Avalon zone: implications for Gondwana break-up. *Geological Society of America, Bulletin*, 119, pp. 681–696. <https://doi.org/10.1130/B26014.1>
- Thompson, M.D., Ramezani, J., Barr, S.M., Hermes, O.D. 2010. High precision U-Pb zircon dates for Ediacaran granitoid rocks in SE New England: Revised magmatic chronology and correlation with other Avalonian terranes. In *From Rodinia to Pangea: The lithotectonic record of the Appalachian region*. Edited by R.P. Tollo, M.J. Bartholomew, J.P. Hibbard, and P.M. Karabinos. Geological Society of America, Memoir, 206, pp. 231–250. [https://doi.org/10.1130/2010.1206\(11\)](https://doi.org/10.1130/2010.1206(11))
- Thompson, M.D., Barr, S.M., Grunow, A.M. 2012. Avalonian perspectives on Cryogenian-Ediacaran paleogeography: Evidence from Sm–Nd isotope geochemistry and detrital zircon geochronology in SE New England. *Geological Society of America, Bulletin*, 124, pp. 517–531. <https://doi.org/10.1130/B30529.1>
- Thompson, M.D., Ramezani, J., and Crowley, J.L. 2014. U-Pb zircon geochronology of the Roxbury Conglomerate, Boston Basin, Massachusetts: Tectono-stratigraphic implications for Avalonia in and beyond SE New England. *American Journal of Science*, 314, pp. 1009–1044. <https://doi.org/10.2475/06.2014.02>
- Tremblay, A. and Pinet, N. 2005. Diachronous supracrustal extension in an intraplate setting and the origin of the Connecticut-Valley Gaspé and Merrimack troughs, northern Appalachians. *Geological Magazine*, 142, pp. 7–

22. <https://doi.org/10.1017/S001675680400038X>
- Tucker, R., Osberg, P., and Berry H.N. 2001. The geology of a part of Acadia and the nature of the Acadian orogeny across central and eastern Maine. *American Journal of Science*, 301, pp. 205–260. <https://doi.org/10.2475/ajs.301.3.205>
- Valverde-Vaquero, P., van Staal, C.R., McNicoll, V., and Dunning, G.R. 2006a. Mid-Late Ordovician magmatism and metamorphism along the Gander margin in central Newfoundland. *Geological Society, London, Journal*, 163, pp. 347–362. <https://doi.org/10.1144/0016-764904-130>
- Valverde-Vaquero, P., Dunning, G.R., and O'Brien, S.J. 2006b. Polycyclic evolution of the Late Neoproterozoic basement in the Hermitage Flexure region (southwest Newfoundland Appalachians): New evidence from the Cinq-Cerf gneiss. *Precambrian Research*, 148, pp. 1–18. <https://doi.org/10.1016/j.precamres.2006.03.001>
- van Staal, C.R. 1994. Brunswick subduction complex in the Canadian Appalachians: Record of the Late Ordovician to Late Silurian collision between Laurentia and the Gander margin of Avalon. *Tectonics*, 13, pp. 946–962. <https://doi.org/10.1029/93TC03604>
- van Staal, C.R. and Barr, S.M. 2012. Lithospheric architecture and tectonic evolution of the Canadian Appalachians and associated Atlantic margin. In *Tectonic styles in Canada: the Lithoprobe perspective*. Edited by J.A. Percival, F.A. Cook, and R.M. Clowes. Geological Association of Canada, Special Paper, 49, pp. 41–95.
- van Staal, C.R., Sullivan, R.W., and Whalen, J.B. 1996. Provenance and tectonic history of the Gander Margin in the Caledonian/Appalachian Orogen: Implications for the origin and assembly of Avalonia. In *Avalonian and Related Peri-Gondwanan Terranes of the circum-North Atlantic*. Edited by R.D. Nance and M.D. Thompson. Geological Society of America, Special Paper, 304, pp. 347–367. <https://doi.org/10.1130/0-8137-2304-3.347>
- van Staal, C.R., Dewey, J.F., MacNiocaill, C., and McKerrow, W.S., 1998. The Cambrian–Silurian tectonic evolution of the northern Appalachians and British Caledonides: history of a complex, west and southwest Pacific-type segment of Iapetus. *Geological Society, London, Special Publications*, 143, pp. 197–242. <https://doi.org/10.1144/GSL.SP.1998.143.01.17>
- van Staal, C.R., Wilson, R.A., Rogers, N., Fyffe, L.R., Langton, J.P., McCutcheon, S.R., McNicoll, V., and Ravenhurst, C.E. 2003. Geology and tectonic history of the Bathurst Supergroup, Bathurst Mining Camp, and its relationships to coeval rocks in southwestern New Brunswick and adjacent Maine-A synthesis. In *Massive sulfide deposits of the Bathurst Mining Camp, New Brunswick, and Northern Maine*. Edited by W.D. Goodfellow, S.R. McCutcheon, and J.M. Peter. *Economic Geology, Monograph*, 11, pp. 37–60. <https://doi.org/10.5382/Mono.11.03>
- van Staal, C.R., Currie, K.L., Rowbotham, G., Goodfellow, W., and Rogers, N. 2008. P-T paths and exhumation of Late Ordovician - Early Silurian blueschists and associated metamorphic nappes of the Salinic Brunswick subduc-
- tion complex, northern Appalachians. *Geological Society of America, Bulletin*, 120, pp. 1455–1477. <https://doi.org/10.1130/B26324.1>
- van Staal, C.R., Whalen, J.B., Valverde-Vaquero, P., Zagorevski, A., and Rogers, N. 2009. Pre-Carboniferous, episodic accretion-related, orogenesis along the Laurentian margin of the northern Appalachians. In *Ancient orogens and modern analogues*. Edited by J.B. Murphy, J.D. Keppe, and A.J. Hynes. Geological Society, London, Special Publications, 327, pp. 271–316. <https://doi.org/10.1144/SP327.13>
- van Staal, C.R., Barr, S.M., and Murphy, J.B. 2012. Provenance and tectonic evolution of Ganderia: Constraints on the evolution of the Iapetus and Rheic oceans. *Geology*, 40, pp. 987–990. <https://doi.org/10.1130/G33302.1>
- van Staal, C.R., Wilson, R.A., Kamo, S.L., McClelland, W.C., and McNicoll, V. 2016. Evolution of the Early to Middle Ordovician Popelogan arc in New Brunswick, Canada, and adjacent Maine, USA: Record of arc-trench migration and multiple phases of rifting. *Geological Society of America, Bulletin*, 128, pp. 122–146. <https://doi.org/10.1130/B31253.1>
- van Staal, C.R., Barr, S.M., McCausland, P.J.A., Thompson, M.D., and White, C. E. 2020. Tonian-Ediacaran tectonomagmatic evolution of West Avalonia and its Ediacaran - early Cambrian interactions with Ganderia: an example of complex terrane transfer due to arc-arc collision? In *Pannotia to Pangaea: Neoproterozoic and Paleozoic orogenic cycles in the circum-Atlantic region*. Edited by J.B. Murphy, R.A. Strachan, and C. Quesada. Geological Society, London, Special Publications, 503, pp. 143–167. <https://doi.org/10.1144/SP503-2020-23>
- Van Wagoner, N.A., Leybourne, M.I., Dadd, L.A., Baldwin, D.K., and McNeil, W. 2002. Late Silurian bimodal volcanism of southwestern New Brunswick, Canada: Products of continental extension. *Geological Society of America, Bulletin*, 114, pp. 400–418. [https://doi.org/10.1130/0016-7606\(2002\)114<0400:LSBVOS>2.0.CO;2](https://doi.org/10.1130/0016-7606(2002)114<0400:LSBVOS>2.0.CO;2)
- Vermeesch, P. 2004. How many grains are needed for a provenance study? *Earth and Planetary Science Letters*, 224, pp. 441–451. <https://doi.org/10.1016/j.epsl.2004.05.037>
- Waldron, J.W.F., White, C.E., Barr, S.M., Simonetti, A., and Heaman, L.M. 2009. Provenance of the Meguma terrane, Nova Scotia: Rifted margin of early Paleozoic Gondwana. *Canadian Journal of Earth Sciences*, v. 46, pp. 1–8. <https://doi.org/10.1139/E09-004>
- Waldron, J.W.F., Schofield, D.I., Dufrane, S.A., Floyd, J.D., Crowley, Q.G., Simonetti, A., Dokken, R.J., and Pothier, H.D. 2014. Ganderia-Laurentia collision in the Caledonides of Great Britain and Ireland. *Geological Society, London, Journal*, 171, pp. 555–569. <https://doi.org/10.1144/jgs2013-131>
- Waldron, J.W.F., Schofield, D.I., and Murphy, J.B. 2018. Diachronous Paleozoic accretion of peri-Gondwanan terranes at the Laurentian margin. In *Fifty years of the Wilson cycle concept in plate tectonics*. Edited by R.W. Wilson, G.A. Houseman, K.J.W. McCaffrey, A.G. Dore',

- and S.J.H. Buiter. Geological Society, London, Special Publications, 470, pp. 289–310. <https://doi.org/10.1144/SP470.11>
- Walsh, G.J. and Merschat, A.J. 2015. Bedrock geologic map of the Worcester South quadrangle, Worcester County, Massachusetts. U.S. Geological Survey, Scientific Investigations, Map 3345, scale 1:24 000. <https://doi.org/10.3133/sim3345>
- Walsh, G.J., Aleinikoff, J.N., and Dorais, M.J. 2009. Tectonic history of the Avalon and Nashoba terranes along the western flank of the Milford antiform, Massachusetts. Geological Society of America, Northeastern Section, 44th Annual Meeting, Abstracts with Programs, 41, no. 3, p. 98. <https://gsa.confex.com/gsa/2009NE/webprogram/Paper155504.html>
- Walsh, G.J., Aleinikoff, J.N., and Dorais, M.J. 2011a. Bedrock geologic map of the Grafton quadrangle, Worcester County, Massachusetts. U.S. Geological Survey, Scientific Investigations, Map 3171, 39 p., 1:24 000. <https://doi.org/10.3133/sim3171>
- Walsh, G.J., Aleinikoff, J.N., Wintsch, R.P., and Ayuso, R.A. 2011b. Origin of the Quinebaug-Marlboro belt in southeastern New England. Geological Society of America, Northeastern (46th Annual) and North-Central (45th Annual) Joint Meeting, Abstracts with Programs, 43, no. 1, p.158. <https://gsa.confex.com/gsa/2011NE/webprogram/Paper184582.html>
- Walsh, G.J., Aleinikoff, J.N., Wintsch, R.P., and Ayuso, R.A. 2013a. Integrated bedrock mapping and geochronology in the terranes of southeastern New England. Geological Society of America, Northeastern Section, 48th Annual Meeting, Abstract with Programs, 45, no. 1, p. 65. <https://gsa.confex.com/gsa/2013NE/webprogram/Paper215305.html>
- Walsh, G.J., Jahns, R.H., and Aleinikoff, J.N. 2013b. Bedrock geologic map of the Nashua South quadrangle, Hillsborough County, New Hampshire, and Middlesex County, Massachusetts. U.S. Geological Survey, Scientific Investigations Map, 3200, 31 p., scale 1:24 000. <https://doi.org/10.3133/sim3200>
- Walsh, G.J., Aleinikoff, J.N., Wintsch, R.P., Ayuso, R.A., McAlleer, R.J., and Mershchat, A.J. 2015. Unravelling the prolonged history of the Ganderian margin of southeastern New England. Geological Society of America, Northeastern Section, 50th Annual Meeting Abstracts with Programs, 47, no. 1, p.42. <https://gsa.confex.com/gsa/2015NE/webprogram/Paper252525.html>
- Walsh, G.J., Aleinikoff, J.N., Ayuso, R.A., and Wintsch, R.P. 2021. Age and tectonic setting of the Quinebaug-Marlboro belt and implications for the history of Ganderian crustal fragments in southeastern New England, USA. *Geosphere*, 17, p. 1–63. <https://doi.org/10.1130/GES02295.1>
- Watts, B.G., Dorais, M.J., and Wintsch, R.P. 2000. Geochemistry of Early Devonian calc-alkaline plutons in the Merrimack Belt; implications for mid-Paleozoic terrane relationships in the New England Appalachians. *Atlantic Geology*, 36, pp. 79–102. <https://doi.org/10.4138/2013>
- West, D. P., Jr. and Condit, C.B. 2016. Stratigraphy, structure, and plutonism in the Wiscasset-Dresden region of mid-coastal Maine. In *Guidebook for field trips along the Maine coast from Maquoit Bay to Muscongus Bay*. Edited by H.N. Berry, IV and D. P. West, Jr. New England Intercollegiate Geological Conference, 108th Annual Meeting, Bath, Maine, Reprographics, Middlebury College, Middlebury, Vermont, pp. 165–182.
- West, D.P., Jr. and Hussey, A.M., II 2016. Middle Ordovician to Early Silurian terranes of the northern Casco Bay region, Maine. In *Guidebook for field trips along the Maine coast from Maquoit Bay to Muscongus Bay*. Edited by H. N. Berry, IV and D.P. West, Jr. New England Intercollegiate Geological Conference, 108th Annual Meetingg, Bath, Maine, Reprographics, Middlebury College, Middlebury, Vermont, pp. 249–266.
- West, D.P., Jr., Ludman, A., and Lux, D. R. 1992. Silurian age for the Pocomoonshine Gabbro-Diorite, southeastern Maine and its regional tectonic implications. *American Journal of Science*, 292, pp. 253–273. <https://doi.org/10.2475/ajs.292.4.253>
- West, D.P., Jr., Beal, H.M., and Grover, T.W. 2003. Silurian deformation and metamorphism of Ordovician arc rocks of the Casco Bay Group, south-central Maine. *Canadian Journal of Earth Sciences*, 40, pp. 887–905. <https://doi.org/10.1139/e03-021>
- West, D.P., Jr., Coish, R.A., and Tomascak, P.B. 2004. Tectonic setting and regional correlation of Ordovician metavolcanic rocks of the Casco Bay Group, Maine; evidence from trace element and isotope geochemistry. *Geological Magazine*, 141, pp. 125–140. <https://doi.org/10.1017/S0016756803008562>
- West, D.P., Jr., Hussey, A.M., II, Berry, H.N., IV, and Cubley, J. 2006. Bedrock geology across the Falmouth-Brunswick-Central Maine sequence boundary in southwestern Maine. In *Guidebook for field trips in Western Maine*. Edited by D. Gibson, J. Daly, and D. Reusch. New England Intercollegiate Geological Conference: 98th Annual Meeting, University of Maine, Farmington, Maine, pp. 44–56.
- West, D.P., Jr., Yates, M.G., Gerbi, C.C., and Bernard, N.Q. 2008. Metamorphosed Ordovician Fe- and Mn-rich rocks in south-central Maine: From peri-Gondwanan deposition through Acadian metamorphism. *The American Mineralogist*, 93, p. 270–282. <https://doi.org/10.2138/am.2008.2592>
- White, C.E., Barr, S.M., Bevier, M.L., and Kamo, S. 1994. A revised interpretation of the Cambrian and Ordovician rocks in the Bourinot belt in central Cape Breton Island, Nova Scotia. *Atlantic Geology*, 30, pp. 123–142. <https://doi.org/10.4138/2125>
- White, C.E. and Barr, S.M. 1996. Geology of the Brookville terrane, southern New Brunswick, Canada. In *Avalon and related peri-Gondwanan terranes of the circum-North Atlantic*. Edited by R.D. Nance and M. D. Thompson. Geological Society of America, Special Paper, 304, pp.

- 133–147. <https://doi.org/10.1130/0-8137-2304-3.133>
- Williams, H. 1978. Tectonic lithofacies map of the Appalachian Orogen. Memorial University of Newfoundland, Map 1, scale 1:1 000 000.
- Willner, A.P., Barr, S.M., Gerdes, A., Massonne, H.J., and White, C.E. 2013. Origin and evolution of Avalonia: evidence from U-Pb and Lu-Hf isotopes in zircon from the Mira terrane, Canada, and the Stavelot-Venn massif, Belgium. Geological Society, London, Journal, 170, pp. 769–784. <https://doi.org/10.1144/jgs2012-152>
- Willner, A.P., Gerdes, A., Massonne, H.J., van Staal, C.R., and Zagorevski, A. 2014. Crustal evolution of the northeast Laurentian margin and the peri-Gondwanan micro-continent Ganderia prior to and during closure of the Iapetus Ocean: Detrital zircon U-Pb and Hf isotope evidence from Newfoundland. Geoscience Canada, 41, pp. 345–364. <https://doi.org/10.12789/geocanj.2014.41.046>
- Wilson, R.A., van Staal, C.R., and McClelland, W.C. 2015. Synaccretionary sedimentary and volcanic rocks in the Ordovician Tetagouche backarc basin, New Brunswick, Canada: Evidence for a transition from foredeep to forearc basin sedimentation. American Journal of Science, 315, pp. 958–1001. <https://doi.org/10.2475/10.2015.03>
- Wilson, R.A., van Staal, C.R., and Komo, S.L. 2017. Rapid transition from the Salinic to Acadian orogenic cycles in the northern Appalachian orogen: Evidence from northern New Brunswick, Canada. American Journal of Science, 317, pp. 449–482. <https://doi.org/10.2475/04.2017.02>
- Wintsch, R.P., Aleinikoff, J.N., Walsh, G.J., Bothner, W.A., Hussey, A.M., and Fanning, C.M. 2007. SHRIMP U-Pb evidence for a late Silurian age of metasedimentary rocks in the Merrimack and Putnam-Nashoba terranes, eastern New England. American Journal of Science, 307, pp. 119–167. <https://doi.org/10.2475/01.2007.05>
- Wones, D.R. and Goldsmith, R. 1991. Intrusive rocks of eastern Massachusetts. In *The bedrock geology of Massachusetts*. Edited by N.L. Hatch, Jr. U.S. Geological Survey, Professional Paper 1366 E-J, pp. I1–I61.
- Yakymchuk, C., Kirkland, C.L., and Clark, C. 2018. Th/U ratios in metamorphic zircon. Journal of Metamorphic Geology, 36, pp. 715–737. <https://doi.org/10.1111/jmg.12307>
- Zagorevski, A. and van Staal, C.R. 2011. The record of Ordovician arc-arc and arc-continent collisions in the Canadian Appalachians during the closure of Iapetus. In *Arc-continent collisions*. Edited by D. Brown and P.D. Ryan. Frontiers in Science, Springer-Verlag, Berlin, Heidelberg, Chapter 12, pp.341–371. [https://doi.org/10.1007/978-3-540-88558-0\\_12](https://doi.org/10.1007/978-3-540-88558-0_12)
- Zagorevski, A., van Staal, C.R., and McNicoll, V.J., 2007a. Distinct Taconic, Salinic and Acadian deformation along the Iapetus suture zone, Newfoundland Appalachians. Canadian Journal of Earth Sciences, 44, pp. 1567–1585. <https://doi.org/10.1139/e07-037>
- Zagorevski, A., van Staal, C.R., McNicoll, V., and Rogers, N. 2007b. Upper Cambrian to Upper Ordovician peri-Gondwanan island arc activity in the Victoria Lake Supergroup, Central Newfoundland: Tectonic development of the northern Ganderian margin. American Journal of Science, 307, pp. 339–370. <https://doi.org/10.2475/02.2007.02>
- Zagorevski, A., van Staal, C.R., McNicoll, V., Rogers, N., and Valverde-Vaquero. P. 2008. Tectonic architecture of an arc-arc collision zone, Newfoundland Appalachians. In *Formation and applications of the sedimentary record in arc collision zones*. Edited by A. Draut, P.D. Clift, and D.W. Scholl. Geological Society of America, Special Paper, 436, pp. 309–334. [https://doi.org/10.1130/2008.2436\(14\)](https://doi.org/10.1130/2008.2436(14))
- Zagorevski, A., van Staal, C.R., Rogers, N., McNicoll, V., Dunning, G.R., and Pollock, J.C. 2010. Middle Cambrian to Ordovician arc-backarc development on the leading edge of Ganderia, Newfoundland Appalachians. In *From Rodinia to Pangea: The lithotectonic record of the Appalachian region*. Edited by R.P. Tollo, M.J. Batholomew, J.P. Hibbard, and P.M. Karabinos. Geological Society of America, Memoir, 206, pp. 367–396. [https://doi.org/10.1130/2010.1206\(16\)](https://doi.org/10.1130/2010.1206(16))
- Zartman, R.E. and Naylor, R.S. 1984. Structural implications of some radiometric ages of igneous rocks in southeastern New England. Geological Society of America, Bulletin, 95, pp. 522–539. [https://doi.org/10.1130/0016-7606\(1984\)95<522:SIOSRA>2.0.CO;2](https://doi.org/10.1130/0016-7606(1984)95<522:SIOSRA>2.0.CO;2)
- Zartman, R.E. and Marvin, R.F. 1991. Radiometric ages of rocks in Massachusetts. In *The bedrock geology of Massachusetts*. Edited by N.L. Hatch, Jr. U.S. Geological Survey, Professional Paper, 1366 E-J, p. J1–J19.
- Zen, E., editor, Goldsmith, R., Ratcliffe, N.M., Robinson, P., and Stanley, R.S., compilers, 1983. Bedrock geologic map of Massachusetts. United States Geological Survey, Special Geologic Map, scale 1:250 000.

*Editorial responsibility:* David P. West, Jr.

## APPENDIX

## Sample Locations and LA-ICPMS U-Pb zircon data

**Table A1.** Sample locations.

Unit name	Sample number	Coordinates	Location description
<b>Nashoba terrane</b>			
Marlboro Formation	MLMR1	42°19'56.21"N, 71°36'01.70"W	Hayes Memorial Drive, Marlborough, MA.
	MLMR2	42°20'49.35"N, 71°32'52.56"W	Main St. in Marlborough, MA. This is the type- locality of Marlboro Formation schist (Emerson, 1917).
	MLMR5	42°23'45.65"N, 71°28'24.11"W	Massachusetts Fire Fighting Academy in Stowe, MA.
	MLMR6	42°21'35.19"N, 71°31'30.10"W	From a small outcrop in a housing development in Marlborough, MA. The unit was located along strike with the Main St. exposures.
Shawsheen Gneiss	MLSG1	42°31'34.98"N, 71°15'17.17"W	Fresh exposures adjacent to the parking lot of an industrial park at 900 Middlesex Turnpike in Billerica, MA. The samples were collected at multiple locations around the industrial park to ensure a statistical representation of detrital zircon populations across layers.
Nashoba Formation	MLNB1	42°19'50.51"N, 71°40'15.87"W	Fresh exposure due to blasting for a new housing development at Church St. Village, Northboro, MA.
	MLBM1	42°22'50.87"N, 71°38'43.12"W	From the spillway of a flood control dam in Berlin, MA.
	MLNS1	42°20'25.45"N, 71°39'48.17"W	Green Street, Northboro, MA.
Tadmuck Brook Schist	MLTMBC	42°31'55.27"N, 71°31'30.25"W	A combination of several samples taken within 50 m along one continuous road outcrop in Littleton, MA.
<b>Merrimack belt</b>			
Kittery Formation	KSCTI	43°5'12.1"N, 070°46' 06.2" W	Stop 1 of the 1995 NEIGC field trip guide, trip II (Fargo and Bothner, 1995). Located on Michael Succi Drive, Portsmouth, NH, near the National Gypsum Plant.
Eliot Formation	KSELI	43°8'53.9"N, 070°58' 38.9"W	Stop 5, trip A2, NEIGC field trip guide, 1995, p. A2-9 (Fargo and Bothner, 1995). Located at Lee Five Corners, Lee, NH at the intersections of Route 155 and Route 4.
Berwick Formation	KSBDI	43°10'51.3"N, 070°56'51.2"W	Located at the MSPCA/Nevins Farm on Route 28, Methuen, MA near the rear of the property next to a storage facility.
Oakdale Formation	KSOKI	42°23'47.5"N, 071°47'03.9"W	Stop 2, trip F2, NEIGC field trip guide, 1976, p. 373 (Hepburn, 1976). Located in West Boylston, MA along a set of railroad tracks about 150 meters west of Prescott St.
Worcester Formation	KWSWI	42°22'14.4"N, 071°44'53.1"W	Stop 1, trip F-2, NEIGC field trip guide, 1976, p. 372 (Hepburn, 1976). Located on the shore of the Wachusett reservoir on the east side of Shalon Point in Boylston, MA.
Paxton Formation	KSPXIII	42°31'12.5"N, 071°46'22.40"W	Located at Barrett Park, located off Chestnut St., Leominster, MA. The outcrop was located along the edge of the parking lot near the information center of the park.
Tower Hill Formation	KSTHI	42°20'59.1"N, 071°44'23.67"W	Located directly behind the Boylston Fire Station off of Main St., Boylston, MA on Diamond Hill.

Table A2. LA-ICPMS data.

Sample/ Analysis	Measured Isotopic Ratios						Calculated Ages (Ma)								Detrital (Ma)		Metamorphic (Ma)		CA-TIMS (Ma)				
	$^{207}\text{Pb}/^{235}\text{U}$	$\pm 1\sigma$	$^{206}\text{Pb}/^{238}\text{U}$	$\pm 1\sigma$	Rho	$^{207}\text{Pb}/^{206}\text{Pb}$	$\pm 1\sigma$	$^{207}\text{Pb}/^{235}\text{U}$	$\pm 1\sigma$	$^{206}\text{Pb}^{238}\text{U}$	$\pm 1\sigma$	$^{207}\text{Pb}/^{206}\text{Pb}$	$\pm 1\sigma$	U-Pb/Pb-Pb concordancy (%)	Concordia age	$\pm 2\sigma$	Probability of concordance	Th/U	For Prob Dens plots age	For Prob Dens plots age	$^{206}\text{Pb}/^{238}\text{U}$	$\pm 2\sigma$	
<b>NASHOBA ERRANE</b>																							
<b>Marlboro Formation (MLMRC)</b>																							
mr04a20	0.442	0.031	0.047	0.004	0.67	0.068	0.001	372	22	293	27	857	23		34	353	43	0.00	0.014				
mr04a19	0.508	0.038	0.058	0.005	0.59	0.063	0.001	417	26	361	31	719	29		50	401	50	0.03	0.023				
mr04a24	0.519	0.015	0.063	0.001	0.37	0.062	0.000	424	10	397	8	666	16		60	406	15	0.01	0.008				
mr04a28	3.142	0.310	0.189	0.017	0.46	0.110	0.002	1443	76	1115	93	1796	25		62	1296	153	0.00	0.455				
mr04a34	5.856	0.301	0.318	0.011	0.34	0.126	0.002	1955	45	1778	55	2044	23		87	1885	83	0.00	0.207				
mr04a33	5.980	0.272	0.318	0.012	0.41	0.129	0.001	1973	40	1780	58	2083	17		85	1927	78	0.00	0.620				
mr04a26	0.452	0.078	0.052	0.009	0.50	0.055	0.001	379	55	324	55	415	50		78	350	96	0.32	0.033		324	55	
mr04a16	0.481	0.015	0.061	0.002	0.46	0.058	0.000	399	10	379	10	525	14		72	389	18	0.07	0.011		379	10	
mr04a35	0.497	0.048	0.061	0.003	0.30	0.055	0.001	410	33	381	21	428	53		89	387	40	0.39	0.035		381	21	
mr04a10	0.529	0.044	0.062	0.005	0.52	0.062	0.000	431	29	386	32	660	16		58	412	53	0.14	0.006		386	32	
mr04a08	0.542	0.033	0.065	0.005	0.61	0.061	0.001	440	22	408	29	639	20		64	435	43	0.18	0.086		408	29	
mr04a14	0.586	0.095	0.066	0.010	0.46	0.065	0.001	468	61	411	60	771	26		53	437	105	0.36	0.111		411	60	
sel14a97	0.507	0.080	0.068	0.004	0.18	0.060	0.003	417	54	424	24	617	96		69	423	46	0.89	0.023		424	24	
mr04a31	0.562	0.053	0.070	0.004	0.32	0.060	0.001	453	35	434	26	594	44		73	439	47	0.61	0.611		434	26	1
mr04a09	0.531	0.028	0.071	0.004	0.52	0.056	0.000	432	19	440	23	453	20		97	434	35	0.73	0.005		440	23	
mr04a17	0.598	0.055	0.071	0.007	0.51	0.062	0.001	476	35	443	40	665	24		67	464	65	0.39	0.039		443	40	
mr04a06	0.589	0.061	0.076	0.008	0.48	0.058	0.002	470	39	470	46	515	93		91	470	72	1.00	0.182		470	46	
sel14a99	0.755	0.092	0.081	0.005	0.25	0.063	0.003	571	53	504	29	715	87		70	514	56	0.22	2.968		504	29	
mr04a05	0.715	0.033	0.086	0.003	0.39	0.059	0.001	548	19	529	18	551	41		96	537	31	0.37	0.889		529	18	
mr04a27	0.784	0.052	0.086	0.005	0.41	0.060	0.001	588	30	531	28	586	29		91	555	49	0.07	0.922		531	28	
mr04a07	0.793	0.062	0.088	0.004	0.27	0.068	0.001	593	35	545	22	879	37		62	555	42	0.20	0.871		545	22	
sel14a98	0.898	0.084	0.104	0.007	0.34	0.062	0.001	651	45	640	39	679	23		94	644	68	0.83	0.240		640	39	
mr04a32	10.966	0.283	0.466	0.010	0.42	0.154	0.001	2520	24	2476	45	2393	11		103	2516	48	0.19	0.364		2393	11	
sel14a95	12.946	0.337	0.511	0.013	0.49	0.172	0.002	2676	25	2661	56	2581	18		103	2676	49	0.77	0.595		2581	18	
sel14a94	30.084	0.955	0.745	0.020	0.42	0.280	0.003	3490	31	3588	73	3364	15		107	3490	62	0.14	0.356		3364	15	
<b>Shawsheen gneiss (MLSGL)</b>																							
mr05a31	0.509	0.025	0.054	0.002	0.33	0.072	0.001	418	16	338	10	980	29		34	352	20	0.00	0.322				
mr06a120	0.788	0.039	0.069	0.003	0.45	0.083	0.001	590	22	428	18	1260	24		34	467	34	0.00	1.083				
mr05a10	0.799	0.033	0.078	0.003	0.44	0.071	0.001	597	19	486	17	963	31		50	527	31	0.00	0.621				
mr06a77	0.845	0.084	0.083	0.005	0.28	0.072	0.002	622	46	512	27	995	67		51	528	52	0.02	0.534				
mr05a39	0.750	0.023	0.083	0.002	0.35	0.064	0.001	568	13	515	11	737	25		70	532	20	0.00	0.326				
mr06a66	0.788	0.031	0.086	0.002	0.35	0.065	0.001	590	17	530	14	787	30		67	548	25	0.00	0.762				
sel13a72	1.002	0.047	0.086	0.003	0.38	0.074	0.001	705	24	533	19	1047	38		51	571	35	0.00	0.189				
mr06a141	0.859	0.062	0.087	0.004	0.30	0.071	0.002	630	34	535	22	964	46		55	554	43	0.01	0.622				
mr06a89	1.068	0.090	0.088	0.003	0.20	0.084	0.001	738	44	541	18	1297	58		42	551	35	0.00	0.262				
sel13a79	1.132	0.044	0.089	0.003	0.37	0.080	0.001	769	21	547	15	1197	25		46	582	29	0.00	0.333				
mr05a13	1.076	0.037	0.090	0.002	0.37	0.086	0.001	742	18	558	14	1340	21		42	596	26	0.00	0.153				
mr06a76	0.904	0.076	0.091	0.012	0.76	0.063	0.001	654	41	561	69	712	42		79	676	77	0.04	0.875				
mr06a81	2.014	0.134	0.092	0.003	0.28	0.151	0.001	1120	45	567	20	2353	43		24	562	40	0.00	1.099				
sel13a70	1.094	0.145	0.095	0.010	0.41	0.079	0.001	750	70	583	60	1163	20		50	632	111	0.02	0.216				
sel13a78	0.875	0.034	0.097	0.001	0.20	0.060	0.001	638	18	600	9	591	30		102	604	17	0.04	0.735				
mr06a69	0.925	0.041	0.099	0.003	0.32	0.066	0.001	665	22	606	16	822	30		74	622	30	0.01	0.652				
mr06a58	1.720	0.119	0.124	0.007	0.39	0.098	0.001	1016	44	751	38	1590	21		47	817	72	0.00	0.212				
mr05a20	1.713	0.095	0.145	0.004	0.27	0.083	0.001	1013	35	872	24	1274	27		68	901	46	0.00	0.066				
sel13a76	1.904	0.160	0.154	0.007	0.29	0.090	0.002	1083	56	922	42	1424	34		65	960	77	0.01	0.445				
sel13a81	2.107	0.108	0.174	0.008	0.43	0.080	0.001	1151	35	1033	42	1187	21		87	1105	66	0.00	0.207				
sel13a62	0.458	0.120	0.175	0.007	0.41	0.099	0.001	1260	35	1042	38	1613	16		65	1147	65	0.00	0.348				
mr06a108	2.737	0.252	0.179	0.010	0.30	0.117	0.001	1339	68	1064	54	1913	19		56	1126	101	0.00	0.163				
mr06a55	2.788	0.255	0.195	0.014	0.39	0.100	0.001	1352	68	1148	75	1621	2										

Table A2. Continued.

Sample/ Analysis	Measured Isotopic Ratios						Calculated Ages (Ma)								Detrital (Ma)		Metamorphic (Ma)			CA-TIMS (Ma)		
	$^{207}\text{Pb}/^{235}\text{U}$	$\pm 1\sigma$	$^{206}\text{Pb}/^{238}\text{U}$	$\pm 1\sigma$	Rho	$^{207}\text{Pb}/^{206}\text{Pb}$	$\pm 1\sigma$	$^{207}\text{Pb}/^{235}\text{U}$	$\pm 1\sigma$	$^{206}\text{Pb}^{2/3}$	$^{207}\text{Pb}/^{206}\text{Pb}$	$\pm 1\sigma$	Concordia age	$\pm 2\sigma$	Probability of concordance (%)	Th/U	For Prob Dens plots age	For Prob Dens plots age	$^{206}\text{Pb}/^{238}$ U	$\pm 1\sigma$		
mr06a99	0.817	0.046	0.091	0.003	0.32	0.065	0.001	607	26	563	19	784	29	72	575	36	0.11	0.551	563	19		
se13a80	0.804	0.048	0.091	0.003	0.26	0.062	0.001	599	27	563	17	685	39	82	570	32	0.20	0.688	563	17		
mr06a50	0.795	0.032	0.092	0.002	0.30	0.062	0.001	594	18	564	13	675	32	84	573	24	0.12	0.631	564	13		
mr04a89	0.724	0.072	0.091	0.005	0.27	0.061	0.002	553	43	564	29	623	57	91	561	54	0.81	0.618	564	29		
mr06a51	0.747	0.070	0.093	0.003	0.18	0.060	0.002	566	41	571	19	604	66	95	570	36	0.92	0.724	571	19		
mr05a53	0.864	0.064	0.093	0.003	0.20	0.071	0.002	632	35	572	16	958	55	60	578	32	0.10	1.059	572	16		
mr06a48	0.740	0.058	0.093	0.004	0.25	0.062	0.002	562	34	573	21	660	64	87	570	40	0.77	0.818	573	21		
mr05a43	0.743	0.037	0.093	0.003	0.27	0.059	0.001	564	22	574	15	561	40	102	572	27	0.65	0.487	574	15		
mr06a15	0.810	0.050	0.093	0.003	0.29	0.061	0.001	603	28	576	20	628	42	92	583	37	0.37	0.565	576	20		
mr06a135	0.799	0.060	0.093	0.003	0.22	0.067	0.002	596	34	576	18	824	55	70	579	35	0.57	0.610	576	18		
mr05a21	0.741	0.038	0.094	0.002	0.23	0.060	0.001	563	22	579	13	608	41	95	576	24	0.49	0.461	579	13		
mr06a59	0.774	0.067	0.094	0.004	0.27	0.060	0.002	582	38	581	26	602	60	97	581	47	0.98	1.541	581	26		
mr06a60	0.770	0.069	0.095	0.008	0.50	0.053	0.002	580	40	584	50	318	71	184	581	75	0.92	0.444	584	50		
mr06a46	0.844	0.069	0.096	0.007	0.42	0.063	0.001	621	38	591	39	698	42	85	606	66	0.46	0.722	591	39		
mr05a08	0.802	0.025	0.097	0.002	0.31	0.061	0.001	598	14	597	11	626	18	95	597	20	0.96	1.087	597	11		
mr05a24	0.824	0.028	0.097	0.003	0.40	0.061	0.001	610	15	599	15	650	18	92	604	26	0.51	0.644	599	15		
mr06a15	0.806	0.029	0.099	0.002	0.33	0.058	0.001	600	16	606	14	534	32	113	604	24	0.72	0.300	606	14		
mr06a148	0.733	0.064	0.099	0.005	0.29	0.054	0.002	559	38	607	29	366	66	166	590	52	0.23	0.509	607	29		
mr06a88	0.940	0.089	0.100	0.010	0.52	0.065	0.001	673	47	613	57	788	44	78	654	89	0.25	0.769	613	57		
mr05a49	0.902	0.060	0.100	0.004	0.33	0.069	0.001	653	32	615	26	901	44	68	627	46	0.27	0.343	615	26		
mr05a37	0.758	0.036	0.100	0.003	0.27	0.059	0.001	573	21	616	15	551	34	112	603	27	0.05	0.391	616	15		
mr05a50	0.910	0.055	0.101	0.004	0.30	0.067	0.002	657	29	619	21	841	47	74	629	39	0.21	0.682	619	21		
mr06a151	0.887	0.069	0.101	0.004	0.29	0.065	0.001	645	37	620	26	787	39	79	626	48	0.52	0.894	620	26		
mr06a13	0.857	0.073	0.101	0.006	0.32	0.061	0.002	628	40	621	33	640	66	97	624	58	0.86	0.880	621	33		
mr06a95	0.868	0.035	0.101	0.003	0.33	0.061	0.001	635	19	622	16	637	30	98	626	28	0.53	0.851	622	16		
mr05a38	0.863	0.086	0.103	0.009	0.45	0.060	0.001	632	47	633	54	600	48	106	632	85	0.99	0.472	633	54		
mr06a57	0.880	0.051	0.104	0.004	0.27	0.058	0.001	597	29	639	21	538	41	119	626	37	0.16	0.560	639	21		
mr06a147	0.900	0.034	0.105	0.003	0.43	0.060	0.001	652	18	641	19	596	23	108	647	32	0.59	0.470	641	19		
mr05a58	0.839	0.034	0.105	0.003	0.29	0.060	0.001	619	19	645	15	604	26	107	636	26	0.20	0.789	645	15		
mr06a145	0.906	0.050	0.107	0.004	0.32	0.061	0.001	655	27	653	22	647	41	101	654	39	0.96	0.797	653	22		
mr06a127	0.898	0.042	0.107	0.003	0.31	0.062	0.001	651	23	654	18	664	34	98	653	32	0.90	0.134	654	18		
mr06a14	0.933	0.111	0.107	0.005	0.21	0.069	0.002	669	58	656	31	892	52	74	658	58	0.82	0.162	656	31		
mr06a86	0.988	0.049	0.108	0.004	0.33	0.061	0.001	698	25	663	21	650	45	102	675	37	0.19	0.710	663	21		
mr06a110	0.981	0.080	0.109	0.011	0.61	0.061	0.001	694	41	669	64	630	28	106	693	82	0.62	0.278	669	64		
mr05a07	0.888	0.039	0.110	0.003	0.31	0.061	0.001	645	21	670	17	623	31	108	661	30	0.26	0.847	670	17		
mr06a157	0.980	0.054	0.110	0.003	0.28	0.064	0.001	694	28	672	20	732	38	92	678	36	0.46	0.074	672	20		
mr05a52	0.904	0.055	0.113	0.004	0.27	0.064	0.001	654	29	689	22	737	48	93	678	39	0.26	0.636	689	22		
mr05a47	1.236	0.214	0.114	0.015	0.37	0.085	0.001	817	97	693	85	1311	26	53	735	153	0.24	0.203	693	85		
mr06a79	1.238	0.092	0.126	0.006	0.35	0.072	0.002	818	42	764	37	985	54	78	785	65	0.24	0.205	764	37		
mr06a129	1.238	0.056	0.129	0.004	0.35	0.066	0.001	818	25	782	23	800	31	98	797	40	0.20	0.215	782	23		
mr05a40	1.369	0.160	0.149	0.008	0.22	0.073	0.002	876	68	897	44	1005	45	89	892	80	0.77	0.601	1005	45		
mr06a68	1.664	0.136	0.153	0.010	0.40	0.076	0.001	995	52	918	55	1084	32	85	958	91	0.19	0.144	1084	32		
mr06a106	1.808	0.102	0.167	0.008	0.43	0.077	0.001	1048	37	994	45	1111	27	89	1029	68	0.21	0.160	1111	27		
mr06a49	1.956	0.099	0.180	0.007	0.41	0.078	0.001	1101	34	1067	41	1138	16	94	1089	62	0.42	0.307	1138	16		
mr06a80	2.212	0.178	0.189	0.012	0.41	0.085	0.001	1185	56	1118	67	1315	34	85	1160	103	0.33	0.542	1315	34		
mr06a45	2.360	0.193	0.192	0.012	0.37	0.086	0.001	1231	58	1132	62	1347	33	84	1183	102	0.15	0.260	1347	33		
mr06a116	2.147	0.050	0.194	0.004	0.42	0.077	0.001	1164	16	1145	21	1126	14	102	1158	30	0.36	0.331	1126	14		
mr05a41	2.742	0.139	0.215	0.008	0.38	0.095	0.001	1340	38	1253	44	1536	25	82	1305	69	0.06	0.204	1536	25		
mr06a70	3.389	0.297	0.230	0.017	0.41	0.104	0.001	1502	69	1336	87	1702	25	78	1442	131	0.05	0.296	1702	25		
mr05a33	3.274	0.188	0.240	0.016	0.57	0.093	0.001	1475	45	1387	82	1486	28	93	1476	89	0.18	0.495	1486	28		
se13a39	2.975	0.178	0.252	0.013	0.43	0.098	0.002	1401	46	1448	67	1581	40	92	1409	88	0.45	0.198	1581	40		
mr05a28	3.269	0.093	0.256	0.007	0.45	0.090	0.001	1474	22	1471	34	1426	22	103	1473	43	0.94	1.670	1426	22		
mr05a17	3.287	0.071	0.257	0.005	0.4																	

Table A2. Continued.

Sample/ Analysis	Measured Isotopic Ratios						Calculated Ages (Ma)								Detrital (Ma)		Metamorphic (Ma)			CA-TIMS (Ma)		
	$^{207}\text{Pb}/^{235}\text{U}$	$\pm 1\sigma$	$^{206}\text{Pb}/^{238}\text{U}$	$\pm 1\sigma$	Rho	$^{207}\text{Pb}/^{206}\text{Pb}$	$\pm 1\sigma$	$^{207}\text{Pb}/^{235}\text{U}$	$\pm 1\sigma$	$^{206}\text{Pb}^2/^{238}\text{U}$	$\pm 1\sigma$	$^{207}\text{Pb}/^{206}\text{Pb}$	$\pm 1\sigma$	Concordia concordancy (%)	age	$\pm 2\sigma$	Probability of concordance	Th/U	For Prob Dens plots age	For Prob Dens plots age	$^{206}\text{Pb}/^{238}\text{U}$	$\pm 2\sigma$
mr02a14	0.449	0.036	0.057	0.002	0.25	0.058	0.001	376	25	360	14	523	46	69	363	27	0.52	0.024		360	14	
mr02a19	0.422	0.033	0.058	0.003	0.30	0.053	0.001	357	23	366	16	312	41	117	364	30	0.72	0.021		366	16	
mr02a15	0.491	0.031	0.060	0.003	0.39	0.056	0.001	405	21	375	18	463	34	81	385	32	0.17	0.019		375	18	
mr04a43	0.459	0.015	0.061	0.001	0.36	0.054	0.001	384	10	384	9	372	28	103	384	15	0.99	0.008		384	9	
mr06a09	0.507	0.023	0.062	0.003	0.49	0.055	0.001	416	15	386	16	415	28	93	403	28	0.06	0.037		386	16	
mr02a44	0.506	0.035	0.063	0.003	0.34	0.057	0.001	416	23	392	18	507	38	77	399	33	0.33	0.157		392	18	
mr02a23	0.519	0.032	0.063	0.002	0.25	0.058	0.001	424	21	393	12	511	44	77	398	23	0.15	0.013		393	12	
mr04a50	0.477	0.016	0.063	0.002	0.38	0.054	0.001	396	11	397	10	390	25	102	397	17	0.95	0.007		397	10	
mr04a46	0.505	0.027	0.064	0.003	0.45	0.056	0.001	418	18	402	19	454	31	89	409	31	0.50	0.029		402	19	
mr06a08	0.472	0.032	0.065	0.003	0.35	0.052	0.001	393	22	404	19	277	47	146	400	33	0.64	0.016		404	19	
mr06a29	0.486	0.021	0.065	0.002	0.27	0.056	0.001	402	15	408	9	470	34	87	406	18	0.71	0.034		408	9	
mr04a64	0.496	0.022	0.067	0.003	0.42	0.055	0.001	409	15	415	15	425	23	98	412	26	0.68	0.030		415	15	
mr02a07	0.485	0.019	0.067	0.001	0.28	0.054	0.001	401	13	419	9	385	29	109	414	16	0.19	0.008		419	9	
mr02a37	0.498	0.023	0.067	0.002	0.38	0.053	0.001	410	16	420	14	343	22	122	416	25	0.55	0.005		420	14	
mr06a28	0.518	0.015	0.068	0.001	0.33	0.055	0.001	424	10	425	8	396	23	107	425	14	0.88	0.184		425	8	
mr02a40	0.491	0.031	0.069	0.002	0.23	0.058	0.001	406	21	429	12	534	39	80	425	23	0.28	0.089		429	12	
mr06a34	0.550	0.028	0.070	0.003	0.35	0.055	0.001	445	19	437	15	428	32	102	440	27	0.69	0.022		437	15	
mr02a17	0.581	0.028	0.071	0.002	0.30	0.057	0.001	465	18	444	12	489	41	91	449	22	0.26	0.0408		444	12	
mr02a67	0.575	0.037	0.072	0.002	0.21	0.063	0.001	461	24	445	12	718	41	62	447	23	0.51	0.032		445	12	
mr02a08	0.538	0.034	0.073	0.002	0.27	0.057	0.001	437	22	451	15	492	43	92	448	27	0.54	0.027		451	15	
mr02a79	0.679	0.115	0.073	0.002	0.09	0.113	0.004	526	69	454	13	1846	57	25	455	26	0.31	0.037		454	13	
mr06a25	0.556	0.030	0.074	0.002	0.31	0.055	0.001	449	20	458	15	405	38	113	455	27	0.67	0.175	458	15		
mr06a39	0.607	0.025	0.074	0.002	0.40	0.058	0.001	482	16	463	15	513	31	90	471	26	0.26	0.439	463	15		
mr04a87	0.532	0.056	0.075	0.004	0.24	0.058	0.001	433	37	468	27	524	47	89	457	49	0.37	0.624	468	27		
mr06a17	0.582	0.025	0.076	0.002	0.33	0.053	0.001	466	16	471	13	339	41	139	469	23	0.76	0.289	471	13		
mr02a31	0.618	0.048	0.077	0.002	0.21	0.061	0.001	488	30	476	15	641	49	74	478	29	0.69	0.208	476	15		
mr06a19	0.564	0.047	0.077	0.004	0.31	0.055	0.001	454	31	477	24	414	54	115	469	43	0.47	0.643	477	24		
mr02a34	0.608	0.037	0.077	0.002	0.26	0.061	0.001	482	23	477	11	657	49	73	478	22	0.82	0.050	477	11		
mr02a06	0.580	0.026	0.077	0.002	0.32	0.057	0.001	464	17	480	13	477	36	101	475	24	0.39	0.445	480	13	465.9 0.7	
mr06a20	0.664	0.034	0.077	0.003	0.37	0.059	0.001	517	20	481	17	556	38	87	494	31	0.09	0.174	481	17		
mr06a07	0.620	0.069	0.078	0.004	0.21	0.056	0.001	490	43	483	21	444	46	109	484	41	0.87	0.591	483	21		
mr02a18	0.661	0.044	0.078	0.003	0.31	0.065	0.001	515	27	484	19	769	44	63	491	35	0.26	0.372	484	19		
mr05a68	0.668	0.036	0.080	0.003	0.36	0.059	0.001	519	22	495	19	578	26	86	504	33	0.30	0.180	495	19		
mr02a10	0.691	0.051	0.080	0.004	0.33	0.062	0.001	534	31	497	23	661	26	75	508	42	0.26	0.081	497	23		
mr04a52	0.607	0.026	0.080	0.003	0.42	0.055	0.001	482	16	499	17	428	25	117	490	28	0.34	1.101	499	17		
mr05a82	0.669	0.034	0.081	0.004	0.44	0.061	0.001	520	21	501	22	622	30	81	511	36	0.40	0.097	501	22		
mr02a49	0.644	0.050	0.081	0.004	0.36	0.057	0.002	505	31	503	27	494	65	102	504	47	0.96	0.028	503	27		
mr06a14	0.671	0.024	0.081	0.002	0.30	0.059	0.001	521	15	504	11	584	25	86	509	19	0.27	1.068	504	11		
mr02a35	0.693	0.063	0.081	0.005	0.31	0.060	0.001	535	38	504	27	586	46	86	512	50	0.43	0.027	504	27		
mr05a87	0.725	0.051	0.082	0.004	0.35	0.061	0.001	554	30	509	24	647	44	79	523	44	0.16	0.245	509	24		
mr02a45	0.734	0.153	0.082	0.014	0.41	0.063	0.002	559	89	510	84	720	60	71	531	146	0.61	0.049	510	84		
mr05a89	0.662	0.031	0.082	0.003	0.36	0.058	0.001	516	19	511	17	526	26	97	513	30	0.80	1.366	511	17		
mr04a62	0.658	0.045	0.083	0.004	0.34	0.060	0.001	518	23	512	23	614	34	83	513	41	0.97	0.724	512	23		
mr04a44	0.625	0.023	0.083	0.002	0.37	0.056	0.002	468	47	519	28	508	68	102	508	52	0.29	1.054	519	28		
mr02a32	0.689	0.029	0.085	0.002	0.34	0.056	0.001	532	17	524	14	462	32	113	527	25	0.65	1.074	524	14		
mr02a80	0.753	0.055	0.085	0.003	0.28	0.071	0.001	570	32	527	20	952	35	55	536	38	0.20	0.321	527	20		
mr04a41	0.635	0.044	0.086	0.004	0.36	0.057	0.001	499	27	531	26	508	30	105	516	43	0.29	1.120	531	26		
mr02a78	0.708	0.023	0.086	0.002	0.41	0.058	0.001	544	13	531	13	537	22	99	537	22	0.36	2.266	531	13		
mr02a13	0.718	0.069	0.086	0.005	0.32	0.061	0.001	550	41	532	31	627	30	85	537	57	0.68	0.929	532	31		
mr04a68	0.679	0.041	0.086	0.004	0.37	0.060	0.001	526	25	532	23	600	19	89	529	39	0.85	0.784	532	23		
mr06a35	0.671	0.045	0.086	0.003	0.30	0.057	0.001	509	53	540	36	505	57	107	532	65	0.57	0.786	540	36		
mr02a42	0.636	0.064	0.086	0.004	0.25	0.059	0.001	500	40	535	26	577	49	93	526	47	0.40	1.040				

Table A2. Continued.

Sample/ Analysis	Measured Isotopic Ratios						Calculated Ages (Ma)								Detrital (Ma)		Metamorphic (Ma)			CA-TIMS (Ma)					
	$^{207}\text{Pb}/^{235}\text{U}$	$\pm 1\sigma$	$^{206}\text{Pb}/^{238}\text{U}$	$\pm 1\sigma$	Rho	$^{207}\text{Pb}/^{206}\text{Pb}$	$\pm 1\sigma$	$^{207}\text{Pb}/^{235}\text{U}$	$\pm 1\sigma$	$^{206}\text{Pb}^2/^{238}\text{U}$	$\pm 1\sigma$	$^{207}\text{Pb}/^{206}\text{Pb}$	$\pm 1\sigma$	Concordia concordancy (%)	age	$\pm 2\sigma$	Probability of concordance	Th/U	For Prob Dens plots age	For Prob Dens plots age	$^{206}\text{Pb}/^{238}\text{U}$	$\pm 2\sigma$	notes		
mr02a87	2.693	0.197	0.228	0.013	0.40	0.082	0.002	1326	54	1322	71	1243	40	106	1325	101	0.95	0.201	1243	40					
mr02a16	2.986	0.105	0.235	0.006	0.34	0.089	0.001	1404	27	1360	30	1396	27	97	1385	46	0.18	0.315	1396	27					
mr04a42	3.279	0.215	0.250	0.012	0.37	0.100	0.001	1476	51	1439	63	1629	17	88	1463	93	0.57	0.272	1629	17					
mr04a48	6.377	0.347	0.365	0.015	0.38	0.128	0.001	2029	48	2007	71	2073	14	97	2025	92	0.75	1.028	2073	14					
mr04a482	6.915	0.166	0.379	0.009	0.49	0.130	0.001	2101	21	2073	42	2105	13	98	2100	43	0.45	0.950	2105	13					
mr02a52	8.364	0.784	0.451	0.044	0.52	0.151	0.007	2271	85	2402	196	2361	76	102	2264	170	0.44	0.176	2361	76					
mr02a41	12.920	0.336	0.507	0.011	0.43	0.180	0.002	2674	25	2644	49	2656	15	100	2673	49	0.50	0.846	2656	15					
mr04a49	13.550	0.895	0.534	0.020	0.28	0.192	0.002	2718	62	2757	84	2759	15	100	2730	112	0.66	0.898	2759	15					
<b>Nashoba Formation schist (MLNS1)</b>																									
se10a263	0.469	0.034	0.054	0.003	0.41	0.058	0.001	390	23	336	19	548	37	61	353	35	0.02	0.012							
se10a264	0.496	0.044	0.054	0.005	0.56	0.057	0.001	409	30	339	33	500	40	68	379	56	0.02	0.011							
se10a246	0.587	0.036	0.055	0.004	0.62	0.063	0.001	469	23	346	26	715	43	48	416	45	0.00	0.010							
se10a239	0.543	0.021	0.056	0.002	0.37	0.061	0.001	440	14	353	10	633	32	56	371	19	0.00	0.019							
se10a235	0.485	0.030	0.057	0.004	0.54	0.055	0.001	402	20	356	23	406	28	88	383	38	0.03	0.017							
se10a243	0.550	0.034	0.057	0.005	0.70	0.059	0.001	445	22	357	30	572	39	62	439	45	0.00	0.009							
se14a45	0.486	0.023	0.057	0.002	0.45	0.054	0.001	402	16	360	15	381	22	94	378	27	0.01	0.011							
se10a176	0.642	0.024	0.059	0.003	0.68	0.064	0.001	503	15	372	18	750	21	50	470	29	0.00	0.050							
se13a10	0.497	0.023	0.060	0.003	0.48	0.055	0.001	410	15	373	16	392	22	95	392	27	0.02	0.006							
se13a11	0.495	0.019	0.061	0.002	0.39	0.055	0.001	408	13	379	11	403	24	94	389	19	0.03	0.011							
se14a35	0.532	0.029	0.062	0.002	0.35	0.058	0.001	433	19	385	14	540	35	71	398	27	0.02	0.021							
se10a172	0.645	0.045	0.062	0.003	0.31	0.070	0.001	505	28	386	16	938	39	41	401	32	0.00	0.023							
se10a256	0.547	0.033	0.062	0.003	0.43	0.059	0.001	443	22	388	19	584	32	66	408	35	0.01	0.020							
se10a216	0.566	0.039	0.063	0.003	0.38	0.060	0.001	455	25	394	20	594	40	66	412	37	0.02	0.047							
se10a168	0.643	0.040	0.064	0.003	0.42	0.064	0.002	504	25	399	20	742	52	54	428	38	0.00	0.010							
se14a19	0.732	0.034	0.064	0.003	0.48	0.072	0.002	570	20	403	17	986	46	41	447	33	0.00	0.302							
se13a19	0.596	0.027	0.069	0.002	0.39	0.059	0.001	475	17	430	15	565	29	76	446	26	0.01	0.470							
se10a199	0.646	0.046	0.070	0.003	0.28	0.063	0.001	506	28	439	17	703	45	62	450	32	0.02	0.061							
se10a253	0.467	0.069	0.052	0.006	0.42	0.060	0.001	389	48	327	40	605	35	54	346	73	0.20	0.013	327	40					
se10a258	0.387	0.039	0.052	0.003	0.27	0.058	0.002	332	29	328	17	511	75	64	329	32	0.89	0.015	328	17					
se10a219	0.486	0.078	0.053	0.006	0.36	0.064	0.002	402	50	531	33	371	740	51	45	345	70	0.18	0.018	331	37				
se14a50	0.377	0.031	0.053	0.002	0.24	0.053	0.001	324	23	331	13	338	48	98	330	24	0.77	0.005	331	13					
se14a15	0.405	0.021	0.053	0.002	0.40	0.053	0.001	345	15	332	14	349	33	95	337	24	0.41	0.113	332	14					
se14a34	0.424	0.031	0.053	0.002	0.30	0.055	0.001	359	22	334	14	402	37	83	339	27	0.27	0.008	334	14					
se10a218	0.494	0.088	0.053	0.008	0.40	0.064	0.001	407	60	335	47	727	44	46	354	87	0.23	0.017	335	47					
se10a224	0.468	0.066	0.054	0.007	0.46	0.058	0.001	390	46	340	42	511	38	67	361	76	0.29	0.010	340	42					
se10a255	0.413	0.048	0.054	0.004	0.33	0.055	0.001	351	34	340	25	425	40	80	343	46	0.74	0.014	340	25					
se10a177	0.477	0.076	0.054	0.004	0.22	0.066	0.002	396	52	341	23	807	48	42	346	45	0.30	0.012	341	23					
se10a203	0.396	0.047	0.054	0.004	0.31	0.051	0.001	339	34	342	25	257	50	133	341	45	0.93	0.017	342	25					
se14a46	0.458	0.029	0.055	0.003	0.42	0.055	0.001	383	21	343	18	428	38	80	358	32	0.06	0.014	343	18					
se10a175	0.492	0.070	0.055	0.005	0.34	0.059	0.001	406	48	344	32	553	51	62	357	61	0.21	0.019	344	32					
se14a77	0.437	0.041	0.055	0.004	0.34	0.055	0.001	368	29	344	22	403	39	85	350	40	0.42	0.012	344	22					
se10a178	0.378	0.064	0.055	0.004	0.19	0.056	0.001	326	47	345	22	459	45	75	343	42	0.68	0.011	345	22					
se10a213	0.412	0.037	0.055	0.002	0.21	0.058	0.001	351	26	346	13	515	46	67	347	25	0.87	0.027	346	13					
se10a198	0.403	0.035	0.055	0.002	0.25	0.055	0.001	344	25	348	15	419	38	83	347	28	0.88	0.016	348	15					
se10a237	0.468	0.042	0.056	0.005	0.52	0.054	0.001	390	29	349	32	375	38	93	373	53	0.17	0.016	349	32					
se10a207	0.443	0.068	0.056	0.007	0.39	0.054	0.001	372	48	349	41	374	41	93	357	74	0.63	0.013	349	41					
se14a07	0.429	0.040	0.056	0.003	0.33	0.055	0.001	362	28	349	21	392	28	89	353	38	0.65	0.028	349	21					
se14a17	0.401	0.045	0.056	0.003	0.26	0.058	0.001	342	33	349	20	513	43	68	348	37	0.83	0.015	349	20					
se14a48	0.422	0.032	0.056	0.003	0.31	0.052	0.001	358	23	351	16	304	52	115	353	30	0.79	0.007	351	16					
se10a223	0.421	0.028	0.056	0.002	0.30	0.052	0.001	357	20	352	14	295	40	119	353	26	0.83	0.012	352	14</td					

Table A2. Continued.

Sample/ Analysis	Measured Isotopic Ratios						Calculated Ages (Ma)								Detrital (Ma)	Metamorphic (Ma)	CA-TIMS (Ma)							
	$^{207}\text{Pb}/^{235}\text{U}$	$\pm 1\sigma$	$^{206}\text{Pb}/^{238}\text{U}$	$\pm 1\sigma$	Rho	$^{207}\text{Pb}/^{206}\text{Pb}$	$\pm 1\sigma$	$^{207}\text{Pb}/^{235}\text{U}$	$\pm 1\sigma$	$^{206}\text{Pb}^2/^{238}\text{U}$	$\pm 1\sigma$	$^{207}\text{Pb}/^{206}\text{Pb}$	$\pm 1\sigma$	Concordia concordancy (%)	age	$\pm 2\sigma$	Probability of concordance	Th/U	For Prob Dens plots age	For Prob Dens plots age	$^{206}\text{Pb}/^{238}\text{U}$	$\pm 2\sigma$	notes	
sel10a182	0.458	0.071	0.60	0.003	0.15	0.066	0.002	383	49	376	17	794	66	47	376	34	0.89	0.015		376	17			
sel14a09	0.396	0.062	0.60	0.003	0.16	0.058	0.001	338	45	377	18	525	47	72	373	35	0.39	0.019		377	18			
sel10a267	0.479	0.069	0.60	0.005	0.29	0.057	0.001	397	47	377	30	495	43	76	381	57	0.67	0.014		377	30			
sel14a10	0.408	0.039	0.60	0.002	0.21	0.055	0.001	348	28	378	15	432	42	88	373	29	0.29	0.016		378	15			
sel10a25	0.462	0.060	0.60	0.005	0.30	0.056	0.001	385	42	378	28	435	38	87	380	53	0.86	0.018		378	28			
sel14a37	0.474	0.051	0.61	0.004	0.31	0.054	0.001	394	35	379	25	389	39	97	383	46	0.67	0.014		379	25			
sel10a195	0.490	0.045	0.61	0.003	0.27	0.058	0.001	405	31	380	18	540	43	70	384	34	0.42	0.011		380	18			
sel10a215	0.466	0.087	0.61	0.008	0.36	0.054	0.001	389	60	380	50	391	49	97	383	89	0.89	0.022		380	50			
sel13a09	0.494	0.020	0.61	0.002	0.35	0.054	0.001	408	13	382	10	381	30	100	389	19	0.06	0.015		382	10			
sel10a163	0.591	0.087	0.61	0.011	0.59	0.059	0.002	471	56	383	65	583	76	66	439	108	0.11	0.011		383	65			
sel10a167	0.505	0.029	0.61	0.002	0.24	0.056	0.001	415	19	383	10	448	38	85	387	19	0.11	0.009		383	10			
sel13a28	0.482	0.056	0.61	0.005	0.38	0.054	0.001	400	39	383	33	389	33	98	389	58	0.67	0.008		383	33			
sel14a28	0.453	0.037	0.61	0.004	0.28	0.055	0.001	379	26	383	17	416	38	92	382	32	0.88	0.014		383	17			
sel13a23	0.463	0.033	0.61	0.004	0.43	0.050	0.001	386	23	383	23	214	31	179	385	39	0.89	0.006		383	23			
sel14a66	0.494	0.037	0.61	0.003	0.32	0.055	0.001	408	25	384	18	405	39	95	390	33	0.35	0.012		384	18			
sel14a29	0.449	0.062	0.61	0.005	0.29	0.054	0.001	377	43	385	29	380	46	101	383	54	0.86	0.013		385	29			
sel13a21	0.461	0.059	0.62	0.004	0.24	0.057	0.001	385	41	385	23	506	51	76	385	43	0.99	0.021		385	23			
sel14a61	0.433	0.045	0.62	0.003	0.21	0.054	0.001	365	32	388	16	361	45	107	384	31	0.48	0.009		388	16			
sel13a17	0.485	0.042	0.62	0.004	0.33	0.055	0.001	401	28	388	22	424	30	92	392	39	0.66	0.007		388	22			
sel10a192	0.475	0.046	0.62	0.004	0.30	0.056	0.001	394	31	389	22	463	37	84	391	41	0.87	0.008		389	22			
sel13a18	0.465	0.026	0.62	0.002	0.33	0.054	0.001	388	18	389	14	355	30	110	389	25	0.97	0.176		389	14			
sel14a38	0.515	0.029	0.63	0.002	0.35	0.055	0.001	422	19	392	15	419	31	94	401	28	0.13	0.038		392	15			
sel14a58	0.572	0.072	0.63	0.005	0.32	0.061	0.001	459	47	392	31	655	43	60	405	59	0.16	0.011		392	31			
sel10a233	0.526	0.137	0.63	0.014	0.44	0.057	0.001	429	91	393	88	486	34	81	410	153	0.70	0.128		393	88			
sel10a229	0.475	0.043	0.63	0.003	0.23	0.057	0.001	395	29	393	16	501	53	78	393	30	0.95	0.016		393	16			
sel14a49	0.462	0.040	0.63	0.002	0.21	0.056	0.001	386	28	394	14	433	41	91	393	26	0.76	0.012		394	14			
sel14a12	0.474	0.045	0.63	0.003	0.23	0.056	0.001	394	31	394	17	454	56	87	394	32	0.99	0.010		394	17			
sel13a12	0.491	0.027	0.63	0.002	0.27	0.054	0.001	405	19	395	12	377	37	105	397	22	0.59	0.010		395	12			
sel13a27	0.487	0.040	0.63	0.003	0.28	0.056	0.001	403	28	396	18	453	36	87	398	33	0.82	0.006		396	18			
sel10a247	0.481	0.043	0.63	0.003	0.27	0.056	0.001	399	29	396	18	440	41	90	396	34	0.91	0.021		396	18			
sel10a173	0.482	0.043	0.64	0.002	0.17	0.056	0.001	399	29	397	11	469	48	85	397	22	0.94	0.030		397	11			
sel10a249	0.484	0.096	0.64	0.005	0.19	0.056	0.001	401	66	398	29	462	56	86	399	56	0.97	0.009		398	29			
sel10a162	0.550	0.039	0.64	0.002	0.20	0.061	0.001	445	25	399	11	645	49	62	403	21	0.08	0.013		399	11			
sel14a08	0.472	0.042	0.64	0.002	0.18	0.061	0.002	393	29	401	13	647	61	62	400	24	0.79	0.009		401	13			
sel10a188	0.464	0.064	0.64	0.004	0.21	0.060	0.001	387	45	402	22	617	52	65	400	43	0.74	0.207		402	22			
sel14a39	0.508	0.040	0.65	0.003	0.30	0.055	0.001	417	27	404	18	401	35	101	407	34	0.64	0.029		404	18			
sel14a13	0.509	0.060	0.65	0.003	0.18	0.058	0.001	418	40	404	17	513	57	79	405	33	0.74	0.012		404	17			
sel10a194	0.465	0.066	0.65	0.003	0.18	0.060	0.001	388	46	405	20	612	51	66	403	38	0.70	0.022		405	20			
sel10a186	0.498	0.047	0.65	0.003	0.28	0.057	0.001	411	32	406	21	475	44	85	407	38	0.89	0.009		406	21			
sel14a36	0.496	0.040	0.65	0.003	0.28	0.054	0.001	409	27	407	18	372	42	109	407	33	0.94	0.017		407	18			
sel14a60	0.509	0.048	0.66	0.003	0.24	0.056	0.001	418	32	410	18	444	49	92	411	34	0.81	0.006		410	18			
sel13a29	0.547	0.040	0.66	0.003	0.28	0.060	0.001	443	26	412	16	595	44	69	418	31	0.24	0.078		412	16			
sel10a193	0.510	0.045	0.66	0.003	0.28	0.056	0.001	418	30	413	20	453	43	91	414	37	0.85	0.037		413	20			
sel10a245	0.511	0.100	0.67	0.005	0.20	0.058	0.001	419	67	416	31	526	54	79	416	61	0.96	0.018		416	31			
sel10a268	0.508	0.110	0.67	0.003	0.09	0.071	0.002	417	74	417	16	944	55	44	417	32	1.00	0.037		417	16			
sel10a166	0.548	0.027	0.67	0.002	0.23	0.056	0.001	444	18	418	9	465	37	90	422	18	0.17	0.028		418	9			
sel10a187	0.515	0.073	0.67	0.003	0.17	0.060	0.002	422	49	419	19	591	62	71	419	38	0.94	0.010		419	19			
sel10a234	0.514	0.044	0.67	0.002	0.17	0.063	0.002	422	29	420	12	709	65	59	420	23	0.95	0.012		420	12			
sel14a76	0.543	0.033	0.69	0.002	0.23	0.056	0.001	440	22	433	12	469	43	92	434	22	0.75	0.022		433	12			
sel13a22	0.620	0.062	0.77	0.005	0.35	0.056	0.001	490	39	477	32	448	38	106	481	57	0.75	0.286	</					

Table A2. Continued.

Sample/ Analysis	Measured Isotopic Ratios						Calculated Ages (Ma)								Detrital (Ma)	Metamorphic (Ma)	CA-TIMS (Ma)						
	$^{207}\text{Pb}/^{235}\text{U}$	$\pm 1\sigma$	$^{206}\text{Pb}/^{238}\text{U}$	$\pm 1\sigma$	Rho	$^{207}\text{Pb}/^{206}\text{Pb}$	$\pm 1\sigma$	$^{207}\text{Pb}/^{235}\text{U}$	$\pm 1\sigma$	$^{206}\text{Pb}^{2}/^{238}\text{U}$	$\pm 1\sigma$	$^{207}\text{Pb}/^{206}\text{Pb}$	$\pm 1\sigma$	U-Pb/Pb-Pb concordancy (%)	Concordia age	$\pm 2\sigma$	Probability of concordance	Th/U	For Prob Dens plots age	For Prob Dens plots age	$^{206}\text{Pb}/^{238}$ U	$\pm 2\sigma$	notes
se10a138	0.489	0.035	0.058	0.004	0.46	0.057	0.001	404	24	361	23	482	21	75	380	40	0.07	0.170		361	23		
se10a103	0.483	0.048	0.058	0.005	0.42	0.057	0.001	400	33	361	29	504	43	72	376	52	0.24	0.140		361	29		
se10a134	0.452	0.047	0.058	0.004	0.33	0.056	0.001	379	33	361	24	466	26	77	365	44	0.60	0.200		361	24		
se10a118	0.437	0.031	0.058	0.003	0.31	0.054	0.001	368	22	361	16	385	32	94	363	29	0.74	0.140		361	16		
se10a110	0.456	0.076	0.058	0.007	0.35	0.055	0.001	382	53	362	40	421	27	86	368	74	0.72	0.150		362	40		
se10a132	0.443	0.055	0.058	0.004	0.29	0.055	0.001	372	39	362	25	411	34	88	365	47	0.80	0.150		362	25		
se10a108	0.458	0.024	0.058	0.002	0.32	0.054	0.001	383	17	364	12	389	27	94	368	22	0.28	0.150		364	12		
se13c102	0.454	0.025	0.058	0.002	0.35	0.054	0.001	380	18	364	14	389	36	94	369	25	0.39	0.160		364	14		
se10a98	0.444	0.033	0.058	0.003	0.35	0.053	0.001	373	23	364	18	338	31	108	367	33	0.69	0.120		364	18		
se13c117	0.463	0.028	0.058	0.003	0.43	0.053	0.001	387	20	366	19	328	28	112	375	32	0.30	0.120		366	19		
se13c105	0.468	0.027	0.059	0.003	0.42	0.053	0.001	390	19	368	17	320	36	115	377	30	0.27	0.130		368	17		
se10a99	0.444	0.023	0.059	0.002	0.31	0.056	0.001	373	16	370	12	451	30	82	371	22	0.84	0.160		370	12		
se10a123	0.464	0.073	0.060	0.006	0.34	0.056	0.001	387	51	376	39	436	31	86	379	71	0.83	0.120		376	39		
se10a141	0.482	0.020	0.060	0.002	0.41	0.055	0.001	399	14	377	13	397	29	95	386	22	0.13	0.190		377	13		
se10a113	0.505	0.030	0.061	0.003	0.39	0.057	0.001	415	20	379	17	502	25	75	391	31	0.09	0.370		379	17		
se13a92	0.461	0.053	0.061	0.005	0.34	0.054	0.001	385	37	379	29	383	40	99	381	53	0.88	0.150		379	29		
se10a128	0.480	0.037	0.061	0.004	0.39	0.055	0.001	398	25	381	22	404	28	94	388	39	0.51	0.130		381	22		
se10a150	0.483	0.021	0.062	0.002	0.35	0.054	0.001	400	14	386	12	385	24	100	391	21	0.36	0.120		386	12		
se13a93	0.475	0.047	0.062	0.004	0.30	0.056	0.001	395	33	387	22	468	33	83	389	41	0.82	0.100		387	22		
se10a114	0.486	0.026	0.062	0.002	0.31	0.057	0.002	402	18	389	12	500	82	78	392	23	0.48	0.120		389	12		
se10a101	0.527	0.026	0.065	0.002	0.31	0.056	0.001	430	17	404	12	451	30	90	410	22	0.15	0.110		404	12		
se10a140	0.557	0.032	0.067	0.003	0.35	0.057	0.001	450	21	418	16	483	25	87	428	29	0.14	0.150		418	16		
se10a122	0.575	0.036	0.067	0.003	0.38	0.058	0.001	461	23	421	19	513	30	82	434	35	0.09	0.130		421	19		
se13c103	0.591	0.037	0.070	0.003	0.38	0.056	0.001	472	24	434	20	455	40	95	447	36	0.13	0.160		434	20		
se10a121	0.657	0.034	0.081	0.004	0.43	0.056	0.001	513	21	500	21	453	26	110	506	36	0.56	0.200		500	21	4	
<b>Tadmuck Brook Schist (MLTMBC)</b>																							
se10a52	0.775	0.169	0.057	0.012	0.49	0.078	0.001	583	96	359	74	1156	23	31	387	145	0.02	1.500					
se10a81	0.685	0.042	0.073	0.003	0.30	0.060	0.001	530	25	455	16	610	25	75	469	31	0.00	0.250					
se10a31	0.798	0.080	0.073	0.005	0.35	0.067	0.001	596	45	456	31	841	37	54	480	59	0.00	1.110					
se09b09	0.762	0.048	0.078	0.003	0.31	0.060	0.001	575	28	482	18	615	38	78	499	34	0.00	0.550					
se09b12	0.955	0.052	0.094	0.004	0.35	0.064	0.001	681	27	577	21	730	22	79	605	39	0.00	0.820					
se09b12	0.955	0.052	0.094	0.004	0.35	0.064	0.001	681	27	577	21	730	22	79	605	39	0.00	0.820					
se10a56	1.013	0.081	0.098	0.005	0.35	0.064	0.001	711	41	605	32	732	28	83	634	59	0.01	0.210					
se10a56	1.013	0.081	0.098	0.005	0.35	0.064	0.001	711	41	605	32	732	28	83	634	59	0.01	0.210					
se09b18	1.033	0.070	0.099	0.005	0.38	0.061	0.001	720	35	609	30	645	47	94	646	55	0.00	0.720					
se09b18	1.033	0.070	0.099	0.005	0.38	0.061	0.001	720	35	609	30	645	47	94	646	55	0.00	0.720					
se09b11	1.113	0.062	0.103	0.004	0.32	0.063	0.001	760	30	634	22	709	45	89	663	41	0.00	0.080					
se10a60	1.519	0.095	0.137	0.004	0.21	0.072	0.001	938	38	830	20	990	42	84	845	39	0.01	0.810					
se09b07	1.792	0.084	0.140	0.005	0.35	0.077	0.001	1043	31	844	26	1134	35	74	902	48	0.00	0.050					
se10a09	2.120	0.276	0.142	0.017	0.45	0.098	0.001	1155	90	856	94	1595	22	54	973	168	0.00	0.600					
se10a32	1.904	0.139	0.152	0.011	0.48	0.073	0.001	1083	49	914	60	1002	30	91	1019	94	0.00	0.160					
se10a80	1.982	0.113	0.166	0.006	0.34	0.074	0.001	1109	39	992	36	1048	24	95	1038	62	0.01	0.820					
se09b23	2.307	0.154	0.172	0.009	0.38	0.090	0.007	1214	47	1025	48	1434	157	71	1108	83	0.00	0.390					
se10a37	4.014	0.322	0.204	0.013	0.41	0.117	0.001	1637	65	1198	72	1911	13	63	1360	128	0.00	0.590					
se09b27	3.682	0.244	0.239	0.010	0.32	0.093	0.004	1568	53	1383	53	1489	80	93	1463	90	0.00	0.220					
se14a84	4.463	0.149	0.286	0.009	0.46	0.102	0.001	1724	28	1622	44	1658	24	98	1708	55	0.01	0.090					
se09b22	6.523	0.415	0.291	0.012	0.32	0.124	0.002	2049	56	1646	58	2018	24	82	1792	102	0.00	0.970					
se09b13	6.011	0.235	0.296	0.012	0.51	0.119	0.001	1977	34	1673	59	1943	16	86	1951	69	0.00	0.030					
se10a19	8.135	0.471	0.359	0.016	0.40	0.147	0.009	2246	52	1979	78	2315	110	85	2178	105	0.00	0.120					
se10a71	0.648	0.121	0.068	0.007	0.29	0.061	0.001	507	74	424	44	657	36	65	437	85	0.28	0.790		424	44		
se10a62	0.577	0.081	0.069	0.004	0.19	0.055	0.001	463	52	432	22	406	48	106	435	43	0.56	0.050		432	22		
se10a49	0.627	0.162	0.070	0.007																			

Table A2. Continued.

Sample/ Analysis	Measured Isotopic Ratios						Calculated Ages (Ma)								Detrital (Ma)		Metamorphic (Ma)			CA-TIMS (Ma)		notes	
	$^{207}\text{Pb}/^{235}\text{U}$	$\pm 1\sigma$	$^{206}\text{Pb}/^{238}\text{U}$	$\pm 1\sigma$	Rho	$^{207}\text{Pb}/^{206}\text{Pb}$	$\pm 1\sigma$	$^{207}\text{Pb}/^{235}\text{U}$	$\pm 1\sigma$	$^{206}\text{Pb}^{2}/^{238}\text{U}$	$\pm 1\sigma$	$^{207}\text{Pb}/^{206}\text{Pb}$	$\pm 1\sigma$	U-Pb/Pb-Pb concordancy (%)	Concordia age	$\pm 2\sigma$	Probability of concordance	Th/U	For Prob Dens plots age	For Prob Dens plots age	$^{206}\text{Pb}/^{238}\text{U}$	$\pm 1\sigma$	
<b>MERRIMACK BELT</b>																							
<b>Kittery Formation (KSkt)</b>																							
mr17b17	0.550	0.017	0.067	0.001	0.28	0.055	0.001	445	11	419	7	417	26	101	424	13	0.03	0.793					
mr17b53	0.644	0.025	0.071	0.002	0.41	0.059	0.001	505	16	441	14	575	39	77	464	25	0.00	0.448					
mr18b48	0.835	0.039	0.076	0.002	0.33	0.066	0.001	617	21	470	14	803	39	59	492	27	0.00	0.258					
mr18a25	0.861	0.050	0.079	0.003	0.33	0.077	0.002	631	27	492	18	1115	42	44	516	35	0.00	0.129					
mr18b30	0.695	0.032	0.079	0.002	0.31	0.058	0.001	536	19	492	14	532	34	93	503	25	0.03	0.719					
mr17b57	0.711	0.030	0.080	0.002	0.27	0.063	0.001	545	18	494	11	724	35	68	503	21	0.00	0.235					
mr17a40	0.775	0.048	0.082	0.004	0.44	0.063	0.001	583	28	506	26	714	32	71	539	46	0.01	0.414					
mr17b37	0.793	0.041	0.087	0.002	0.27	0.063	0.001	593	23	540	14	702	35	77	550	27	0.03	0.315					
mr17b20	1.130	0.089	0.099	0.005	0.33	0.078	0.001	768	42	607	30	1158	24	52	639	57	0.00	0.217					
mr18a40	1.881	0.089	0.118	0.006	0.53	0.102	0.002	1074	32	717	34	1665	37	43	847	63	0.00	0.405					
mr17b29	2.015	0.094	0.157	0.005	0.31	0.092	0.002	1120	32	939	25	1461	32	64	988	46	0.00	0.709					
mr18b29	1.954	0.053	0.175	0.004	0.40	0.074	0.001	1100	18	1042	21	1050	20	99	1076	32	0.01	0.754					
mr18a30	2.622	0.245	0.176	0.012	0.35	0.104	0.001	1307	69	1046	63	1700	18	61	1129	114	0.00	0.431					
mr17a42	2.038	0.059	0.177	0.004	0.40	0.077	0.001	1128	20	1053	22	1132	22	93	1094	36	0.00	0.431					
mr17b28	1.439	0.090	0.179	0.008	0.34	0.074	0.002	905	37	1060	41	1050	50	101	964	62	0.00	1.216					
mr17a49	2.249	0.097	0.179	0.006	0.41	0.087	0.002	1197	30	1062	34	1349	39	79	1137	55	0.00	1.060					
mr17b33	2.682	0.192	0.195	0.010	0.34	0.099	0.003	1323	53	1151	51	1599	49	72	1221	89	0.00	0.392					
mr17b19	2.531	0.087	0.196	0.005	0.36	0.087	0.001	1281	25	1153	26	1364	21	85	1214	43	0.00	0.372					
mr18b23	2.495	0.151	0.198	0.009	0.39	0.088	0.001	1271	44	1164	50	1375	22	85	1225	79	0.04	0.326					
mr18b10	2.715	0.148	0.204	0.009	0.40	0.090	0.002	1322	41	1195	48	1418	34	84	1275	75	0.00	0.351					
mr18b40	2.593	0.098	0.209	0.005	0.33	0.088	0.001	1299	28	1223	28	1381	20	89	1259	46	0.02	0.200					
mr18a54	2.641	0.062	0.215	0.003	0.34	0.083	0.001	1312	17	1253	18	1259	20	99	1283	29	0.00	0.461					
mr18a23	5.218	1.062	0.231	0.014	0.15	0.197	0.006	1856	173	1339	76	2799	51	48	1359	150	0.02	0.606					
mr18a08	3.307	0.159	0.232	0.010	0.44	0.091	0.002	1483	38	1343	52	1440	39	93	1445	73	0.00	0.808					
mr18b31	2.946	0.066	0.233	0.004	0.40	0.086	0.001	1394	17	1348	22	1342	14	100	1380	32	0.03	0.368					
mr18a53	3.109	0.120	0.233	0.006	0.34	0.088	0.001	1435	30	1349	32	1374	22	98	1394	51	0.02	0.193					
mr18a47	3.348	0.107	0.234	0.005	0.36	0.096	0.001	1492	25	1355	28	1549	17	88	1430	45	0.00	0.528					
mr18a36	3.121	0.068	0.235	0.005	0.45	0.088	0.001	1438	17	1360	24	1382	14	98	1421	32	0.00	0.428					
mr18a57	3.104	0.091	0.238	0.005	0.38	0.090	0.001	1434	23	1376	28	1418	21	97	1413	41	0.04	0.531					
mr18b13	3.495	0.144	0.238	0.008	0.40	0.102	0.001	1526	33	1378	41	1670	17	83	1473	62	0.00	0.185					
mr18b27	3.250	0.121	0.239	0.006	0.34	0.093	0.001	1469	29	1384	31	1493	23	93	1429	50	0.01	0.362					
mr18b42	3.263	0.083	0.240	0.004	0.35	0.090	0.001	1472	20	1388	22	1422	18	98	1436	35	0.00	0.647					
mr18b50	3.468	0.066	0.241	0.004	0.44	0.095	0.001	1520	15	1390	21	1538	11	90	1487	29	0.00	0.171					
mr18a19	3.395	0.083	0.245	0.004	0.35	0.093	0.001	1503	19	1412	22	1491	18	95	1464	34	0.00	0.472					
mr17b22	3.319	0.105	0.246	0.005	0.30	0.094	0.001	1486	25	1416	24	1501	30	94	1448	40	0.02	0.343					
mr17b23	3.507	0.077	0.250	0.004	0.38	0.094	0.001	1529	17	1440	22	1511	13	95	1498	32	0.00	0.455					
mr17b13	3.329	0.080	0.251	0.004	0.33	0.091	0.001	1488	19	1441	20	1451	13	99	1467	32	0.04	0.278					
mr17b14	3.655	0.110	0.254	0.005	0.34	0.096	0.001	1562	24	1460	27	1541	22	95	1516	42	0.00	0.371					
mr18b45	3.856	0.097	0.264	0.005	0.38	0.100	0.001	1604	20	1510	26	1630	16	93	1573	38	0.00	0.1991					
mr17b09	3.790	0.132	0.264	0.005	0.27	0.097	0.001	1591	28	1513	25	1560	23	97	1544	43	0.02	0.304					
mr17a11	4.020	0.121	0.266	0.007	0.45	0.098	0.001	1638	25	1519	37	1585	19	96	1615	48	0.00	0.726					
mr18a15	3.831	0.097	0.267	0.006	0.43	0.096	0.001	1599	20	1526	30	1557	17	98	1583	40	0.01	0.466					
mr18b39	3.963	0.105	0.269	0.005	0.37	0.098	0.001	1627	21	1538	27	1578	15	97	1595	40	0.00	0.692					
mr17b42	3.917	0.106	0.273	0.005	0.37	0.099	0.001	1617	22	1557	27	1597	18	97	1596	40	0.03	0.973					
mr18b07	4.140	0.119	0.275	0.006	0.36	0.102	0.001	1662	24	1565	28	1660	21	94	1625	43	0.00	0.453					
mr18b32	4.557	0.284	0.276	0.015	0.44	0.108	0.002	1741	52	1573	27	1763	31	89	1705	103	0.02	0.928					
mr17a29	4.102	0.137	0.277	0.006	0.34	0.105	0.001	1655	27	1576	32	1710	24	92	1623	49	0.02	0.988					
mr18a12	4.217	0.107	0.280	0.006	0.41	0.101	0.001	1677	21	1593	29	1642	17	97	1656	40	0.00	0.271					
mr18a24	4.458	0.066	0.296	0.004	0.45	0.099	0.001	1722	12	1670	19	1600	10	104	1715	24	0.00	0.128			</td		

Table A2. Continued.

Sample/ Analysis	Measured Isotopic Ratios						Calculated Ages (Ma)								Detrital (Ma)		Metamorphic (Ma)		CA-TIMS (Ma)			
	$^{207}\text{Pb}/^{235}\text{U}$	$\pm 1\sigma$	$^{206}\text{Pb}/^{238}\text{U}$	$\pm 1\sigma$	Rho	$^{207}\text{Pb}/^{206}\text{Pb}$	$\pm 1\sigma$	$^{207}\text{Pb}/^{235}\text{U}$	$\pm 1\sigma$	$^{206}\text{Pb}^{238}\text{U}$	$\pm 1\sigma$	$^{207}\text{Pb}/^{206}\text{Pb}$	$\pm 1\sigma$	U-Pb/Pb-Pb concordancy (%)	Concordia age	$\pm 2\sigma$	Probability of concordance	Th/U	For Prob Dens plots age	For Prob Dens plots age	$^{206}\text{Pb}^{238}\text{U}$	$\pm 2\sigma$
mr17b41	1.209	0.090	0.123	0.007	0.37	0.069	0.001	805	42	749	39	904	22	83	773	67	0.23	0.098	749	39		
mr17b38	1.156	0.139	0.128	0.006	0.19	0.065	0.002	780	65	776	33	774	73	100	776	63	0.95	0.524	776	33		
mr17a39	1.677	0.075	0.159	0.005	0.36	0.072	0.000	1000	28	953	28	977	13	98	975	47	0.15	0.199	977	13		
mr17a12	1.663	0.076	0.160	0.004	0.25	0.077	0.001	995	29	956	21	1127	29	85	966	37	0.22	0.320	1127	29		
mr17b54	1.657	0.093	0.165	0.005	0.28	0.074	0.001	992	36	986	29	1038	39	95	988	51	0.86	0.668	1038	39		
mr17a38	1.751	0.041	0.168	0.003	0.35	0.073	0.001	1028	15	1001	15	1009	16	99	1014	25	0.13	0.521	1009	16		
mr18b38	1.784	0.077	0.170	0.005	0.32	0.073	0.001	1040	28	1012	26	1002	36	101	1024	44	0.38	1.435	1002	36		
mr18b24	1.845	0.071	0.171	0.004	0.33	0.074	0.001	1062	25	1016	24	1047	29	97	1036	40	0.10	0.418	1047	29		
mr18a26	1.652	0.163	0.171	0.006	0.18	0.072	0.002	990	62	1019	34	983	48	104	1014	64	0.65	0.417	983	48		
mr18b52	1.662	0.096	0.174	0.005	0.27	0.073	0.002	994	36	1033	29	1026	44	101	1019	51	0.33	0.799	1026	44		
mr17b39	1.827	0.053	0.180	0.004	0.40	0.073	0.001	1055	19	1066	23	1014	15	105	1059	34	0.65	0.259	1014	15		
mr18a43	2.038	0.088	0.183	0.004	0.26	0.083	0.002	1128	29	1083	23	1272	37	85	1097	40	0.16	0.453	1272	37		
mr17b30	2.104	0.104	0.188	0.006	0.32	0.079	0.001	1150	34	1113	32	1175	34	95	1129	54	0.34	0.460	1175	34		
mr17a18	1.900	0.176	0.189	0.010	0.30	0.072	0.002	1081	62	1116	57	977	53	114	1100	95	0.61	0.390	977	53		
mr17a22	2.140	0.067	0.191	0.004	0.30	0.076	0.001	1162	22	1125	19	1091	24	103	1140	33	0.13	0.098	1091	24		
mr18b28	2.316	0.067	0.201	0.004	0.32	0.079	0.001	1217	21	1179	20	1178	20	100	1197	33	0.11	0.490	1178	20		
mr17a50	2.030	0.099	0.203	0.005	0.28	0.073	0.001	1126	33	1190	29	1012	33	118	1162	49	0.09	0.804	1012	33		
mr18a13	2.144	0.069	0.203	0.004	0.31	0.076	0.001	1163	22	1190	21	1099	22	108	1177	35	0.30	0.124	1099	22		
mr17a17	2.593	0.114	0.211	0.006	0.34	0.084	0.002	1299	32	1234	33	1285	37	96	1266	54	0.09	0.559	1285	37		
mr17a48	2.556	0.084	0.211	0.005	0.37	0.082	0.001	1288	24	1235	27	1237	20	100	1266	42	0.07	0.445	1237	20		
mr18b51	2.767	0.191	0.214	0.009	0.31	0.087	0.001	1347	51	1250	49	1363	29	92	1291	83	0.10	0.183	1363	29		
mr17b24	2.640	0.182	0.215	0.008	0.27	0.087	0.001	1312	51	1254	42	1366	20	92	1275	74	0.31	0.191	1366	20		
mr18b17	2.555	0.117	0.215	0.006	0.28	0.084	0.001	1288	34	1254	30	1289	27	97	1268	50	0.38	0.171	1289	27		
mr17b10	2.767	0.110	0.221	0.006	0.32	0.089	0.001	1347	30	1286	29	1415	25	91	1314	48	0.08	0.882	1415	25		
mr17b08	2.700	0.178	0.221	0.009	0.32	0.086	0.001	1328	49	1287	49	1344	25	96	1307	81	0.47	0.380	1344	25		
mr17b51	2.705	0.106	0.224	0.005	0.31	0.085	0.001	1330	29	1303	28	1307	24	100	1316	47	0.43	0.550	1307	24		
mr18a29	2.866	0.457	0.224	0.018	0.25	0.090	0.002	1373	120	1305	93	1431	48	91	1326	165	0.61	0.205	1431	48		
mr18a46	2.829	0.129	0.226	0.006	0.29	0.088	0.001	1363	34	1314	32	1375	30	96	1335	53	0.21	0.124	1375	30		
mr17b50	2.881	0.088	0.228	0.005	0.34	0.085	0.001	1377	23	1325	25	1322	24	100	1354	40	0.06	0.645	1322	24		
mr17b52	2.889	0.113	0.230	0.005	0.30	0.090	0.001	1379	30	1335	29	1417	23	94	1356	48	0.21	0.548	1417	23		
mr17b27	2.852	0.081	0.232	0.004	0.30	0.086	0.001	1369	21	1343	21	1347	20	100	1355	34	0.28	0.452	1347	20		
mr18a41	2.801	0.112	0.232	0.006	0.31	0.083	0.001	1356	30	1347	30	1267	25	106	1351	48	0.79	0.473	1267	25		
mr18a32	2.889	0.115	0.235	0.005	0.26	0.090	0.001	1379	30	1360	26	1435	24	95	1367	44	0.57	0.369	1435	24		
mr17b34	3.426	0.453	0.238	0.026	0.41	0.102	0.004	1510	104	1378	136	1657	68	83	1468	199	0.32	0.395	1657	68		
mr18b22	3.267	0.166	0.239	0.008	0.34	0.096	0.002	1473	40	1382	43	1548	31	89	1431	69	0.06	0.864	1548	31		
mr17b59	2.836	0.151	0.241	0.007	0.27	0.097	0.002	1365	40	1390	36	1570	46	89	1379	59	0.58	0.080	1570	46		
mr18a34	3.167	0.088	0.243	0.005	0.33	0.095	0.001	1449	22	1400	23	1526	19	92	1427	37	0.06	0.503	1526	19		
mr18b18	3.352	0.169	0.243	0.008	0.32	0.098	0.001	1493	39	1402	40	1580	20	89	1446	66	0.05	0.874	1580	20		
mr18b09	3.121	0.073	0.243	0.003	0.28	0.088	0.001	1438	18	1402	17	1385	17	101	1417	28	0.09	0.284	1385	17		
mr17b07	3.225	0.121	0.245	0.007	0.37	0.092	0.001	1463	29	1414	36	1475	19	96	1446	53	0.18	0.286	1475	19		
mr17b18	3.360	0.141	0.255	0.007	0.31	0.093	0.001	1495	33	1463	34	1482	20	99	1480	55	0.42	0.703	1482	20		
mr17b11	3.272	0.101	0.255	0.004	0.27	0.088	0.001	1474	24	1464	22	1388	25	105	1469	37	0.71	0.401	1388	25		
mr17a27	3.251	0.108	0.257	0.006	0.38	0.086	0.001	1469	26	1474	33	1347	31	109	1471	47	0.90	0.598	1347	31		
mr18b49	3.915	0.282	0.262	0.016	0.53	0.098	0.001	1617	47	1501	83	1585	14	95	1612	95	0.10	0.120	1585	14		
mr18b14	3.455	0.096	0.263	0.005	0.37	0.091	0.001	1517	22	1505	27	1442	16	104	1513	40	0.68	0.467	1442	16		
mr17a14	3.517	0.179	0.264	0.007	0.27	0.098	0.002	1531	40	1510	37	1581	31	95	1519	62	0.65	0.107	1581	31		
mr17a13	3.631	0.069	0.266	0.004	0.39	0.093	0.001	1556	15	1522	20	1490	15	102	1547	28	0.09	0.456	1490	15		
mr18a11	3.291	0.083	0.267	0.005	0.41	0.086	0.001	1479	20	1528	28	1329	22	115	1496	37	0.07	0.373	1329	22		
mr17b49	3.656	0.091	0.269	0.005	0.38	0.094	0.001	1562	20	1533	26	1515	20	101	1553	37	0.27	0.307	1515	20		
mr17b47	3.796	0.076	0.271	0.005	0.45	0.095	0.001	1592	16	1548	25	1531	13	101	1585	32	0.05	0.068	1531	13		
mr18a10	3.920	0.112	0.274	0.006	0.37	0.100	0.001	1618	23	1562	29	1628	22	96	1599	43	0.06	1.057	1628	22		
mr17a30																						

Table A2. Continued.

Sample/ Analysis	Measured Isotopic Ratios						Calculated Ages (Ma)								Detrital (Ma)		Metamorphic (Ma)		CA-TIMS (Ma)		notes		
	$^{207}\text{Pb}/^{235}\text{U}$	$\pm 1\sigma$	$^{206}\text{Pb}/^{238}\text{U}$	$\pm 1\sigma$	Rho	$^{207}\text{Pb}/^{206}\text{Pb}$	$\pm 1\sigma$	$^{207}\text{Pb}/^{235}\text{U}$	$\pm 1\sigma$	$^{206}\text{Pb}^{i2}/^{238}\text{U}$	$\pm 1\sigma$	$^{207}\text{Pb}/^{206}\text{Pb}$	$\pm 1\sigma$	U-Pb/Pb-Pb concordancy (%)	Concordia age	$\pm 2\sigma$	Probability of concordance	Th/U	For Prob Dens plots age	For Prob Dens plots age	$^{206}\text{Pb}/^{238}\text{U}$	$\pm 2\sigma$	
mr10b117	1.090	0.171	0.091	0.014	0.48	0.080	0.001	748	83	563	81	1204	22	47	631	146	0.03	0.100					
mr10b101	0.957	0.044	0.094	0.003	0.40	0.061	0.001	682	23	577	21	623	27	93	615	37	0.00	0.655					
mr10b99	1.172	0.111	0.102	0.006	0.32	0.076	0.001	787	52	626	36	1093	25	57	657	69	0.00	0.186					
mr10b131	1.550	0.176	0.118	0.012	0.46	0.090	0.001	950	70	717	71	1420	22	50	808	127	0.00	0.160					
mr11a08	1.764	0.103	0.133	0.006	0.37	0.093	0.001	1032	38	802	32	1497	29	54	864	59	0.00	0.388					
mr10b55	2.180	0.100	0.147	0.008	0.55	0.087	0.001	1175	32	885	42	1365	25	65	1082	66	0.00	0.134					
mr10b96	1.853	0.111	0.159	0.006	0.31	0.075	0.001	1064	39	949	33	1073	22	88	987	59	0.01	0.795					
mr11a07	1.983	0.098	0.160	0.004	0.27	0.087	0.001	1110	33	957	24	1369	27	70	993	45	0.00	0.877					
mr10b38	1.701	0.060	0.160	0.003	0.30	0.073	0.001	1009	23	958	19	1009	28	95	976	33	0.04	0.407					
mr10b68	2.152	0.072	0.161	0.004	0.36	0.087	0.001	1166	23	965	21	1352	30	71	1035	38	0.00	0.532					
mr10b80	1.870	0.057	0.166	0.003	0.32	0.077	0.001	1070	20	990	18	1120	22	88	1020	31	0.00	0.011					
mr10b85	2.766	0.223	0.168	0.008	0.30	0.119	0.002	1346	60	1003	45	1941	30	52	1061	86	0.00	0.574					
mr10b69	1.917	0.068	0.169	0.004	0.30	0.076	0.001	1087	24	1007	20	1085	23	93	1034	35	0.00	0.219					
mr10b64	2.675	0.129	0.186	0.008	0.44	0.093	0.003	1322	36	1099	42	1486	52	74	1225	68	0.00	0.411					
mr10b54	2.594	0.194	0.190	0.011	0.40	0.092	0.001	1299	55	1119	62	1460	18	77	1214	101	0.01	0.279					
mr10b28	2.251	0.048	0.195	0.003	0.35	0.076	0.001	1197	15	1150	16	1094	18	105	1174	25	0.01	0.585					
mr10b74	2.555	0.090	0.205	0.005	0.33	0.082	0.001	1288	26	1202	26	1257	26	96	1242	43	0.00	0.222					
mr10b34	3.222	0.126	0.213	0.008	0.50	0.101	0.001	1462	30	1244	44	1642	22	76	1416	61	0.00	0.479					
mr10d40	2.998	0.090	0.216	0.006	0.43	0.092	0.001	1407	23	1263	29	1465	18	86	1359	44	0.00	0.312					
mr10b82	4.190	0.281	0.218	0.014	0.48	0.127	0.003	1672	55	1272	74	2062	40	62	1526	115	0.00	0.108					
mr10b70	3.094	0.135	0.220	0.010	0.50	0.092	0.001	1431	34	1281	51	1471	14	87	1407	67	0.00	0.324					
mr10b63	3.067	0.099	0.221	0.007	0.47	0.093	0.001	1425	25	1285	36	1496	11	86	1394	49	0.00	0.275					
mr10b58	3.039	0.085	0.226	0.006	0.44	0.087	0.001	1417	21	1316	30	1360	25	97	1392	42	0.00	0.735					
mr10b54	3.017	0.098	0.230	0.004	0.30	0.092	0.001	1425	25	1335	23	1457	19	92	1368	39	0.01	0.367					
mr10b30	3.341	0.118	0.231	0.006	0.37	0.099	0.001	1491	28	1340	31	1608	19	83	1423	50	0.00	0.546					
mr10b27	3.177	0.151	0.232	0.008	0.38	0.092	0.001	1452	37	1345	44	1463	18	92	1411	68	0.02	0.688					
mr10a09	3.392	0.197	0.232	0.009	0.33	0.089	0.001	1503	46	1347	47	1405	16	96	1420	78	0.00	0.381					
mr10b72	3.257	0.138	0.236	0.007	0.33	0.089	0.002	1471	33	1364	35	1405	35	97	1417	56	0.01	0.445					
mr10b111	4.727	0.318	0.243	0.017	0.53	0.111	0.001	1772	56	1401	90	1811	17	77	1716	117	0.00	0.243					
mr10c10	3.436	0.132	0.243	0.009	0.49	0.095	0.001	1513	30	1401	48	1521	15	92	1498	60	0.01	0.549					
mr10b20	3.847	0.209	0.243	0.009	0.34	0.093	0.001	1603	44	1403	47	1497	25	94	1500	78	0.00	0.517					
mr10b12	3.547	0.198	0.244	0.009	0.33	0.099	0.001	1538	44	1405	47	1609	20	87	1470	76	0.01	0.224					
mr10b84	3.530	0.094	0.247	0.006	0.45	0.093	0.001	1534	21	1421	31	1494	18	95	1510	41	0.00	0.301					
mr10b97	3.843	0.178	0.248	0.009	0.40	0.093	0.001	1602	37	1428	48	1495	14	95	1540	71	0.00	0.324					
mr10b21	3.585	0.113	0.249	0.006	0.38	0.095	0.001	1546	25	1435	30	1528	13	94	1504	46	0.00	0.590					
mr10b74	3.528	0.077	0.256	0.005	0.41	0.093	0.001	1533	17	1471	24	1496	11	98	1517	33	0.01	0.115					
mr10b93	3.755	0.153	0.257	0.007	0.34	0.099	0.002	1583	33	1474	36	1602	31	92	1533	57	0.01	0.747					
mr10b19	3.638	0.105	0.257	0.005	0.34	0.097	0.001	1558	23	1475	26	1571	24	94	1521	40	0.00	0.192					
mr10b98	4.005	0.165	0.258	0.010	0.48	0.102	0.001	1635	33	1481	52	1652	18	90	1612	67	0.00	1.100					
mr10b58	3.910	0.158	0.263	0.006	0.30	0.098	0.002	1616	33	1379	33	1759	28	86	1557	54	0.01	1.016					
mr10b918	3.743	0.076	0.265	0.005	0.44	0.097	0.001	1581	16	1516	24	1566	15	97	1568	32	0.00	0.274					
mr10b29	4.049	0.111	0.270	0.006	0.41	0.098	0.004	1644	22	1540	31	1760	67	87	1617	43	0.00	0.696					
mr10b103	4.281	0.239	0.271	0.008	0.26	0.109	0.001	1690	46	1543	40	1784	25	86	1595	70	0.01	0.606					
mr10b112	4.841	0.180	0.271	0.008	0.41	0.107	0.001	1792	31	1545	42	1752	14	88	1712	62	0.00	0.741					
mr11a20	4.034	0.150	0.273	0.008	0.38	0.104	0.001	1641	30	1555	38	1692	17	97	2018	46	0.00	0.259					
mr10b17	4.325	0.151	0.283	0.006	0.31	0.102	0.001	1698	29	1608	31	1664	25	97	1656	49	0.01	1.033					
mr10a13	6.484	0.829	0.287	0.021	0.28	0.153	0.002	2044	112	1625	103	2382	20	68	1739	188	0.00	0.142					
mr10b34	4.990	0.334	0.292	0.017	0.43	0.116	0.002	1817	57	1653	48	1895	25	87	1781	112	0.04	1.386					
mr10b73	4.533	0.101	0.296	0.005	0.42	0.103	0.001	1737	18	1669	27	1678	16	100	1723	36	0.01	0.691					
mr10a14	5.614	0.303	0.303	0.015	0.45	0.105	0.001	1918	46	1706	37	1709	14	100	1880	93	0.00	0.294					
mr10b31	6.426	0.168	0.348	0.008	0.42	0.123	0.001	2036	23	1926	37	1995	17	130	409	19	0.06	0.259					
mr10b23	5.124	0.313																					

Table A2. Continued.

Sample/ Analysis	Measured Isotopic Ratios						Calculated Ages (Ma)								Detrital (Ma)		Metamorphic (Ma)		CA-TIMS (Ma)		notes		
	$^{207}\text{Pb}/^{235}\text{U}$	$\pm 1\sigma$	$^{206}\text{Pb}/^{238}\text{U}$	$\pm 1\sigma$	Rho	$^{207}\text{Pb}/^{206}\text{Pb}$	$\pm 1\sigma$	$^{207}\text{Pb}/^{235}\text{U}$	$\pm 1\sigma$	$^{206}\text{Pb}^{238}\text{U}$	$\pm 1\sigma$	$^{207}\text{Pb}/^{206}\text{Pb}$	$\pm 1\sigma$	U-Pb/Pb-Pb concordancy (%)	Concordia age	$\pm 2\sigma$	Probability of concordance	Th/U	For Prob Dens plots age	For Prob Dens plots age	$^{206}\text{Pb}/^{238}\text{U}$	U	$\pm 2\sigma$
mr10b42	0.645	0.205	0.072	0.011	0.24	0.063	0.001	505	127	450	67	693	49	65	457	129	0.67	0.499	450	67			
mr10b51	0.560	0.086	0.072	0.003	0.16	0.056	0.001	452	56	450	21	432	41	104	450	41	0.97	0.377	450	21			
mr11a19	0.541	0.116	0.072	0.007	0.24	0.057	0.001	439	76	451	44	478	49	94	448	84	0.88	0.651	451	44			
mr10b110	0.742	0.198	0.073	0.010	0.26	0.070	0.001	563	116	452	62	921	37	49	464	120	0.36	0.352	452	62			
mr09b68	0.631	0.049	0.073	0.004	0.37	0.060	0.001	497	31	453	26	595	47	76	468	46	0.18	0.608	453	26			
mr10b33	0.583	0.018	0.073	0.001	0.26	0.056	0.001	466	11	453	7	465	21	97	455	13	0.25	0.606	453	7			
mr09b13	0.613	0.033	0.073	0.002	0.22	0.061	0.001	486	21	455	10	648	39	70	459	20	0.15	0.691	455	10			
mr09b55	0.562	0.044	0.073	0.003	0.22	0.061	0.001	453	29	455	15	631	50	72	454	29	0.96	0.810	455	15			
mr10b14	0.547	0.024	0.073	0.001	0.17	0.058	0.001	443	16	456	7	520	32	88	454	13	0.43	0.784	456	7			
mr10a19	0.612	0.058	0.073	0.003	0.21	0.057	0.001	485	37	456	18	490	41	93	459	34	0.45	0.323	456	18			
mr10b127	0.651	0.094	0.074	0.006	0.29	0.063	0.001	509	58	461	37	698	33	66	470	69	0.42	0.448	461	37			
mr09b09	0.574	0.024	0.074	0.001	0.23	0.058	0.001	460	16	463	9	520	34	89	462	17	0.90	0.293	463	9			
mr10b53	0.550	0.039	0.075	0.002	0.20	0.054	0.001	445	25	464	13	391	33	119	461	24	0.47	0.497	464	13			
mr09b93	0.604	0.055	0.075	0.003	0.24	0.065	0.001	480	35	464	20	762	43	61	467	37	0.67	0.166	464	20			
mr09b79	0.561	0.016	0.075	0.001	0.30	0.048	0.001	452	11	468	8	76	34	613	463	15	0.16	0.676	468	8			
mr10b45	0.610	0.025	0.076	0.001	0.22	0.057	0.001	484	16	471	8	479	30	98	473	16	0.44	0.245	471	8			
mr09b59	0.609	0.018	0.076	0.001	0.33	0.054	0.001	483	11	473	9	366	31	129	476	16	0.37	0.180	473	9			
mr09b99	0.565	0.082	0.077	0.005	0.21	0.053	0.001	455	53	481	28	334	64	144	477	53	0.63	0.643	481	28			
mr09b76	0.642	0.033	0.078	0.002	0.26	0.057	0.001	504	20	484	12	504	27	96	488	23	0.35	0.123	484	12			
mr09b65	0.613	0.029	0.079	0.002	0.23	0.057	0.001	486	18	490	10	506	35	97	489	19	0.82	0.308	490	10			
mr11a18	0.898	0.261	0.080	0.012	0.26	0.100	0.002	651	139	495	72	1615	30	31	509	140	0.29	0.361	495	72			
mr10b107	0.838	0.122	0.083	0.009	0.36	0.064	0.001	618	67	512	51	739	26	69	538	95	0.13	0.091	512	51			
mr11a14	0.746	0.134	0.085	0.008	0.25	0.067	0.001	566	78	523	45	851	40	61	530	86	0.60	0.569	523	45			
mr10b22	0.712	0.040	0.094	0.002	0.21	0.063	0.001	546	24	579	13	695	36	83	572	25	0.18	0.703	579	13			
mr09b38	0.821	0.029	0.095	0.002	0.36	0.060	0.001	609	16	583	14	591	34	99	593	25	0.15	0.748	583	14			
mr10b07	0.858	0.052	0.095	0.004	0.33	0.063	0.001	629	29	586	23	708	28	83	599	41	0.16	0.331	586	23			
mr09b41	0.922	0.054	0.109	0.004	0.35	0.057	0.002	664	28	667	26	502	58	133	666	44	0.90	0.896	667	26			
mr10b100	1.326	0.235	0.116	0.012	0.29	0.084	0.001	857	103	709	69	1297	28	55	737	131	0.18	0.322	709	69			
mr10a16	1.268	0.186	0.124	0.009	0.25	0.068	0.001	832	83	755	52	858	31	88	770	98	0.39	0.307	755	52			
mr09b62	1.206	0.152	0.132	0.006	0.18	0.082	0.002	803	70	799	33	1257	46	64	800	64	0.96	0.332	799	33			
mr09b43	1.176	0.149	0.134	0.007	0.20	0.075	0.002	790	69	811	39	1071	42	76	807	73	0.76	0.816	1071	42			
mr09b60	1.237	0.105	0.137	0.009	0.37	0.067	0.001	818	48	828	49	851	43	97	823	80	0.85	0.367	851	43			
mr09b08	1.397	0.072	0.142	0.006	0.42	0.069	0.001	888	31	854	34	903	32	95	874	55	0.35	0.457	903	32			
mr10b109	1.383	0.522	0.142	0.023	0.21	0.083	0.001	882	222	857	128	1271	31	67	862	240	0.92	0.156	1271	31			
mr09b42	1.388	0.074	0.145	0.004	0.26	0.071	0.001	884	32	872	23	960	27	91	875	41	0.73	0.595	960	27			
mr09b32	1.398	0.150	0.150	0.006	0.19	0.077	0.002	888	64	901	33	1134	39	79	899	63	0.85	0.336	1134	39			
mr09b52	1.565	0.062	0.153	0.004	0.33	0.071	0.001	957	24	919	22	955	27	96	934	38	0.17	0.820	955	27			
mr10b50	1.421	0.314	0.154	0.011	0.16	0.079	0.001	898	132	924	60	1168	35	79	920	114	0.85	0.253	1168	35			
mr10c08	1.411	0.149	0.157	0.005	0.16	0.089	0.002	893	63	939	29	1408	49	67	932	56	0.48	0.492	1408	49			
mr10c19	1.766	0.170	0.163	0.006	0.18	0.086	0.002	1033	62	972	32	1334	41	73	981	61	0.36	0.827	1334	41			
mr09b70	1.756	0.058	0.165	0.004	0.33	0.073	0.001	1029	21	983	20	1013	23	97	1003	34	0.06	0.386	1013	23			
mr10b71	1.721	0.086	0.165	0.006	0.36	0.074	0.001	1016	32	986	33	1031	32	96	1001	54	0.40	1.302	1031	32			
mr09b39	1.688	0.067	0.170	0.005	0.38	0.068	0.001	1024	25	1011	28	876	36	115	1007	44	0.81	0.695	876	36			
mr10b75	1.752	0.069	0.170	0.004	0.29	0.074	0.001	1028	21	1013	21	1041	27	97	1019	37	0.61	0.796	1041	27			
mr09b97	1.756	0.201	0.172	0.008	0.21	0.082	0.002	1029	74	1023	46	1237	41	83	1025	29	0.12	0.250	1237	41			
mr09b95	2.177	0.209	0.194	0.009	0.23	0.089	0.001	1174	67	1142	47	1415	27	81	1150	85	0.66	0.280	1415	27			
mr10a15	2.374	0.673	0.205	0.020	0.20	0.098	0.002	1349	181	1202	108	1583	40	76	1227	204	0.46	0.662	1583	40			
mr09b19	2.332	0.090	0.121	0.004	0.23	0.084	0.001	1222	27	1240	20	1299	26	95	1234	35	0.56	0.746	1299	26			
mr11a23	2.568	0.168	0.213	0.008	0.29	0.088	0.002	1292	48	1245	43	1388	39	90	1264	74	0.40	0.395	1388	39			
mr10c17	2.834	0.181	0.218	0.009	0.31	0.092	0.001	1365	48	1270	46	1466	23	87	1311	77	0.09	0.399					

Table A2. Continued.

Sample/ Analysis	Measured Isotopic Ratios						Calculated Ages (Ma)								Detrital (Ma)		Metamorphic (Ma)		CA-TIMS (Ma)		notes		
	$^{207}\text{Pb}/^{235}\text{U}$	$\pm 1\sigma$	$^{206}\text{Pb}/^{238}\text{U}$	$\pm 1\sigma$	Rho	$^{207}\text{Pb}/^{206}\text{Pb}$	$\pm 1\sigma$	$^{207}\text{Pb}/^{235}\text{U}$	$\pm 1\sigma$	$^{206}\text{Pb}^{i2}/^{238}\text{U}$	$\pm 1\sigma$	$^{207}\text{Pb}/^{206}\text{Pb}$	$\pm 1\sigma$	U-Pb/Pb-Pb concordancy (%)	Concordia age	$\pm 2\sigma$	Probability of concordance	Th/U	For Prob Dens plots age	For Prob Dens plots age	$^{206}\text{Pb}/^{238}\text{U}$	$\pm 1\sigma$	
mr05a125	1.352	0.161	0.178	0.007	0.18	0.072	0.002	868	70	1054	41	998	59	106	1005	73	0.01	0.415					
mr04b92	2.127	0.084	0.178	0.004	0.28	0.078	0.001	1158	27	1057	21	1136	28	93	1087	38	0.00	0.584					
mr05a114	2.358	0.093	0.178	0.005	0.32	0.083	0.002	1230	28	1052	25	1263	37	84	1116	45	0.00	0.527					
mr04b50	2.397	0.176	0.189	0.007	0.24	0.087	0.006	1242	53	1114	36	1367	133	81	1142	66	0.03	0.402					
mr05a137	2.571	0.207	0.192	0.014	0.45	0.095	0.001	1293	59	1131	75	1520	14	74	1238	114	0.02	0.441					
mr04b30	2.293	0.061	0.193	0.004	0.38	0.078	0.001	1210	19	1151	21	1151	20	99	1178	33	0.00	0.417					
mr05a25	2.459	0.078	0.195	0.005	0.41	0.085	0.001	1260	23	1150	27	1322	20	87	1216	42	0.00	0.863					
mr05a26	2.727	0.106	0.213	0.005	0.28	0.087	0.001	1326	29	1244	25	1365	29	91	1277	43	0.01	0.396					
mr05a10	2.831	0.122	0.215	0.008	0.42	0.089	0.001	1364	32	1257	41	1402	15	90	1328	61	0.01	0.391					
mr04b25	4.616	0.680	0.216	0.007	0.11	0.136	0.016	1752	123	1260	36	2176	206	58	1268	72	0.00	0.279					
mr05a20	2.782	0.060	0.217	0.004	0.47	0.085	0.001	1351	16	1266	23	1327	17	95	1334	32	0.00	0.446					
mr04b48	2.987	0.088	0.220	0.006	0.47	0.087	0.001	1404	22	1282	32	1365	25	94	1379	44	0.00	0.781					
mr05a22	2.835	0.084	0.223	0.005	0.41	0.086	0.001	1365	22	1297	29	1338	14	97	1344	42	0.02	0.582					
mr05a50	2.936	0.101	0.229	0.005	0.29	0.088	0.001	1391	26	1330	24	1390	22	96	1355	40	0.04	0.579					
mr05a120	3.630	0.151	0.235	0.006	0.31	0.101	0.003	1556	33	1358	31	1636	46	83	1433	54	0.00	0.438					
mr05a82	2.991	0.064	0.235	0.005	0.45	0.089	0.001	1405	16	1359	24	1397	12	97	1396	32	0.03	0.437					
mr09a21	3.173	0.105	0.239	0.005	0.31	0.089	0.001	1451	25	1379	25	1399	15	99	1412	41	0.02	0.394					
mr05a86	3.203	0.069	0.244	0.004	0.37	0.093	0.001	1458	17	1406	20	1479	12	95	1438	30	0.01	0.361					
mr04b15	3.268	0.081	0.244	0.004	0.36	0.092	0.001	1473	19	1407	23	1474	15	95	1447	35	0.01	0.525					
mr05a90	3.583	0.087	0.248	0.006	0.47	0.098	0.001	1546	19	1426	29	1591	21	90	1525	38	0.00	0.864					
mr05a77	3.339	0.085	0.249	0.005	0.41	0.093	0.001	1490	20	1431	27	1489	13	96	1474	38	0.02	0.446					
mr04b81	3.356	0.102	0.249	0.006	0.37	0.094	0.001	1494	24	1432	29	1503	15	95	1472	43	0.04	0.669					
mr05a11	3.627	0.051	0.256	0.003	0.44	0.093	0.001	1555	11	1468	16	1497	12	98	1536	22	0.00	0.565					
mr09a40	3.829	0.126	0.259	0.007	0.40	0.094	0.001	1599	26	1487	35	1507	13	99	1564	50	0.00	0.768					
mr04b32	9.834	1.295	0.261	0.009	0.13	0.198	0.025	2419	121	1493	45	2812	206	53	1498	91	0.00	0.376					
mr05a12	4.152	0.129	0.261	0.007	0.41	0.102	0.001	1665	25	1497	34	1656	20	90	1611	49	0.00	0.490					
mr05a21	3.886	0.127	0.266	0.005	0.28	0.102	0.001	1611	26	1522	25	1659	19	92	1559	41	0.00	0.284					
mr09a12	3.988	0.159	0.267	0.007	0.31	0.098	0.001	1632	32	1525	33	1590	20	96	1577	54	0.01	0.410					
mr05a94	3.906	0.101	0.268	0.006	0.43	0.101	0.002	1615	21	1532	31	1644	33	93	1597	41	0.00	0.086					
mr05a27	4.049	0.098	0.273	0.005	0.36	0.101	0.001	1644	20	1554	24	1647	15	94	1610	36	0.00	0.069					
mr04b78	4.078	0.091	0.273	0.006	0.50	0.101	0.001	1650	18	1557	31	1638	12	95	1643	37	0.00	0.327					
mr04b90	4.140	0.125	0.276	0.006	0.38	0.102	0.001	1662	25	1571	32	1652	18	95	1632	46	0.00	0.986					
mr05a83	4.139	0.103	0.276	0.005	0.37	0.103	0.001	1662	20	1573	26	1676	13	94	1631	38	0.00	0.617					
mr05a58	4.051	0.092	0.278	0.005	0.40	0.100	0.001	1645	18	1582	25	1629	14	97	1627	35	0.01	0.648					
mr05a14	4.224	0.083	0.279	0.005	0.46	0.101	0.001	1679	16	1586	25	1651	12	96	1664	32	0.00	0.527					
mr04b38	4.301	0.116	0.283	0.006	0.42	0.102	0.001	1694	22	1604	32	1656	13	97	1673	43	0.00	0.685					
mr04b46	4.898	0.237	0.286	0.009	0.32	0.128	0.002	1802	41	1622	45	2069	28	78	1713	72	0.00	1.076					
mr09a30	4.618	0.163	0.287	0.007	0.36	0.107	0.001	1753	29	1626	36	1748	15	93	1705	54	0.00	0.510					
mr09a33	3.762	0.154	0.297	0.007	0.39	0.092	0.002	1585	33	1679	35	1474	31	114	1624	54	0.02	0.803					
mr04b57	2.537	0.117	0.316	0.007	0.49	0.111	0.001	1859	19	1772	33	1819	11	97	1853	38	0.00	0.108					
mr04b13	5.587	0.109	0.327	0.005	0.43	0.114	0.001	1914	17	1822	27	1862	14	98	1899	33	0.00	0.530					
mr05a16	9.547	0.348	0.352	0.012	0.48	0.180	0.001	2392	34	1944	58	2649	13	73	2332	70	0.00	0.521					
mr05a32	11.294	0.365	0.444	0.013	0.45	0.177	0.002	2548	30	2368	58	2624	21	90	2538	61	0.00	1.021					
mr05a17	12.225	0.287	0.484	0.010	0.44	0.166	0.002	2622	22	2544	43	2520	17	101	2618	44	0.04	0.423					
mr09a35	0.549	0.094	0.663	0.006	0.28	0.061	0.001	442	62	396	37	648	46	61	405	71	0.45	0.328	396	37			
mr05a47	0.513	0.066	0.664	0.006	0.36	0.055	0.001	421	44	398	35	412	23	97	406	64	0.63	0.566	398	35			
mr09a39	0.489	0.024	0.664	0.002	0.26	0.054	0.001	404	16	402	10	359	25	112	402	18	0.86	0.989	402	10			
mr05a133	0.518	0.094	0.665	0.006	0.26	0.055	0.001	424	63	405	37	417	45	97	408	71	0.76	0.551	405	37			
mr09a34	0.473	0.020	0.665	0.002	0.31	0.052	0.001	393	13	406	10	288	54	141	402	18	0.35	0.273	406	10			
mr04b29	0.530	0.016	0.666	0.001	0.31	0.055	0.001	432	11	414	8	398	22	104	419	14	0.11	0.689	414	8	486.35	0.47	
mr05a118	0.519	0.058	0.666	0.003	0.23	0.059	0.001	425	39	414	21	568	30	73	416	40							

Table A2. Continued.

Sample/ Analysis	Measured Isotopic Ratios						Calculated Ages (Ma)								Detrital (Ma)		Metamorphic (Ma)		CA-TIMS (Ma)			
	$^{207}\text{Pb}/^{235}\text{U}$	$\pm 1\sigma$	$^{206}\text{Pb}/^{238}\text{U}$	$\pm 1\sigma$	Rho	$^{207}\text{Pb}/^{206}\text{Pb}$	$\pm 1\sigma$	$^{207}\text{Pb}/^{235}\text{U}$	$\pm 1\sigma$	$^{206}\text{Pb}^{238}\text{U}$	$\pm 1\sigma$	$^{207}\text{Pb}/^{206}\text{Pb}$	$\pm 1\sigma$	U-Pb/Pb-Pb concordancy (%)	Concordia age	$\pm 2\sigma$	Probability of concordance	Th/U	For Prob Dens plots age	For Prob Dens plots age	$^{206}\text{Pb}^{238}\text{U}$	$\pm 2\sigma$
mr05a147	1.692	0.431	0.155	0.023	0.29	0.082	0.001	1005	163	927	126	1237	25	75	950	228	0.66	0.209	1237	25		
mr04b09	1.688	0.073	0.163	0.004	0.27	0.076	0.001	1004	28	973	21	1102	26	88	983	37	0.30	0.787	1102	26		
mr05a13	1.686	0.065	0.164	0.004	0.29	0.073	0.001	1003	25	978	20	1003	30	97	987	35	0.35	0.323	1003	30		
mr05a23	1.594	0.174	0.164	0.008	0.22	0.071	0.001	968	68	978	44	965	37	101	796	81	0.88	1.396	965	37		
mr05a81	1.661	0.056	0.165	0.004	0.32	0.073	0.001	994	21	986	20	1010	25	98	990	33	0.74	0.318	1010	25		
mr05a80	1.643	0.059	0.166	0.004	0.31	0.071	0.001	987	23	988	20	964	27	102	987	34	0.98	0.359	964	27		
mr09a18	1.537	0.131	0.167	0.005	0.16	0.079	0.002	945	52	997	26	1164	41	86	989	49	0.33	0.491	1164	41		
mr04b39	1.779	0.065	0.168	0.004	0.33	0.072	0.001	1038	24	1002	23	987	23	101	1018	38	0.18	0.342	987	23		
mr05a39	1.664	0.065	0.169	0.005	0.38	0.072	0.001	995	25	1006	28	981	32	103	1000	43	0.70	0.287	981	32		
mr05a31	1.832	0.104	0.174	0.009	0.46	0.076	0.002	1057	37	1036	50	1101	42	94	1052	71	0.65	0.571	1101	42		
mr05a79	1.699	0.079	0.177	0.005	0.28	0.073	0.001	1008	30	1049	26	1009	29	104	1032	44	0.22	0.605	1009	29		
mr05a89	1.873	0.046	0.179	0.003	0.35	0.075	0.001	1071	16	1061	16	1071	22	99	1066	27	0.56	0.272	1071	22		
mr09a29	1.849	0.247	0.180	0.011	0.24	0.075	0.003	1063	88	1065	62	1079	79	99	1065	112	0.98	12.598	1079	79		
mr05a51	2.002	0.079	0.180	0.005	0.36	0.076	0.001	1116	27	1068	28	1099	25	97	1093	45	0.12	0.566	1099	25		
mr04b68	2.027	0.098	0.180	0.004	0.24	0.079	0.001	1125	33	1069	23	1171	34	91	1084	42	0.12	0.624	1171	34		
mr04b57	1.923	0.064	0.182	0.004	0.33	0.075	0.001	1089	22	1070	22	1070	25	101	1083	36	0.63	0.386	1070	25		
mr05a135	1.854	0.090	0.183	0.005	0.28	0.079	0.001	1065	32	1081	27	1161	27	93	1075	47	0.65	0.344	1161	27		
mr04b53	2.050	0.079	0.185	0.005	0.34	0.074	0.001	1132	26	1093	27	1050	23	104	1112	44	0.20	1.003	1050	23		
mr05a144	2.107	0.105	0.186	0.006	0.34	0.082	0.001	1151	34	1102	35	1247	21	88	1126	57	0.22	0.417	1247	21		
mr04b23	2.117	0.080	0.188	0.005	0.33	0.081	0.001	1154	26	1110	25	1229	32	90	1130	42	0.14	0.295	1229	32		
mr05a42	2.130	0.055	0.193	0.004	0.39	0.078	0.001	1158	18	1139	21	1152	16	99	1151	32	0.36	0.077	1152	16		
mr05a51	2.284	0.149	0.199	0.009	0.34	0.084	0.001	1207	46	1167	48	1286	23	91	1188	78	0.46	0.178	1286	23		
mr04b24	2.294	0.064	0.199	0.003	0.30	0.081	0.001	1210	20	1170	18	1231	25	95	1187	31	0.07	0.380	1231	25		
mr05a40	2.067	0.068	0.200	0.004	0.28	0.079	0.001	1138	22	1177	20	1163	25	101	1161	33	0.12	0.595	1163	25		
mr05a30	2.425	0.124	0.202	0.006	0.29	0.087	0.001	1250	37	1189	32	1355	17	88	1212	55	0.14	0.284	1355	17		
mr09a22	2.679	0.534	0.203	0.029	0.36	0.089	0.001	1323	147	1189	157	1397	18	85	1256	258	0.44	0.080	1397	18		
mr09a24	2.329	0.186	0.204	0.009	0.29	0.080	0.001	1221	57	1198	51	1204	36	100	1208	86	0.72	0.379	1204	36		
mr05a128	2.332	0.177	0.211	0.008	0.24	0.088	0.002	1222	54	1236	42	1380	35	90	1231	73	0.81	1.003	1380	35		
mr04b18	2.552	0.088	0.215	0.004	0.29	0.083	0.001	1287	25	1254	23	1275	19	98	1268	39	0.25	0.303	1275	19		
mr04b72	2.632	0.121	0.215	0.007	0.35	0.085	0.001	1310	34	1257	37	1312	26	96	1286	58	0.19	0.805	1312	26		
mr04b67	2.785	0.112	0.229	0.006	0.32	0.085	0.001	1352	30	1330	31	1312	23	101	1341	50	0.55	0.487	1312	23		
mr09a08	2.745	0.204	0.235	0.007	0.20	0.105	0.003	1341	55	1362	36	1714	53	79	1356	66	0.73	0.313	1714	53		
mr09a31	2.945	0.165	0.236	0.007	0.26	0.091	0.001	1394	43	1365	36	1438	26	95	1376	62	0.55	0.467	1438	26		
mr05a56	2.971	0.088	0.237	0.005	0.35	0.093	0.001	1400	23	1372	25	1497	27	92	1389	39	0.30	0.652	1497	27		
mr05a107	3.247	0.294	0.239	0.019	0.44	0.088	0.001	1469	70	1384	99	1387	14	100	1448	136	0.36	0.378	1387	14		
mr05a126	3.472	0.388	0.243	0.018	0.33	0.088	0.001	1521	88	1400	93	1760	16	80	1460	152	0.26	0.999	1760	16		
mr05a92	3.204	0.114	0.243	0.009	0.50	0.095	0.001	1458	28	1401	45	1531	24	92	1452	55	0.14	0.927	1531	24		
mr09a13	3.161	0.145	0.244	0.006	0.26	0.091	0.001	1448	35	1408	30	1448	19	97	1424	52	0.33	0.029	1448	19		
mr05a138	3.166	0.201	0.244	0.010	0.31	0.096	0.001	1449	49	1409	50	1548	23	91	1429	81	0.49	1.167	1548	23		
mr05a141	3.304	0.123	0.245	0.007	0.38	0.095	0.001	1482	29	1412	35	1525	20	93	1456	53	0.06	0.632	1525	20		
mr05a59	3.058	0.093	0.246	0.004	0.25	0.090	0.002	1422	23	1418	19	1420	41	100	1420	33	0.87	0.612	1420	41		
mr04b49	3.195	0.077	0.251	0.006	0.46	0.085	0.001	1456	19	1444	29	1312	17	110	1454	37	0.64	0.325	1312	17		
mr04b60	3.396	0.121	0.253	0.007	0.38	0.092	0.001	1503	28	1453	36	1475	17	99	1487	52	0.16	0.362	1475	17		
mr05a43	3.443	0.171	0.253	0.006	0.23	0.095	0.005	1514	39	1455	29	1535	107	95	1473	52	0.18	0.297	1535	107		
mr05a109	3.336	0.213	0.256	0.010	0.31	0.093	0.001	1490	50	1467	51	1480	21	99	1479	82	0.71	0.249	1480	21		
mr05a53	3.551	0.082	0.268	0.005	0.38	0.093	0.001	1539	18	1529	24	1490	16	103	1536	34	0.69	0.310	1490	16		
mr05a145	3.569	0.158	0.269	0.007	0.31	0.098	0.001	1543	35	1536	38	1609	18	95	1540	59	0.87	0.239	1609	18		
mr04b83	3.907	0.141	0.272	0.006	0.30	0.102	0.001	1615	29	1550	30	1667	21	93	1583	49	0.06	0.952	1667	21		
mr05a61	3.520	0.078	0.275	0.005	0.41	0.091	0.001	1532	17	1567	25	1452	14	108	1539	33	0.14	0.211	1452	14		
mr05a140	3.947	0.131	0.278	0.007	0.37	0.102	0.001	1623	27	1579	34	1669	17	95	1609	50	0.20	0.300	1669	17		
mr05a36	3.832	0.120	0.279	0.005	0.29	0.101	0.001	1599	25	1585	25	1650	18	96	1592	40	0.63	0.820	1650	18		
mr																						

Table A2. Continued.

Sample/ Analysis	Measured Isotopic Ratios						Calculated Ages (Ma)										Detrital (Ma)		Metamorphic (Ma)		CA-TIMS (Ma)			
	$^{207}\text{Pb}/^{235}\text{U}$	$\pm 1\sigma$	$^{206}\text{Pb}/^{238}\text{U}$	$\pm 1\sigma$	Rho	$^{207}\text{Pb}/^{206}\text{Pb}$	$\pm 1\sigma$	$^{207}\text{Pb}/^{235}\text{U}$	$\pm 1\sigma$	$^{206}\text{Pb}^{+2}/^{238}\text{U}$	$\pm 1\sigma$	$^{207}\text{Pb}/^{206}\text{Pb}$	$\pm 1\sigma$	U-Pb/Pb-Pb concordancy (%)	Concordia age	$\pm 2\sigma$	Probability of concordance	Th/U	For Prob Dens plots age	For Prob Dens plots age	$^{206}\text{Pb}/^{238}\text{U}$	$\pm 2\sigma$	notes	
mrl6a10	0.676	0.022	0.074	0.002	0.41	0.059	0.001	524	13	463	12	571	30	81	486	21	0.00	0.195						
mrl6b42	0.675	0.036	0.074	0.003	0.35	0.068	0.002	523	22	463	16	864	53	54	479	30	0.01	0.872						
mrl6b34	0.725	0.051	0.075	0.003	0.30	0.065	0.002	554	30	465	19	774	57	60	481	36	0.00	0.977						
mrl6a32	0.505	0.018	0.075	0.002	0.30	0.047	0.001	415	12	467	10	71	34	655	448	17	0.00	0.166						
mrl6a07	0.747	0.047	0.075	0.002	0.26	0.078	0.001	566	27	467	15	1146	35	41	479	28	0.00	0.764						
mrl6a23	0.486	0.026	0.078	0.003	0.35	0.049	0.001	402	18	482	17	136	37	354	442	28	0.00	0.369						
mrl6b31	0.667	0.020	0.078	0.002	0.40	0.058	0.001	519	12	485	11	522	29	93	499	20	0.01	0.670						
mrl6b07	0.759	0.038	0.081	0.003	0.36	0.065	0.002	574	22	499	17	776	54	64	521	32	0.00	0.350						
mrl6b29	0.738	0.025	0.084	0.002	0.38	0.061	0.001	561	14	521	13	639	30	81	536	22	0.01	0.127						
mrl6b92	0.828	0.032	0.085	0.004	0.58	0.063	0.001	613	18	526	22	705	27	75	590	34	0.00	0.241						
mrl6a13	0.884	0.029	0.089	0.003	0.55	0.065	0.001	643	16	548	19	766	25	71	612	30	0.00	0.116						
mrl6b65	0.887	0.033	0.096	0.003	0.39	0.062	0.001	645	18	591	16	669	29	88	612	29	0.00	0.548						
mrl6b62	1.028	0.050	0.099	0.003	0.31	0.076	0.001	718	25	609	18	1085	23	56	632	33	0.00	0.291						
mrl6b84	1.137	0.040	0.102	0.004	0.53	0.070	0.001	771	19	627	22	938	29	67	715	36	0.00	0.172						
mrl6b27	1.051	0.048	0.105	0.003	0.32	0.070	0.001	730	24	643	18	927	42	69	666	33	0.00	0.400						
mrl6b21	1.072	0.054	0.108	0.004	0.41	0.066	0.001	740	26	663	21	813	46	82	698	45	0.01	0.532						
mrl2c17	1.264	0.070	0.117	0.005	0.37	0.073	0.001	830	31	713	28	1018	24	70	753	49	0.00	0.047						
mrl6c18	0.838	0.062	0.149	0.007	0.31	0.055	0.002	618	34	896	39	416	80	215	715	56	0.00	1.144						
mrl6b14	1.855	0.060	0.155	0.004	0.41	0.076	0.001	1065	21	931	23	1108	29	84	999	38	0.00	0.169						
mrl6a37	1.821	0.071	0.163	0.006	0.48	0.072	0.001	1053	26	976	34	991	21	98	1032	49	0.01	0.443						
mrl6b82	1.874	0.048	0.165	0.003	0.36	0.078	0.001	1072	17	984	17	1146	21	86	1025	29	0.00	1.093						
mrl6b13	1.898	0.048	0.172	0.003	0.36	0.073	0.001	1080	17	1023	17	1020	21	100	1051	29	0.00	0.100						
mrl2c10	2.125	0.076	0.186	0.005	0.36	0.079	0.001	1157	25	1098	26	1171	24	94	1129	43	0.04	0.366						
mrl6b19	2.331	0.109	0.188	0.007	0.41	0.081	0.001	1222	33	1112	39	1227	33	91	1177	61	0.01	0.515						
mrl6b51	2.477	0.076	0.192	0.005	0.39	0.086	0.001	1265	22	1134	25	1332	18	85	1200	40	0.00	0.174						
mrl6a14	2.761	0.202	0.195	0.012	0.42	0.097	0.001	1345	55	1149	65	1569	19	73	1262	104	0.00	0.371						
mrl6b39	2.348	0.064	0.196	0.004	0.36	0.081	0.001	1227	20	1152	21	1232	21	94	1192	34	0.00	0.501						
mrl2c31	4.342	0.488	0.203	0.016	0.34	0.150	0.002	1701	93	1190	84	2350	26	51	1285	160	0.00	0.236						
mrl6b32	2.899	0.217	0.210	0.013	0.40	0.092	0.001	1382	57	1226	67	1475	15	83	1317	105	0.02	0.030						
mrl6b41	2.788	0.095	0.210	0.005	0.38	0.092	0.001	1352	25	1228	29	1458	16	84	1298	46	0.00	0.491						
mrl2c20	2.762	0.081	0.215	0.004	0.35	0.088	0.001	1345	22	1257	24	1385	20	91	1304	38	0.00	0.235						
mrl6b47	2.849	0.073	0.222	0.005	0.44	0.085	0.001	1369	19	1294	26	1320	20	98	1349	37	0.00	0.556						
mrl6b70	3.145	0.133	0.223	0.007	0.38	0.099	0.001	1444	33	1296	37	1605	24	81	1378	59	0.00	0.395						
mrl6b69	3.406	0.161	0.224	0.008	0.39	0.100	0.001	1506	37	1305	43	1630	23	80	1416	69	0.00	0.505						
mrl6b60	5.470	0.230	0.234	0.008	0.41	0.161	0.001	1896	36	1353	42	2465	15	55	1555	75	0.00	0.342						
mrl6b73	3.319	0.087	0.237	0.005	0.43	0.094	0.001	1486	20	1373	28	1511	23	91	1455	40	0.00	0.594						
mrl6b89	3.201	0.084	0.243	0.005	0.40	0.093	0.001	1457	20	1400	27	1484	17	94	1440	38	0.03	0.379						
mrl2c23	3.782	0.159	0.253	0.008	0.40	0.103	0.002	1589	34	1453	43	1673	34	87	1542	64	0.00	0.971						
mrl6b49	3.790	0.148	0.254	0.008	0.43	0.100	0.002	1591	31	1457	43	1625	33	90	1555	61	0.00	1.004						
mrl6b96	3.711	0.195	0.255	0.009	0.32	0.104	0.001	1574	42	1462	44	1695	18	86	1518	72	0.03	0.681						
mrl6b83	4.023	0.099	0.270	0.006	0.47	0.100	0.001	1639	20	1542	32	1617	15	95	1626	40	0.00	0.290						
mrl6b75	4.152	0.163	0.272	0.007	0.34	0.105	0.002	1665	32	1550	36	1709	28	91	1614	57	0.00	0.212						
mrl6b85	4.156	0.103	0.277	0.007	0.49	0.099	0.001	1665	20	1574	34	1607	15	98	1656	40	0.00	0.164						
mrl6c24	3.391	0.205	0.295	0.007	0.19	0.101	0.002	1502	47	1666	34	1649	38	101	1600	58	0.00	0.212						
mrl6b44	4.882	0.120	0.297	0.006	0.41	0.107	0.001	1799	21	1675	30	1745	18	96	1768	40	0.00	0.675						
mrl6c09	3.713	0.208	0.314	0.010	0.29	0.099	0.002	1574	45	1759	49	1611	39	109	1646	72	0.00	1.018						
mrl6c28	14.712	0.302	0.305	0.009	0.50	0.195	0.002	2797	20	2654	41	2785	14	95	2794	39	0.00	0.482						
mrl6b119	0.473	0.020	0.062	0.003	0.49	0.047	0.001	393	14	389	16	61	43	637	392	25	0.78	0.530	389	16				
mrl6b23	0.515	0.031	0.065	0.003	0.35	0.055	0.001	422	21	409	17	392	49	104	413	30	0.54	0.312	409	17	425.53	0.64		
mrl2c44	0.543	0.048	0.066	0.002	0.30	0.065	0.002	441	31	413	14	765	50	54	416	27	0.39	0.429	413	14				
mrl6b55	0.516	0.023	0.067	0.002	0.31	0.05																		

Table A2. Continued.

Sample/ Analysis	Measured Isotopic Ratios						Calculated Ages (Ma)								Detrital (Ma)		Metamorphic (Ma)			CA-TIMS (Ma)					
	$^{207}\text{Pb}/^{235}\text{U}$	$\pm 1\sigma$	$^{206}\text{Pb}/^{238}\text{U}$	$\pm 1\sigma$	Rho	$^{207}\text{Pb}/^{206}\text{Pb}$	$\pm 1\sigma$	$^{207}\text{Pb}/^{235}\text{U}$	$\pm 1\sigma$	$^{206}\text{Pb}^{238}\text{U}$	$\pm 1\sigma$	$^{207}\text{Pb}/^{206}\text{Pb}$	$\pm 1\sigma$	U-Pb/Pb-Pb concordancy (%)	Concordia age	$\pm 2\sigma$	Probability of concordance	Th/U	For Prob Dens plots age	For Prob Dens plots age	$^{206}\text{Pb}/^{238}\text{U}$	U	$\pm 2\sigma$	notes	
mr12c18	0.678	0.037	0.082	0.003	0.30	0.055	0.001	526	22	510	16	429	44	119	515	30	0.51	0.516	510	16					
mr16a20	0.656	0.027	0.082	0.002	0.35	0.058	0.001	512	17	511	15	532	38	96	511	26	0.95	0.761	511	15					
mr16c08	0.539	0.079	0.084	0.005	0.21	0.055	0.001	438	52	517	31	418	55	124	499	58	0.14	0.525	517	31					
mr16b40	0.738	0.037	0.084	0.003	0.38	0.060	0.002	561	21	523	19	616	55	85	538	34	0.09	0.788	523	19					
mr16b91	0.771	0.055	0.086	0.004	0.34	0.064	0.001	581	31	531	25	757	29	70	546	45	0.13	0.149	531	25					
mr16a38	0.715	0.034	0.088	0.003	0.36	0.054	0.001	548	20	544	18	375	37	145	546	31	0.86	0.482	544	18					
mr16b28	0.728	0.047	0.089	0.003	0.27	0.062	0.001	555	28	551	18	686	44	80	552	34	0.89	0.479	551	18					
mr16b18	0.727	0.040	0.090	0.002	0.19	0.059	0.001	555	23	553	11	584	34	95	553	21	0.93	0.769	553	11					
mr16b59	0.804	0.036	0.090	0.003	0.36	0.061	0.001	599	20	557	17	631	25	88	572	31	0.05	0.507	557	17					
mr16b10	0.836	0.057	0.094	0.003	0.25	0.066	0.001	617	31	581	19	791	47	73	587	36	0.27	0.197	581	19					
mr16b66	0.848	0.036	0.096	0.002	0.27	0.065	0.001	624	20	594	13	779	31	76	601	25	0.15	0.851	594	13					
mr16b123	0.954	0.293	0.097	0.017	0.28	0.092	0.001	680	152	594	98	1459	26	41	611	186	0.59	0.350	594	98					
mr16c23	0.786	0.049	0.100	0.004	0.33	0.056	0.001	589	28	613	24	463	35	132	603	42	0.42	0.029	613	24					
mr16b74	0.816	0.046	0.100	0.003	0.22	0.063	0.001	606	26	614	15	703	41	87	613	28	0.75	1.100	614	15					
mr12c29	0.857	0.054	0.102	0.003	0.23	0.058	0.001	629	30	624	17	513	44	122	625	32	0.89	0.815	624	17					
mr16b54	0.897	0.040	0.106	0.003	0.28	0.062	0.001	650	21	647	15	661	33	98	648	27	0.88	0.253	647	15					
mr16b113	0.898	0.036	0.106	0.003	0.37	0.063	0.001	651	19	649	18	698	21	93	650	31	0.92	0.242	649	18					
mr16b52	0.901	0.029	0.107	0.002	0.36	0.058	0.001	652	15	653	14	542	33	121	653	24	0.95	0.004	653	14					
mr16b20	0.959	0.047	0.112	0.004	0.39	0.058	0.001	683	24	682	24	530	56	129	683	41	0.97	0.576	682	24					
mr16b33	1.122	0.094	0.122	0.005	0.24	0.067	0.001	764	45	745	29	834	40	89	749	53	0.68	0.570	745	29					
mr12c08	1.377	0.066	0.144	0.005	0.34	0.065	0.001	879	28	869	27	790	38	110	874	45	0.76	0.306	790	38					
mr16c20	1.396	0.116	0.150	0.007	0.29	0.075	0.002	887	49	899	40	1078	43	83	895	70	0.83	0.592	1078	43					
mr16b90	1.451	0.069	0.154	0.004	0.26	0.068	0.001	910	29	922	21	878	37	105	919	38	0.70	0.203	878	37					
mr16b11	1.655	0.076	0.166	0.004	0.29	0.072	0.001	992	29	988	24	997	28	99	989	42	0.90	0.738	997	28					
mr12c33	1.722	0.079	0.171	0.004	0.27	0.074	0.001	1017	29	1019	23	1031	32	99	1018	41	0.94	0.903	1031	32					
mr16b08	2.026	0.112	0.175	0.007	0.37	0.082	0.001	1124	38	1038	39	1255	27	83	1081	65	0.05	0.254	1255	27					
mr12c13	1.921	0.069	0.179	0.004	0.33	0.076	0.001	1089	24	1062	23	1083	21	98	1074	38	0.33	0.471	1083	21					
mr16b37	2.156	0.092	0.190	0.006	0.36	0.082	0.001	1167	30	1122	32	1234	25	91	1146	51	0.19	0.641	1234	25					
mr16b30	2.142	0.095	0.192	0.005	0.27	0.077	0.001	1162	31	1132	24	1129	27	100	1142	43	0.38	0.497	1129	27					
mr16b124	2.237	0.194	0.197	0.010	0.29	0.082	0.001	1193	61	1158	54	1257	28	92	1172	92	0.62	0.646	1257	28					
mr16b122	2.221	0.133	0.198	0.007	0.29	0.085	0.001	1188	42	1162	36	1311	24	89	1172	62	0.59	0.228	1311	24					
mr16b109	2.256	0.195	0.200	0.010	0.30	0.090	0.001	1199	61	1174	56	1425	29	82	1185	95	0.72	0.192	1425	29					
mr16a34	2.197	0.171	0.203	0.006	0.18	0.081	0.002	1180	54	1189	30	1222	44	97	1187	55	0.87	0.372	1222	44					
mr12c09	2.273	0.099	0.205	0.005	0.29	0.083	0.001	1204	31	1204	27	1274	27	95	1204	46	0.99	0.636	1274	27					
mr16b58	2.612	0.182	0.206	0.007	0.24	0.093	0.001	1304	51	1209	37	1496	29	81	1235	68	0.09	0.286	1496	29					
mr12c21	2.306	0.137	0.210	0.006	0.26	0.079	0.001	1214	42	1229	34	1177	30	104	1224	59	0.75	0.337	1177	30					
mr16c21	2.599	0.131	0.211	0.009	0.40	0.088	0.001	1300	37	1234	45	1375	21	90	1277	68	0.15	0.421	1375	21					
mr16c13	2.720	0.139	0.230	0.008	0.35	0.086	0.001	1334	38	1336	44	1344	27	99	1335	66	0.97	0.981	1344	27					
mr16c25	3.088	0.177	0.252	0.009	0.30	0.097	0.002	1430	44	1451	45	1560	35	93	1439	72	0.69	0.588	1560	35					
mr16a09	3.211	0.063	0.254	0.004	0.41	0.089	0.001	1460	15	1460	21	1394	14	105	1466	29	1.00	0.499	1394	14					
mr16c19	3.043	0.225	0.259	0.011	0.28	0.095	0.002	1418	56	1483	55	1532	43	97	1451	87	0.33	0.767	1532	43					
mr16c14	3.619	0.325	0.275	0.011	0.23	0.112	0.002	1554	71	1564	57	1835	33	85	1560	98	0.90	0.507	1835	33					
mr16c10	4.054	0.262	0.283	0.012	0.34	0.106	0.001	1645	53	1605	62	1723	25	93	1629	93	0.54	0.731	1723	25					
mr16c24	3.964	0.169	0.286	0.008	0.32	0.102	0.002	1627	35	1623	39	1655	28	98	1625	59	0.93	0.728	1655	28					
mr16c207	4.454	0.146	0.315	0.006	0.31	0.098	0.001	1722	27	1766	32	1592	22	111	1739	47	0.21	0.086	1592	22					
mr16b43	4.735	0.130	0.316	0.008	0.40	0.100	0.001	1773	23	1770	41	1625	18	109	1773	46	0.93	0.349	1625	18					
mr16c111	4.740	0.173	0.317	0.010	0.42	0.105	0.001	1774	31	1773															

Table A2. Continued.

Sample/ Analysis	Measured Isotopic Ratios						Calculated Ages (Ma)								Detrital (Ma)		Metamorphic (Ma)		CA-TIMS (Ma)		notes		
	$^{207}\text{Pb}/^{235}\text{U}$	$\pm 1\sigma$	$^{206}\text{Pb}/^{238}\text{U}$	$\pm 1\sigma$	Rho	$^{207}\text{Pb}/^{206}\text{Pb}$	$\pm 1\sigma$	$^{207}\text{Pb}/^{235}\text{U}$	$\pm 1\sigma$	$^{206}\text{Pb}^{+2}/^{238}\text{U}$	$\pm 1\sigma$	$^{207}\text{Pb}/^{206}\text{Pb}$	$\pm 1\sigma$	U-Pb/Pb-Pb concordancy (%)	Concordia age	$\pm 2\sigma$	Probability of concordance	Th/U	For Prob Dens plots age	For Prob Dens plots age	$^{206}\text{Pb}/^{238}\text{U}$	$\pm 1\sigma$	
mr03a64	2.261	0.041	0.191	0.003	0.42	0.079	0.001	1200	13	1128	16	1171	14	96	1176	24	0.00	0.690					
mr02a37	2.194	0.066	0.191	0.005	0.40	0.080	0.001	1179	21	1128	25	1198	15	94	1159	38	0.04	0.670					
mr02a80	2.352	0.065	0.220	0.004	0.30	0.083	0.001	1228	20	1282	19	1258	24	102	1255	31	0.02	0.360					
mr03a74	3.443	0.124	0.225	0.007	0.45	0.102	0.001	1514	28	1306	38	1669	13	78	1450	56	0.00	0.540					
mr03a41	3.346	0.225	0.231	0.011	0.36	0.103	0.002	1492	53	1338	59	1679	40	80	1420	94	0.02	0.120					
mr04a10	3.143	0.059	0.231	0.004	0.45	0.091	0.001	1443	15	1341	21	1440	14	93	1420	28	0.00	0.340					
mr02a21	2.518	0.086	0.237	0.004	0.23	0.083	0.001	1277	25	1369	19	1269	20	108	1335	33	0.00	0.130					
mr02a141	3.510	0.120	0.246	0.006	0.33	0.096	0.001	1530	27	1416	29	1553	21	91	1474	47	0.00	0.430					
mr02a54	2.682	0.091	0.253	0.006	0.35	0.080	0.001	1323	25	1456	31	1192	25	122	1364	44	0.00	0.520					
mr03a81	3.897	0.074	0.268	0.004	0.40	0.096	0.001	1613	15	1532	21	1549	15	99	1591	29	0.00	0.380					
mr03a104	4.680	0.167	0.276	0.007	0.38	0.120	0.001	1764	30	1569	37	1960	15	80	1689	57	0.00	0.820					
mr04a17	4.317	0.109	0.284	0.006	0.40	0.104	0.001	1697	21	1613	29	1690	16	95	1675	40	0.00	0.550					
mr03a55	4.493	0.089	0.290	0.005	0.40	0.104	0.001	1730	16	1641	23	1702	13	96	1707	31	0.00	0.790					
mr02a34	4.568	0.113	0.299	0.006	0.38	0.110	0.001	1743	21	1687	28	1797	10	94	1728	39	0.04	0.870					
mr03a98	5.771	0.105	0.322	0.006	0.48	0.121	0.001	1942	16	1799	28	1966	9	92	1930	32	0.00	0.930					
mr02a12	5.422	0.141	0.365	0.006	0.31	0.111	0.001	1888	22	2006	28	1818	17	110	1924	39	0.00	0.560					
mr02a119	0.494	0.026	0.064	0.002	0.28	0.058	0.001	408	17	399	11	527	22	76	401	21	0.64	0.900	399	11			
mr02a114	0.502	0.022	0.066	0.002	0.26	0.059	0.001	413	15	410	9	553	26	74	410	17	0.85	0.140	410	9			
mr02a145	0.543	0.020	0.068	0.002	0.31	0.056	0.001	440	13	424	9	447	23	95	428	17	0.25	0.140	424	9			
mr02a123	0.579	0.026	0.070	0.002	0.36	0.057	0.001	464	17	434	14	480	19	90	444	25	0.09	0.190	434	14			
mr02a142	0.541	0.021	0.070	0.002	0.29	0.058	0.001	439	14	435	9	532	25	82	436	17	0.77	0.450	435	9			
mr02a117	0.491	0.025	0.070	0.003	0.40	0.055	0.001	406	17	436	17	412	39	106	420	28	0.10	0.990	436	17	486.29	5.04	
mr03a45	0.564	0.017	0.070	0.001	0.25	0.056	0.001	454	11	439	6	448	24	98	441	12	0.18	1.050	439	6			
mr02a63	0.514	0.025	0.071	0.002	0.24	0.055	0.001	421	17	444	10	423	28	105	439	19	0.18	0.500	444	10			
mr02a122	0.580	0.042	0.072	0.004	0.40	0.055	0.001	465	27	448	25	421	25	106	455	43	0.55	0.170	448	25			
mr02a84	0.535	0.017	0.072	0.001	0.29	0.055	0.000	435	12	450	8	417	18	108	446	15	0.21	0.130	450	8			
mr03a75	0.590	0.023	0.073	0.001	0.24	0.058	0.001	471	15	453	8	515	29	88	456	16	0.24	0.1370	453	8			
mr02a38	0.548	0.022	0.073	0.002	0.27	0.058	0.001	444	14	454	9	538	22	84	451	17	0.49	0.840	454	9	483.52	1.25	
mr02a99	0.602	0.028	0.073	0.003	0.40	0.057	0.001	479	18	455	16	496	21	92	465	28	0.21	0.170	455	16			
mr03a30	0.584	0.034	0.073	0.002	0.30	0.058	0.001	467	22	456	15	527	21	87	459	28	0.64	0.370	456	15			
mr02a24	0.558	0.018	0.073	0.001	0.31	0.057	0.000	450	12	456	9	494	17	92	454	16	0.67	0.080	456	9			
mr02a107	0.607	0.023	0.073	0.002	0.41	0.057	0.001	481	14	457	13	487	25	94	467	23	0.10	0.380	457	13			
mr03a85	0.595	0.019	0.074	0.001	0.27	0.057	0.001	474	12	459	8	486	31	94	462	14	0.21	0.600	459	8			
mr03a91	0.585	0.015	0.074	0.001	0.25	0.056	0.000	468	9	460	6	447	18	103	462	11	0.42	0.080	460	6			
mr03a31	0.539	0.059	0.074	0.004	0.24	0.059	0.001	438	39	460	23	558	42	82	455	43	0.59	0.810	460	23			
mr02a67	0.560	0.037	0.074	0.003	0.26	0.056	0.001	451	24	461	15	437	25	105	459	29	0.71	0.770	461	15			
mr03a86	0.571	0.024	0.074	0.001	0.24	0.055	0.001	459	15	461	9	412	33	112	461	17	0.89	0.710	461	9			
mr02a62	0.546	0.039	0.074	0.003	0.24	0.056	0.001	442	26	462	15	468	31	99	458	29	0.46	0.590	462	15			
mr04a22	0.606	0.019	0.075	0.001	0.31	0.056	0.000	481	12	465	9	453	18	103	469	16	0.19	0.210	465	9			
mr02a113	0.623	0.040	0.075	0.003	0.30	0.060	0.001	492	25	466	17	586	35	79	472	32	0.31	0.430	466	17			
mr04a21	0.597	0.022	0.075	0.002	0.28	0.055	0.001	475	14	466	9	431	27	108	469	17	0.54	0.850	466	9			
mr03a70	0.609	0.024	0.075	0.002	0.28	0.057	0.000	483	15	467	10	504	19	93	471	18	0.30	0.280	467	10			
mr03a48	0.592	0.021	0.075	0.002	0.32	0.055	0.001	472	13	468	10	406	25	115	469	19	0.76	0.620	468	10			
mr03a26	0.649	0.034	0.075	0.003	0.40	0.058	0.000	508	21	469	19	536	27	88	485	33	0.08	0.770	469	19			
mr04a19	0.582	0.024	0.075	0.001	0.24	0.056	0.001	466	15	469	9	453	27	103	468	17	0.87	1.250	469	9			
mr02a58	0.567	0.019	0.076	0.001	0.27	0.057	0.000	456	13	470	8	492	19	96	467	16	0.27	0.140	470	8			
mr03a106	0.600	0.019	0.076	0.001	0.25	0.057	0.001	477	12	472	7	487	27	97	473	14	0.65	0.620	472	7			
mr02a109	0.622	0.020	0.076	0.002	0.28	0.057	0.001	491	13	475	11	494	21	96	482	20	0.22	0.620	475	11			
mr02a90	0.569	0.029	0.076	0.001	0.18	0.056	0.001	457	19	475	8	461	28	103	473	16	0.35	0.850	477	8			
mr03a79	0.604	0.022	0.076	0.002	0.36	0.055	0.000	480	14	475	12	474	20	112	476	21	0.72	0.130	475	12			
mr02a120	0.558	0.028	0.077	0.002	0.26	0.055																	

Table A2. Continued.

Sample/ Analysis	Measured Isotopic Ratios						Calculated Ages (Ma)								Detrital (Ma)		Metamorphic (Ma)			CA-TIMS (Ma)			
	$^{207}\text{Pb}/^{235}\text{U}$	$\pm 1\sigma$	$^{206}\text{Pb}/^{238}\text{U}$	$\pm 1\sigma$	Rho	$^{207}\text{Pb}/^{206}\text{Pb}$	$\pm 1\sigma$	$^{207}\text{Pb}/^{235}\text{U}$	$\pm 1\sigma$	$^{206}\text{Pb}^{2/3}$	$\pm 1\sigma$	$^{207}\text{Pb}/^{206}\text{Pb}$	$\pm 1\sigma$	U-Pb/Pb-Pb concordancy (%)	Concordia age	$\pm 2\sigma$	Probability of concordance	Th/U	For Prob Dens plots age	For Prob Dens plots age	$^{206}\text{Pb}/^{238}\text{U}$	$\pm 2\sigma$	notes
mr02a42	0.745	0.053	0.101	0.003	0.22	0.058	0.001	565	31	618	19	540	34	115	606	35	0.10	0.360	618	19			
mr02a44	0.766	0.070	0.101	0.003	0.18	0.059	0.001	578	40	619	20	579	35	107	613	37	0.31	0.580	619	20			
mr03a47	1.066	0.205	0.101	0.013	0.34	0.074	0.001	737	101	728	1052	144	27	59	650	144	0.27	0.520	620	78			
mr02a09	0.854	0.036	0.102	0.003	0.29	0.061	0.001	627	20	627	15	651	22	96	627	27	0.99	0.360	627	15			
mr02a71	0.808	0.047	0.104	0.003	0.25	0.059	0.001	601	27	637	17	567	34	112	628	32	0.20	0.410	637	17			
mr04a13	0.899	0.035	0.104	0.002	0.23	0.061	0.001	651	18	639	11	648	33	99	641	20	0.52	0.740	639	11			
mr03a54	0.898	0.036	0.106	0.002	0.29	0.061	0.001	651	19	649	14	630	23	103	649	26	0.91	0.220	649	14			
mr03a27	0.925	0.069	0.113	0.004	0.21	0.066	0.001	665	36	689	21	799	29	86	684	39	0.53	0.290	689	21			
mr02a40	0.991	0.047	0.115	0.003	0.28	0.065	0.001	699	24	704	18	769	28	92	703	32	0.84	0.350	704	18			
mr03a20	0.948	0.085	0.118	0.005	0.24	0.063	0.001	677	44	717	29	710	39	101	707	53	0.38	0.970	717	29			
mr04a31	1.143	0.043	0.120	0.003	0.31	0.065	0.001	770	24	732	16	776	19	94	745	29	0.06	0.410	732	16			
mr02a60	1.325	0.083	0.124	0.004	0.31	0.070	0.001	767	29	744	23	844	26	91	750	40	0.33	0.500	744	23			
mr03a87	1.221	0.053	0.127	0.004	0.32	0.067	0.001	810	24	771	20	836	30	92	785	36	0.14	0.790	771	20			
mr03a49	1.245	0.068	0.131	0.004	0.28	0.065	0.001	821	31	795	23	780	37	102	802	41	0.43	0.800	795	23			
mr04a29	1.223	0.046	0.132	0.003	0.29	0.063	0.001	811	21	797	16	704	31	113	801	29	0.52	0.540	797	16			
mr02a118	1.464	0.061	0.156	0.004	0.28	0.071	0.001	915	25	936	20	954	25	98	928	36	0.47	0.390	954	25			
mr04a07	1.651	0.090	0.158	0.005	0.30	0.073	0.001	990	35	947	29	1006	18	94	963	51	0.26	0.360	1006	18			
mr02a87	1.679	0.059	0.162	0.004	0.35	0.076	0.001	1001	23	967	22	1086	24	89	983	37	0.18	0.590	1086	24			
mr03a22	1.666	0.184	0.163	0.012	0.34	0.073	0.002	996	70	975	67	1020	57	96	984	112	0.79	0.470	1020	57			
mr03a23	1.748	0.266	0.164	0.018	0.36	0.076	0.001	1026	98	980	99	1090	21	90	1002	164	0.68	0.290	1090	21			
mr02a52	1.631	0.047	0.165	0.003	0.33	0.072	0.001	982	18	986	17	974	17	101	984	29	0.85	0.300	974	17			
mr02a17	1.779	0.104	0.167	0.008	0.43	0.085	0.001	1038	38	996	46	1314	28	76	1023	70	0.36	0.650	1314	28			
mr03a94	1.774	0.076	0.172	0.004	0.25	0.073	0.001	1036	28	1024	20	1024	19	100	1027	37	0.68	0.210	1024	19			
mr02a111	1.704	0.082	0.174	0.005	0.30	0.072	0.001	1010	31	1032	28	986	19	105	1022	47	0.53	0.330	986	19			
mr02a30	1.738	0.085	0.174	0.004	0.25	0.084	0.001	1023	31	1033	23	1297	30	80	1030	41	0.77	0.920	1297	30			
mr02a69	1.780	0.090	0.175	0.007	0.39	0.073	0.001	1038	33	1039	37	1009	22	103	1038	58	0.99	0.510	1009	22			
mr02a111	1.799	0.066	0.182	0.004	0.26	0.076	0.001	1045	24	1080	19	1097	22	98	1067	33	0.18	0.280	1097	22			
mr02a07	1.998	0.058	0.190	0.004	0.33	0.077	0.001	1115	20	1121	20	1111	21	101	1118	32	0.80	0.340	1111	21			
mr03a89	2.142	0.056	0.190	0.003	0.32	0.079	0.001	1162	18	1124	17	1172	17	96	1141	29	0.07	0.370	1172	17			
mr02a91	2.135	0.137	0.201	0.006	0.23	0.079	0.001	1160	44	1183	31	1162	30	102	1176	56	0.63	0.400	1162	30			
mr02a82	2.099	0.076	0.205	0.005	0.31	0.077	0.001	1148	25	1202	24	1118	23	107	1175	39	0.07	0.380	1118	23			
mr04a14	2.208	0.097	0.207	0.004	0.22	0.078	0.001	1184	31	1212	21	1141	20	106	1204	38	0.39	0.180	1141	20			
mr02a110	2.226	0.166	0.208	0.010	0.31	0.080	0.001	1189	52	1219	51	1189	19	103	1204	83	0.62	0.320	1189	19			
mr03a32	2.440	0.176	0.209	0.010	0.32	0.084	0.001	1254	52	1221	52	1290	18	95	1237	85	0.58	0.710	1290	18			
mr02a39	2.569	0.093	0.212	0.005	0.31	0.092	0.001	1292	26	1237	25	1468	17	84	1262	42	0.07	0.620	1468	17			
mr02a92	2.167	0.110	0.212	0.005	0.24	0.077	0.001	1171	35	1240	27	1117	24	111	1214	47	0.07	0.180	1117	24			
mr02a145	2.504	0.095	0.216	0.005	0.31	0.087	0.001	1273	28	1259	27	1367	25	92	1266	44	0.66	0.850	1367	25			
mr02a18	2.309	0.088	0.216	0.005	0.27	0.081	0.001	1215	27	1263	24	1219	19	104	1242	40	0.12	0.610	1219	19			
mr03a97	2.665	0.126	0.219	0.008	0.39	0.082	0.001	1319	35	1276	43	1245	26	102	1304	64	0.32	0.410	1245	26			
mr02a61	2.645	0.072	0.220	0.004	0.36	0.086	0.001	1301	23	1243	23	1347	13	95	1301	35	0.22	0.350	1347	13			
mr02a102	2.386	0.083	0.221	0.005	0.30	0.081	0.001	1238	25	1287	24	1232	17	105	1263	39	0.09	0.580	1232	17			
mr02a93	2.530	0.153	0.225	0.009	0.34	0.082	0.001	1281	44	1309	48	1235	15	106	1293	75	0.60	0.090	1235	15			
mr02a72	2.581	0.097	0.231	0.007	0.40	0.081	0.001	1295	27	1341	36	1222	26	110	1308	51	0.20	0.390	1222	26			
mr02a103	2.648	0.090	0.235	0.005	0.31	0.083	0.001	1314	25	1359	26	1265	28	107	1335	41	0.13	0.490	1265	28			
mr03a65	4.137	0.236	0.286	0.009	0.29	0.108	0.002	1662	47	1623	47	1765	33	92	1642	76	0.49	1.530	1765	33			
mr02a94	4.296	0.194	0.317	0.008	0.28	0.102	0.001	1693	37	1775	39	1670	21	106	1729	60	0.07	0.960	1670	21			
mr02a08	4.864	0.154	0.319	0.007	0.35	0.113	0.001	1796	27	1783	34	1847	18	97	1792	48	0.72	1.010	1847	18			
mr03a67	5.273	0.177	0.328	0.008	0.37	0.112	0.001	1865	29	1828	39	1832	18	100	1854	54	0.35	0.770	1832	18			
mr02a68	5.744	0.132	0.343	0.007	0.44	0.117	0.001	1938	20	1901	33	1908	13	100	1934	39	0.22	1.030	1908	13			
mr04a11	6.892	0.143	0.376	0.007	0.42																		

Table A2. Continued.

Sample/ Analysis	Measured Isotopic Ratios						Calculated Ages (Ma)								Detrital (Ma)		Metamorphic (Ma)		CA-TIMS (Ma)		notes
	$^{207}\text{Pb}/^{235}\text{U}$	$\pm 1\sigma$	$^{206}\text{Pb}/^{238}\text{U}$	$\pm 1\sigma$	Rho	$^{207}\text{Pb}/^{206}\text{Pb}$	$\pm 1\sigma$	$^{207}\text{Pb}/^{235}\text{U}$	$\pm 1\sigma$	$^{206}\text{Pb}^{+2}/^{238}\text{U}$	$\pm 1\sigma$	$^{207}\text{Pb}/^{206}\text{Pb}$	$\pm 1\sigma$	U-Pb/Pb-Pb concordancy (%)	Concordia age	$\pm 2\sigma$	Probability of concordance	Th/U	For Prob Dens plots age	For Prob Dens plots age	$^{206}\text{Pb}/^{238}$ U
se07b13	0.548	0.013	0.069	0.002	0.46	0.055	0.001	444	9	428	9	430	25	100	437	15	0.11	0.948	428	9	
se09a34	0.538	0.019	0.069	0.001	0.26	0.056	0.001	437	12	428	8	470	27	91	430	14	0.49	0.489	428	8	
au26a61	0.526	0.024	0.069	0.002	0.26	0.056	0.001	429	16	409	10	464	22	92	428	18	0.93	0.630	428	10	
se08b34	0.533	0.012	0.070	0.001	0.34	0.056	0.000	434	8	435	7	444	18	98	435	12	0.85	0.913	435	7	
au26a52	0.558	0.029	0.072	0.002	0.33	0.055	0.001	450	19	445	15	415	21	107	447	27	0.82	0.524	445	15	
au26a64	0.596	0.030	0.072	0.002	0.27	0.061	0.001	475	19	448	12	622	40	72	453	22	0.16	0.932	448	12	
au26a60	0.583	0.037	0.072	0.003	0.37	0.056	0.001	466	24	450	21	454	46	99	456	37	0.51	0.518	450	21	
se08b14	0.557	0.037	0.072	0.002	0.24	0.056	0.001	450	24	450	14	462	43	98	450	26	0.98	0.416	450	14	
se07b12	0.610	0.083	0.073	0.003	0.16	0.061	0.001	484	52	454	19	656	35	69	456	37	0.58	0.546	454	19	
se09a14	0.574	0.022	0.073	0.001	0.26	0.055	0.001	460	14	455	9	414	28	110	456	16	0.72	0.840	455	9	
se09a63	0.598	0.020	0.074	0.002	0.34	0.057	0.001	476	13	457	10	510	23	90	463	18	0.17	0.589	457	10	
au26a33	0.581	0.049	0.073	0.003	0.23	0.058	0.001	465	32	457	17	518	37	88	458	33	0.81	0.139	457	17	
au26a12	0.596	0.020	0.074	0.001	0.27	0.056	0.001	475	13	458	8	465	26	99	462	15	0.21	0.431	458	8	
au26a17	0.602	0.046	0.074	0.003	0.28	0.061	0.001	478	29	458	19	624	30	73	462	35	0.49	0.149	458	19	
se09a52	0.596	0.020	0.074	0.002	0.35	0.057	0.001	474	13	459	10	489	22	94	464	18	0.25	0.365	459	10	
au26a19	0.612	0.022	0.074	0.002	0.29	0.058	0.001	485	14	460	9	526	22	87	466	18	0.09	0.600	460	9	
se09a46	0.544	0.024	0.075	0.002	0.25	0.056	0.001	441	16	463	10	434	31	107	459	18	0.16	0.082	463	10	
se08b30	0.547	0.031	0.075	0.002	0.24	0.056	0.001	443	20	463	12	442	41	105	459	23	0.33	0.747	463	12	
se08b17	0.562	0.023	0.074	0.002	0.30	0.056	0.000	453	15	463	11	446	20	104	460	20	0.54	0.234	463	11	
au26a63	0.617	0.032	0.075	0.002	0.24	0.060	0.001	488	20	468	11	615	39	76	471	21	0.33	0.522	468	11	
se09a21	0.584	0.015	0.075	0.001	0.38	0.056	0.000	467	10	469	9	440	17	106	468	15	0.86	0.008	469	9	
au26a13	0.625	0.029	0.077	0.002	0.28	0.058	0.001	493	18	479	12	544	41	88	482	22	0.45	0.670	479	12	
se09a22	0.660	0.103	0.077	0.007	0.28	0.066	0.001	515	63	479	41	809	26	59	486	77	0.58	0.175	479	41	
se07b19	0.638	0.021	0.077	0.001	0.29	0.059	0.001	501	13	481	9	578	32	83	485	16	0.14	0.834	481	9	
se07b11	0.639	0.025	0.077	0.002	0.27	0.058	0.001	502	16	481	10	535	23	90	485	18	0.19	0.075	481	10	
au26a09	0.669	0.035	0.079	0.002	0.27	0.062	0.001	520	21	490	13	691	38	71	496	24	0.16	0.820	490	13	
se09a67	0.646	0.030	0.079	0.003	0.36	0.058	0.001	506	19	492	16	544	34	90	497	28	0.49	0.583	492	16	
se08b12	0.647	0.016	0.080	0.001	0.31	0.057	0.001	507	10	499	8	508	20	98	501	14	0.47	0.541	499	8	
se08b11	0.596	0.142	0.085	0.006	0.14	0.063	0.002	474	90	528	35	714	53	74	523	67	0.55	0.103	528	35	
se09a28	0.725	0.051	0.088	0.003	0.25	0.061	0.001	553	30	541	18	647	28	84	543	34	0.69	0.081	541	18	
se09a09	0.815	0.027	0.095	0.002	0.26	0.062	0.001	605	15	586	10	677	25	87	591	18	0.23	1.340	586	10	
au26a11	0.918	0.049	0.103	0.003	0.31	0.063	0.001	661	26	635	20	697	24	91	643	36	0.34	0.021	635	20	
se08b21	1.145	0.054	0.126	0.006	0.52	0.064	0.001	775	26	764	35	752	18	102	773	50	0.71	0.064	764	35	
se08b19	1.536	0.054	0.149	0.005	0.46	0.082	0.001	945	21	895	27	1246	27	72	929	40	0.05	0.225	1246	27	
au26a30	1.534	0.053	0.150	0.003	0.28	0.072	0.001	944	21	899	16	989	26	91	913	29	0.05	0.387	989	26	
se07b24	1.561	0.065	0.156	0.004	0.28	0.073	0.001	955	26	932	20	1011	25	92	939	36	0.42	0.389	1011	25	
se07b25	1.565	0.079	0.156	0.004	0.28	0.075	0.001	957	31	933	24	1066	39	88	941	43	0.49	0.773	1066	39	
au26a41	1.552	0.065	0.158	0.004	0.30	0.069	0.001	951	26	945	22	902	32	105	948	38	0.84	0.440	902	32	
se09a07	1.642	0.057	0.159	0.003	0.27	0.073	0.001	987	22	953	16	1008	29	95	963	30	0.16	1.120	1008	29	
se07b28	1.695	0.044	0.164	0.004	0.46	0.072	0.001	1007	16	979	22	972	17	101	999	31	0.17	0.572	972	17	
au26a43	1.813	0.069	0.167	0.004	0.32	0.074	0.001	1050	25	996	22	1051	31	95	1017	39	0.05	0.337	1051	31	
se08b33	1.762	0.078	0.167	0.005	0.35	0.076	0.001	1032	29	996	29	1085	28	92	1013	48	0.28	0.335	1085	28	
se09a30	1.677	0.056	0.167	0.003	0.30	0.074	0.001	1000	21	996	18	1051	26	95	998	31	0.87	0.399	1051	26	
se09a61	1.743	0.060	0.172	0.004	0.35	0.074	0.001	1024	22	1023	23	1049	28	98	1024	37	0.96	0.755	1049	28	
au26a54	1.834	0.058	0.173	0.004	0.35	0.074	0.001	1058	21	1029	21	1033	21	100	1043	34	0.23	0.607	1033	21	
se09a43	1.767	0.045	0.175	0.003	0.35	0.074	0.001	1033	17	1041	17	1045	19	100	1037	28	0.68	0.583	1045	19	
se07b22	1.846	0.054	0.175	0.003	0.27	0.076	0.001	1062	19	1042	15	1103	23	94	1048	27	0.34	0.420	1103	23	
au26a58	1.960	0.105	0.176	0.006	0.30	0.076	0.001	1102	36	1046	31	1087	34	96	1067	55	0.16	0.384	1087	34	
se09a33	1.925	0.038	0.180	0.003	0.40	0.075	0.001	1090	13	1069	16	1079	11	99	1082	24	0.19	0.933	1079	11	
au26a14	1.983	0.134	0.180	0.007	0.29	0.080	0.001	1110	46	1069	38	1199	35	89	1083	66	0.42	0.732	1199	35	
se09a54	2.072	0.071	0.188	0.006	0.45	0.080	0.001	1140	23	1121	31	1200	12	95	1132	44	0.36	0.353	1200	12	
se08b41	2.182	0.063	0.199	0.004	0.35	0.079	0.001	1175	20	1167	22	1170	17	100	1172	35	0.75	0.285	1170	17	
se08b23	2																				

Table A2. Continued.

Sample/ Analysis	Measured Isotopic Ratios						Calculated Ages (Ma)								Detrital (Ma)		Metamorphic (Ma)			CA-TIMS (Ma)			
	$^{207}\text{Pb}/^{235}\text{U}$	$\pm 1\sigma$	$^{206}\text{Pb}/^{238}\text{U}$	$\pm 1\sigma$	Rho	$^{207}\text{Pb}/^{206}\text{Pb}$	$\pm 1\sigma$	$^{207}\text{Pb}/^{235}\text{U}$	$\pm 1\sigma$	$^{206}\text{Pb}^{238}\text{U}$	$\pm 1\sigma$	$^{207}\text{Pb}/^{206}\text{Pb}$	$\pm 1\sigma$	U-Pb/Pb-Pb concordancy (%)	Concordia age	$\pm 2\sigma$	Probability of concordance	Th/U	For Prob Dens plots age	For Prob Dens plots age	$^{206}\text{Pb}/^{238}\text{U}$	$\pm 2\sigma$	notes
se09a24	4.157	0.060	0.293	0.004	0.46	0.101	0.001	1666	12	1657	19	1647	11	101	1665	23	0.63	0.282	1647	11			
se09a23	4.333	0.187	0.299	0.010	0.37	0.098	0.001	1700	36	1689	47	1582	20	107	1696	66	0.82	0.603	1582	20			
se08b27	4.225	0.071	0.301	0.003	0.34	0.102	0.001	1679	14	1697	17	1655	13	103	1685	25	0.30	1.270	1655	13			
au26a40	4.589	0.125	0.302	0.006	0.38	0.104	0.001	1747	23	1702	31	1698	21	100	1734	43	0.13	0.711	1698	21			
se08b07	4.418	0.074	0.305	0.005	0.48	0.104	0.001	1716	14	1716	24	1693	14	101	1716	27	0.98	0.576	1693	14			
au26a10	4.727	0.235	0.311	0.010	0.31	0.111	0.002	1772	42	1747	47	1819	35	96	1761	71	0.63	0.294	1819	35			
au26a68	4.985	0.125	0.315	0.005	0.35	0.108	0.001	1817	21	1763	27	1766	16	100	1798	39	0.06	0.911	1766	16			
se08a09	12.907	0.182	0.505	0.007	0.52	0.181	0.001	2673	13	2635	31	2662	7	99	2675	26	0.16	0.463	2662	7			
se08b24	13.554	0.235	0.526	0.008	0.44	0.184	0.001	2719	16	2723	34	2686	9	101	2719	33	0.89	0.475	2686	9			
<b>Tower Hill Formation (KSTH1)</b>																							
mrl2a56	0.449	0.032	0.050	0.002	0.27	0.057	0.001	376	23	315	12	499	33	63	322	23	0.01	0.092					
mrl1c81	0.753	0.052	0.081	0.004	0.36	0.065	0.002	570	30	503	24	778	49	65	523	43	0.03	1.089					
mrl1b46	0.747	0.020	0.087	0.002	0.36	0.057	0.000	567	12	540	10	496	18	109	550	18	0.03	0.588					
mrl2a59	0.841	0.059	0.088	0.003	0.26	0.061	0.001	620	33	542	19	654	37	83	555	37	0.02	0.473					
mrl1c19	0.881	0.028	0.092	0.003	0.51	0.062	0.001	641	15	565	17	674	22	84	612	28	0.00	0.356					
mrl1c79	0.849	0.036	0.094	0.002	0.23	0.067	0.001	624	20	581	11	846	36	69	588	21	0.03	0.516					
mrl2b11	1.660	0.325	0.095	0.008	0.21	0.126	0.004	993	124	586	46	2045	53	29	591	92	0.01	1.607					
mrl1b34	0.698	0.041	0.096	0.003	0.28	0.054	0.001	537	24	591	19	383	49	154	573	33	0.04	0.594					
mrl1c14	0.877	0.022	0.097	0.002	0.41	0.061	0.000	639	12	596	12	635	17	94	616	20	0.00	0.177					
mrl2b42	0.955	0.061	0.097	0.004	0.29	0.062	0.001	681	32	596	21	668	43	89	614	40	0.01	0.855					
mrl2b20	1.236	0.139	0.097	0.006	0.27	0.080	0.002	817	63	597	35	1189	55	50	618	68	0.00	0.815					
mrl2b56	0.944	0.040	0.098	0.002	0.27	0.061	0.001	675	21	603	13	652	30	92	617	25	0.00	0.978					
mrl1b27	1.211	0.099	0.099	0.007	0.42	0.080	0.002	806	45	608	40	1190	38	51	664	74	0.00	1.139					
mrl1b47	0.715	0.033	0.101	0.002	0.26	0.052	0.001	548	20	619	14	285	39	217	596	25	0.00	0.525					
mrl2a63	1.016	0.065	0.102	0.003	0.26	0.068	0.005	712	33	625	20	868	159	72	640	38	0.01	0.702					
mrl2a28	0.998	0.040	0.103	0.003	0.30	0.066	0.001	703	20	631	15	808	29	78	649	27	0.00	0.357					
mrl1b45	0.981	0.048	0.104	0.003	0.34	0.064	0.001	694	25	639	20	748	32	85	656	36	0.04	0.208					
mrl1b48	0.990	0.034	0.105	0.002	0.30	0.063	0.001	698	17	643	13	696	29	92	658	23	0.00	0.395					
mrl1c78	0.995	0.023	0.105	0.002	0.42	0.062	0.000	701	12	646	12	682	17	95	673	20	0.00	0.574					
mrl1c21	1.158	0.066	0.107	0.003	0.25	0.073	0.001	781	31	654	18	1015	38	64	672	34	0.00	0.836					
mrl2b13	1.078	0.066	0.108	0.003	0.21	0.063	0.001	743	32	659	16	718	36	92	670	32	0.01	0.845					
mrl2b39	1.090	0.061	0.108	0.003	0.27	0.063	0.001	748	29	664	19	699	27	95	681	36	0.01	0.073					
mrl1c08	1.285	0.107	0.118	0.007	0.37	0.072	0.002	839	48	717	42	996	61	72	759	76	0.02	0.729					
mrl2a65	1.251	0.077	0.120	0.004	0.25	0.068	0.001	824	35	730	21	879	28	83	747	41	0.01	0.194					
mrl1b33	1.168	0.036	0.123	0.002	0.30	0.068	0.001	786	17	747	13	875	25	85	760	24	0.04	0.351					
mrl2b37	1.341	0.091	0.124	0.005	0.29	0.068	0.001	864	40	751	28	862	25	87	777	53	0.01	0.616					
mrl1c71	1.200	0.039	0.125	0.003	0.37	0.065	0.001	801	18	758	17	785	25	97	777	29	0.03	0.860					
mrl2a66	1.396	0.101	0.129	0.006	0.31	0.065	0.001	887	43	782	33	775	27	101	810	60	0.02	0.356					
mrl2b19	1.457	0.121	0.130	0.005	0.25	0.068	0.001	913	50	785	30	865	35	91	806	58	0.02	0.545					
mrl2b12	1.661	0.062	0.136	0.004	0.36	0.071	0.001	994	24	822	21	945	31	87	879	38	0.00	0.522					
mrl1c69	1.565	0.117	0.139	0.006	0.31	0.080	0.001	956	46	842	36	1200	19	70	874	66	0.02	0.131					
mrl2b52	1.561	0.087	0.143	0.004	0.24	0.071	0.001	955	34	863	21	957	29	90	880	40	0.01	1.423					
mrl1b22	1.243	0.038	0.147	0.003	0.32	0.061	0.001	820	17	887	16	637	31	139	855	27	0.00	0.303					
mrl1c82	1.617	0.037	0.155	0.003	0.39	0.071	0.001	977	15	927	15	967	17	95	954	25	0.00	0.322					
mrl1c70	1.798	0.075	0.158	0.006	0.43	0.075	0.001	1045	27	945	31	1057	27	89	1003	50	0.00	0.632					
mrl2b21	1.820	0.085	0.160	0.005	0.35	0.077	0.001	1053	30	956	29	1128	28	85	997	50	0.00	0.100					
mrl2b31	2.091	0.064	0.161	0.005	0.47	0.074	0.001	1146	21	964	26	1041	22	93	1076	41	0.00	0.106					
mrl1b32	1.794	0.069	0.162	0.004	0.33	0.076	0.001	1043	25	967	23	1098	27	88	998	40	0.01	0.318					
mrl1b38	1.845	0.094	0.163	0.008	0.45	0.074	0.001	1032	34	976	42	1036	20	94	1033	64	0.03	0.124					
mrl2b27	2.188	0.172	0.166	0.009	0.34	0.080	0.001	1177	55	989	48	1186	30	83	1051	87	0.00	0.324					
mrl1c62	1.834	0.056	0.168	0.004	0.37	0.076	0.001	1058	41	1175	46	1358	28	87	1264	75	0.00	0.209					
mrl1b18	2.430	0.046	0.203	0.003	0.44	0.081	0																

Table A2. Continued.

Sample/ Analysis	Measured Isotopic Ratios						Calculated Ages (Ma)								Detrital (Ma)		Metamorphic (Ma)			CA-TIMS (Ma)				
	$^{207}\text{Pb}/^{235}\text{U}$	$\pm 1\sigma$	$^{206}\text{Pb}/^{238}\text{U}$	$\pm 1\sigma$	Rho	$^{207}\text{Pb}/^{206}\text{Pb}$	$\pm 1\sigma$	$^{207}\text{Pb}/^{235}\text{U}$	$\pm 1\sigma$	$^{206}\text{Pb}^2/^{238}\text{U}$	$\pm 1\sigma$	$^{207}\text{Pb}/^{206}\text{Pb}$	$\pm 1\sigma$	U-Pb/Pb-Pb concordancy (%)	Concordia age	$\pm 2\sigma$	Probability of concordance	Th/U	For Prob Dens plots age	For Prob Dens plots age	$^{206}\text{Pb}/^{238}\text{U}$	$\pm 2\sigma$	notes	
mr12a39	11.176	0.233	0.455	0.009	0.45	0.162	0.002	2538	19	2418	38	2482	17	97	2532	39	0.00	0.441						
mr11c44	14.156	0.328	0.507	0.013	0.54	0.195	0.001	2760	22	2645	54	2783	8	95	2768	43	0.01	0.245						
mr12a30	0.576	0.020	0.074	0.001	0.29	0.057	0.001	462	13	463	9	472	28	98	463	16	0.94	0.501	463	9				
mr12b53	0.686	0.068	0.079	0.003	0.19	0.058	0.001	531	41	490	18	530	41	93	494	34	0.34	1.247	490	18				
mr11c23	0.661	0.035	0.080	0.002	0.28	0.060	0.001	515	21	497	14	601	24	83	501	26	0.40	0.957	497	14				
mr12b16	0.797	0.095	0.082	0.005	0.24	0.065	0.001	595	53	506	27	782	45	65	516	53	0.11	0.650	506	27				
mr11b11	0.690	0.031	0.083	0.002	0.30	0.057	0.001	533	19	517	13	476	28	108	521	24	0.40	1.403	517	13				
mr11c68	0.666	0.033	0.084	0.002	0.22	0.059	0.001	518	20	519	11	583	33	89	519	21	0.98	2.675	519	11				
mr11c83	0.715	0.023	0.085	0.002	0.31	0.057	0.001	547	14	526	10	509	24	103	532	18	0.13	0.484	526	10				
mr11c64	0.717	0.034	0.086	0.003	0.31	0.061	0.001	549	20	530	15	633	40	84	535	27	0.38	0.658	530	15				
mr12a42	0.705	0.039	0.086	0.002	0.24	0.059	0.001	542	24	530	14	576	31	92	532	26	0.62	0.985	530	14				
mr11b43	0.690	0.030	0.086	0.002	0.33	0.053	0.001	533	18	531	14	310	37	171	532	26	0.94	0.910	531	14				
mr11b07	0.700	0.036	0.088	0.003	0.33	0.058	0.001	539	22	543	18	546	45	100	542	31	0.85	1.041	543	18				
mr12a08	0.732	0.058	0.089	0.004	0.25	0.063	0.001	558	34	552	21	694	35	80	553	39	0.87	0.635	552	21				
mr12b30	0.835	0.074	0.090	0.003	0.21	0.063	0.001	617	41	555	20	707	33	78	562	39	0.15	0.266	555	20				
mr11c72	0.775	0.065	0.090	0.003	0.23	0.070	0.002	583	37	556	20	925	47	60	560	39	0.49	1.444	556	20				
mr11c38	0.740	0.072	0.090	0.006	0.31	0.061	0.001	563	42	557	33	640	42	87	558	59	0.89	0.824	557	33				
mr12a53	0.886	0.071	0.092	0.004	0.27	0.062	0.001	644	38	568	24	666	40	85	582	45	0.06	0.169	568	24				
mr12b08	0.832	0.057	0.092	0.003	0.21	0.058	0.001	614	32	570	16	537	54	106	575	30	0.17	1.365	570	16				
mr11c63	0.849	0.069	0.093	0.006	0.39	0.064	0.002	624	38	572	35	726	65	79	593	61	0.20	1.605	572	35				
mr11c73	0.765	0.028	0.094	0.002	0.26	0.058	0.001	577	16	578	11	535	32	108	578	20	0.96	0.373	578	11				
mr12b61	0.901	0.080	0.094	0.004	0.23	0.065	0.001	652	43	580	23	781	45	74	590	44	0.11	0.825	580	23				
mr11c27	0.791	0.041	0.095	0.002	0.23	0.062	0.001	592	23	583	13	660	29	88	584	25	0.70	0.369	583	13				
mr12b36	0.724	0.072	0.095	0.004	0.19	0.057	0.001	553	43	585	22	509	50	115	580	41	0.46	0.737	585	22				
mr11b17	0.845	0.032	0.096	0.002	0.29	0.062	0.001	622	17	593	12	680	25	87	601	23	0.12	0.946	593	12				
mr12b07	0.846	0.079	0.097	0.004	0.22	0.063	0.001	622	44	596	23	699	47	85	600	44	0.56	0.577	596	23				
mr11b51	0.761	0.044	0.097	0.004	0.31	0.056	0.001	574	25	597	21	468	44	127	588	36	0.41	0.776	597	21				
mr12b60	0.943	0.096	0.098	0.004	0.18	0.068	0.002	674	50	604	21	857	50	70	610	42	0.18	0.819	604	21				
mr12a09	0.832	0.032	0.098	0.003	0.38	0.059	0.001	615	18	605	17	578	24	105	610	29	0.61	0.844	605	17				
mr11b28	0.869	0.027	0.100	0.002	0.29	0.059	0.001	635	15	612	11	555	27	110	618	19	0.13	0.555	612	11				
mr11b29	0.845	0.037	0.101	0.002	0.28	0.059	0.001	622	20	617	14	562	32	110	619	26	0.83	0.613	617	14				
mr12b48	0.906	0.078	0.101	0.004	0.24	0.064	0.001	655	42	618	24	735	42	84	624	46	0.39	0.014	618	24				
mr11c54	0.751	0.077	0.101	0.004	0.18	0.062	0.001	569	45	619	22	674	39	92	611	42	0.27	0.314	619	22				
mr12a64	0.999	0.089	0.101	0.004	0.25	0.066	0.001	704	45	620	26	793	31	78	634	50	0.08	0.259	620	26				
mr11c65	0.914	0.037	0.101	0.002	0.27	0.064	0.001	659	19	621	13	733	38	85	629	24	0.06	0.424	621	13				
mr12b63	0.894	0.055	0.101	0.003	0.25	0.061	0.001	649	29	623	18	628	39	99	628	34	0.40	0.710	623	18				
mr11c31	0.943	0.045	0.102	0.003	0.28	0.065	0.001	674	23	627	16	782	36	80	638	30	0.06	0.616	627	16				
mr11c39	0.856	0.047	0.102	0.002	0.20	0.068	0.001	628	26	629	13	855	34	74	629	25	0.99	1.333	629	13				
mr11b19	0.932	0.038	0.103	0.003	0.32	0.061	0.001	669	20	633	16	639	26	99	644	28	0.10	1.137	633	16				
mr11b29	0.958	0.044	0.104	0.002	0.21	0.066	0.001	682	23	636	12	793	39	80	642	22	0.06	0.639	636	12				
mr12a55	0.829	0.073	0.104	0.003	0.18	0.063	0.002	613	40	636	19	694	62	92	633	36	0.57	0.595	636	19				
mr11c59	0.940	0.033	0.104	0.003	0.34	0.062	0.001	673	17	638	15	670	28	95	650	26	0.06	0.384	638	15				
mr12a54	1.029	0.087	0.104	0.004	0.25	0.066	0.001	718	43	641	26	793	28	81	654	49	0.09	0.381	641	26				
mr12b28	0.942	0.069	0.105	0.004	0.27	0.054	0.001	674	36	649	23	858	35	107	650	45	0.41	0.875	643	24				
mr11e60	0.860	0.058	0.106	0.004	0.28	0.063	0.001	630	32	647	23	722	45	90	642	42	0.63	1.072	647	23				
mr11c50	0.899	0.048	0.106	0.003	0.25	0.062	0.001	651	26	647	17	658	33	98	648	31	0.87	0.460	647	17				
mr12b41	0.959	0.051	0.107	0.020	0.14	0.061	0.001	683	337	653	118	639	51	102	655	232	0.93	0.159	653	118				
mr11c51	0.882	0.035	0.107	0.003	0.32	0.062	0.001	642	19	654	16	657	30	99	649	27	0.56	0.530	654	16				
mr12a38	0.966	0.033	0.108	0.002	0.27	0.060	0.001	686	17	666	11	612	30	108	667	21	0.14	0.525	660	11				
mr11b41	0.971	0.0																						

Table A2. Continued.

Sample/ Analysis	Measured Isotopic Ratios						Calculated Ages (Ma)								Detrital (Ma)		Metamorphic (Ma)		CA-TIMS (Ma)		notes	
	$^{207}\text{Pb}/^{235}\text{U}$	$\pm 1\sigma$	$^{206}\text{Pb}/^{238}\text{U}$	$\pm 1\sigma$	Rho	$^{207}\text{Pb}/^{206}\text{Pb}$	$\pm 1\sigma$	$^{207}\text{Pb}/^{235}\text{U}$	$\pm 1\sigma$	$^{206}\text{Pb}^{238}\text{U}$	$\pm 1\sigma$	$^{207}\text{Pb}/^{206}\text{Pb}$	$\pm 1\sigma$	U-Pb/Pb-Pb concordancy (%)	Concordia age	$\pm 2\sigma$	Probability of concordance	Th/U	For Prob Dens plots age	For Prob Dens plots age	$^{206}\text{Pb}/^{238}\text{U}$	$\pm 1\sigma$
mr11b37	2.123	0.098	0.200	0.005	0.28	0.075	0.001	1156	32	1177	28	1058	31		111	1169	47	0.56	0.282	1058	31	
mr12b21	2.160	0.163	0.203	0.006	0.20	0.083	0.002	1168	52	1191	32	1277	49		93	1186	59	0.68	0.796	1277	49	
mr12a40	2.455	0.155	0.206	0.007	0.25	0.080	0.002	1259	46	1210	35	1194	38		101	1225	63	0.33	0.283	1194	38	
mr11b20	2.451	0.070	0.211	0.004	0.32	0.082	0.001	1258	20	1232	20	1236	21		100	1245	33	0.28	0.314	1236	21	
mr12b09	2.683	0.132	0.215	0.006	0.28	0.085	0.001	1324	36	1257	31	1325	32		95	1282	54	0.11	0.246	1325	32	
mr12a35	3.823	0.242	0.259	0.012	0.37	0.102	0.002	1598	51	1484	63	1652	32		90	1555	94	0.08	1.241	1652	32	
mr11c53	3.383	0.225	0.264	0.010	0.30	0.089	0.001	1500	52	1508	53	1395	25		108	1504	84	0.90	0.106	1395	25	
mr11c58	4.776	0.126	0.327	0.007	0.39	0.107	0.001	1781	22	1825	33	1742	12		105	1789	42	0.16	0.195	1742	12	
mr12b40	8.309	0.612	0.394	0.017	0.29	0.131	0.002	2265	67	2143	79	2116	26		101	2214	119	0.16	0.486	2116	26	
mr11c55	7.647	0.171	0.410	0.008	0.44	0.130	0.001	2190	20	2216	37	2103	15		105	2192	40	0.45	0.276	2103	15	
mr12b38	18.029	1.144	0.599	0.033	0.44	0.210	0.002	2991	61	3025	134	2906	13		104	2992	122	0.78	0.109	2906	13	

## Footnotes

Data in grey - probability of concordance &lt;0.05

Data in red - interpreted as metamorphic, based on morphology and generally low Th/U

Data in blue - youngest detrital zircon age population

Data in black - all other detrital zircon data

## Notes

1. abundant cracks and an amorphous shaped core; included in metamorphic population despite high Th/U

2. relatively low probability of concordance

3. older age but low Th/U

4. excluded from weighted average in text and figure; reversely discordant outlier